タイプ・トークンの相互作用からみた集団現象の創発

新里，高行

(Degree)
博士（理学）

(Date of Degree)
2012-03-25

(Date of Publication)
2012-09-11

(Resource Type)
doctoral thesis

(Report Number)
甲5586

(URL)
https://hdl.handle.net/20.500.14094/D1005586

博士論文

タイプ・トークンの相互作用からみた集団現象の創発

平成２４年１月

神戸大学大学院理学研究科

新里 高行

博士論文

タイプ・トークンの相互作用からみた集団現象の創発

平成２４年１月

神戸大学大学院理学研究科

新里 高行

1. Introduction

1.1. To Understand Living System

It is important to understand a living system in the context of the relation between "parts and whole". A living system makes itself by itself and maintains its systemic property by using its parts. Obviously, we distinguish between "a system" and "making a system" as distinct concepts. A "system", revealing its own entity, has to be distinguished from other systems. On the other hand, "making a system" is very different from "a system"; the notion of "making a system" implies a process of individualizing a system. Therefore, we usually have asked the relation between "system" and "making system" or "parts" and "whole" or "self" and "making self" when we consider the system theory [1-14]. "Making system" usually is accepted as a result of interactions between parts.

One famous example is a cellular automaton [15]. Cellular automata, which are developed by Wolfram, are generally constructed by cells, which have two states, on the one-dimensional line. (Of course, there are many types of cellular automata such as two-dimensional model (Game of Life) or the number of states over two (Universal cellular automata). Here, we can consider the most popular case without losing generality.) In the cellular automata, each cell can interact with nearest neighbor. Each cell determines next state by the state of its two neighbors and its own state. Therefore, there are 2^8=256 patterns of changing rule for the cellular automaton. Wolfram examined the behavior of automata for all pattern of rule. He found that some rules showed simple periodic or stable behavior but some rules shows a complete random behavior. He classified four types for these behaviors of cellular automaton such as Class I, Class II, Class III and Class IV. When the rule is Class I, all cells rapidly converge into a uniform state. When the rule is Class II, all cells rapidly converge into a periodic state. There is no strangeness so far because simple rules result simple behavior. However, when the rule is Class III, Rule 30 for example, the behavior of cellular automata becomes complete random state. The most intriguing case is Class IV. When the rule is Class IV, Rule 110 for example, the behavior of cellular automata never shows periodic neither random. Generally, it is hard to obtain Class IV in the cellular automaton because there are very few cases, which show Class IV behavior in all 256 rules.

Wolfram found that we can compute AND, OR and NOT by using Class IV [15, 16]. In other words, cellular automata have an equivalent computational capability with Turing machine. Wolfram suggests the principle of computational equivalence, which means that the computational performance becomes equivalent if the computing machine exceeds a certain threshold. He also suggested that the threshold of universal computation is very low. Wolfram insists that these universal computations would be common phenomena in nature. However, we should set the initial condition precisely when we compute the problem by using the cellular automata. We could list other examples of needing precise initial condition such as a billiard ball computation [17]. Of cause, some researchers argue against the concept of the principle of computational equivalence. Melanie Mitchell, who is known for researches of the genetic algorithm, compared with *C. elegans* and a brain of human and criticized that it must not be the same such as a sophistication, for example the computational speed or accuracy in the living organisms. We consider, however, that these intuitive arguments never criticize essentially Wolfram's idea. If we really try to criticize Wolfram's idea, we must criticize his framework of the principle of computational equivalence. We will back to this problem about Class IV latter.

What the concept of Class IV brings into the system theory is a critical property [18]. In other words, Class IV is on the boarder of regularity and randomness. Many researchers have discussed the relation between criticality and living system when they consider the emergent behaviors. For example, Kauffman suggests that the living system is on the edge of chaos, which means that the living systems are on the boarder of order and disorder [19, 20]. Other recent example is the neural network. Copelli et al. [21, 22] suggested the famous psychophysics law (a Weber-Fechner logarithmic law or a Stevens power law [23]) could be explained by using a simple cell automaton model when the responsibility of the excited media was on the critical state. Bertschinger and Natschläger showed the computational performance of random connected neural networks reached maximum when the neural networks were on the

criticality [24].

Why is the criticality so important? We can list here two reasons to answer this question. One is that the emergent properties in a living system would need events of chance [15, 18, 21, 23]. If the living system only shows regularity, the system never would evolve. To avoid this disadvantage, the living system is desirable to have both properties, which are the regularity and the accident. Another reason is that the criticality would be well-fitted to the existing idea of the condensed physics. The critical property is often compared with the phase transition.

1.2. Why Does We Consider Collective Phenomena

Here we introduce Vicsek's model for the collective behavior [25, 26]. The detail of his model will be discussed later (Chapter 2). He considered that a set of self-propelled particles is the individual units, which interact with other individuals within a fixed-radius neighborhood. Each individual tries to align its directions within its interaction range. Therefore, each individual imitates each other. As a result, they consist several groups and sometimes behave as one collective. The degree of collectiveness can be tuned by a noise parameter. If the noise is high, individuals is hardly to make groups. However, individuals behave as one collective if the noise is very small. It can be observed the phase transition by the noise tuning. If the noise parameter exceeds a certain threshold, each individual suddenly shows a group behavior [25, 26].

Although there is no obvious central control such as a brain in the aggregation, we can acknowledge that the aggregation moves as though it has one body or one mind [27, 28, 29]. In fact, birds flocking, fish schooling and other collective phenomena are sometimes discussed in the context of self-organization [30, 31]. Global properties emerge only from local interactions of each individual. Recently, a more accurate analysis of flocking behavior can be achieved than was formerly possible [32, 33, 34]. Cavagna et al. measured velocity fluctuations of real birds (a precise definition will be discussed later) and found that the range of the spatial correlation does not have a constant value, but it scales with the linear size of the flock [34]. The size of correlation domain is obviously larger than the interaction range of each bird. Birds share more information than they can interact. Cavagna and others called this phenomenon "scale-free correlation". This is a very suggestive result because scale-free correlation indicates that a flock cannot divide into independent subparts. If one individual in a flock changes his direction, its influence would spread to all individuals. Cavagna's empirical results sometimes are compared with the criticality in condensed physics [35]. Real flocking spontaneously approaches to the critical state. This phenomenon is called self-organized criticality (SOC in short) [36, 37, 38]. Real flocks in the critical state can respond external perturbation (such as predator's attack) quickly [34].

Here we found the common ground for the Class IV, which has high computational ability, and SOC. We note that we never agree on the attitude, which such situation would important when we discuss the living system. We argue the problems, which are emerged through such criticality, when we believe "collective phenomena is on the critical state". In the critical state, it is considered that the fixed point would connect the whole and parts. Therefore, whole system is given in advance. However, in the collective phenomena, it is not trivial problem to determine what is one collective in natural flocks. It is still vague for the criterion of a flock. Self (what is a flock) is not prepared in advance.

This is why we take the theme of this paper as the collective phenomena. The collective phenomena contain important problems of the relation between "parts" and "whole". If we cannot prepare a "self", then what does mean "making self"? Many system theories miss this point. Returning to the definition of the word "self-organize", we point out that the word must contain two levels, which are "self" (parts) and "making self" (whole), at least. However, the word "self" would contain other elements, which never belongs to "self" in advance, because the "self" can make progress by actively taking in unknown factors when he adapts to changing environment. "Self" itself must be defined as incomplete in the self-organization. Changing "self" also requires changing "making self" as a whole. Therefore, the relation between "self" and "making self" must be dynamic. To overcome these problems, we use the concept of type (e.g., kind, classes, roles, variables) and token cognition (e.g., individuals, instances, filters,

values). Types and tokens are essential characteristics of physical symbol systems hypothesized in human and nonhuman mental representation [39, 40, 41]. Although it has been reported that nonhuman animals appear to reason on the basis of particular sets of features shared by members (tokens) rather than on abstract roles (types), we have to consider ambiguity between types and tokens when we consider the dynamical relation between parts and whole. The model of Chapter 2 and Chapter 3 are constructed by regarding the type and toke cognition. Each individual of our model adjusts a dynamical relation between type and token cognition though its own experience.

1.3. Construction of This Paper

In Chapter2, we will discuss about the flocking phenomena. Recently, the analysis of the flocking behavior can be more accurately analyzed than it was used to be. These researches make us reconsider to the notion of the neighborhood for the theoretical model. Topological distance is regarded as one of results. The topological distance elaborates that a birds never interacts with his or her neighbors in the neighborhood in a fixed length (they call "metric distance"), but interacts with the nearest 1^{st} - 7^{th} neighbors. Cavagna et al., moreover, found the new phenomenon in flocks explained by neither the metric distance nor topological distance. They found that the correlated domain in a flock is larger than the metric and topological distance, and discovered that this domain is proportional to the flock size. To synthesize topological and metric distance, we propose the metric-topological interaction model that reveals both metric and the topological distance. This model shows the various behaviors of a flock without any external noise. The metric-topological interaction model also shows the scale-free correlation in a flock, and simulating results are well-fitted to the empirical data obtained by Cavagna et al in two- and three dimensions. We also will discuss many properties for the fluctuation such as SOC and releasing and storing fluctuation.

In Chapter 3, we will discuss the ecological evolutional system. There are two contradictory aspects for the adaptive process in evolution. The one is that species must optimally increase its own fitness in a given environment. The other is that species must keep their variation ready to changing environment. In a strict sense, these two aspects might be exclusive with each other. If species is adapted to the optimal, the variation of species which can be trapped to the suboptimal decreases, and *vice versa*. To resolve this dilemma, we have to find the balancing between the optimal adaptation and the robust adaptation. Finding balance between them, however, needs the complete and static information for the locality and globality. The balancing between them must be more dynamic. In this study, we proposed the model that shows dynamical negotiation between global and local information by using a lattice theory. By using lattice theory, we never only can represent dynamic global information from local incomplete information. Species of our model show the power law of the lifespan distribution and $1/f$ fluctuation for adapting process. Finally, we argue that our model enables the balance between the optimal adaptation and the robust adaptation without any parameter. Incompleteness of information positively helps ecosystem to adapt to a given environment optimally.

2. Metric-Topological Interaction Model in Collective Behavior

2.1. Background

Collective behavior is observed in many biological systems in nature [30, 31, 42, 43, 44, 45]. Common examples include bird flocks [32, 33], fish schools [46, 47, 48, 49], human trails [50], swarms of insects [51] and bacterial cultures [52, 53]. Much is unknown about why animals exhibit collective behavior. Parrish et al. point out that there is a trade-off between individual and aggregation [47]. Aggregation would increase the survival chances and reproductive success of any new member. On the other hand, aggregations attract predators. Decision-making of each individual in a group is also an important aspect of collective behavior. The collective behavior sometimes seems to behave as if controlled by one mind [27, 28]. The individuals emerge as one collective through the decision of each individual under various conditions. Fish schools [48] and locust swarms [51], for example, adopt their environment by making different formations.

There are many models to explain these collective behaviors. The basic property of the model mainly has two aspects: (i) each individual unit (particle, bird, fish, etc.) interacts *locally* within a given space; and (ii) the global collective properties emerge from the interactions of individual units [54]. The key point is that the collective behavior, in particular the aggregation of the individual units, has a global property, which is not observed in the behavior of an isolated unit, through the interaction of the individual units; it is global even though individual units interact only locally, i.e., within a limited local space. Therefore, collective behavior can be considered an example of the concept of self-organization because the collective behavior emerges without the need for centralized control.

Many theoretical models of collective behavior have been proposed. The one of the famous models is the flocking and schooling model of Reynolds [55], whose computer simulations showed that the aggregation of individuals could reproduce various patterns. Vicsek's model, also called the self-propelled particle system (SPPs), can be considered as an abstraction of Reynold's model [25, 26, 56, 57]. Roughly speaking, this model assumes that each particle interacts with other particles only within a fixed neighborhood; it exhibits an order-disorder phase transition as a noise parameter is increased. Vicseck's physics-based model has been extended in several abstract ways. For example, Grégoire et al. showed that a system could change its collective behavior from a solid phase to a liquid phase by varying its parameter that determines the strength of a force between particles [29, 58]. There are some studies of the collective behavior by using the equation of the motion. Dossetti et al. examined the phase transition of the particle's behavior when non-liner noise is introduced into the equation of the motion [73].

Huth and Wissel introduced the idea that each individual had a repulsion zone within which other individuals are avoided and an attraction zone within which other individuals are attracted [59]. After Huth's study, Couzin et al. showed that the individuals using three interaction zones could reproduce various aggregation patterns by varying the sizes of these two zones. From their results, they noted the existence of a collective memory in the patterns formed by the aggregation of individuals [28]. In other words, a formation of the flock is affected by their past history. Another point of this model was that they used the field of perception. Each individual has the area of blindness. Several studies suggest that this kind of a limit of the animal cognition would play an important role in the collective behavior [60, 61, 62, 63].

Recently, another approach to collective behavior has developed from fieldwork [32, 33]. From careful research, Ballerini et al. proposed an alternative model of bird flocking in which the interactions of each bird depend on topological distance (the rank of the distance between two birds, e.g., first, second, third, etc., neighbors) rather than on metric distance (the length separation between them). It was a fixed radius neighborhood, that is SPP model, for example, that they mentioned "metric distance" here. Each bird interacts with a fixed number of its closest neighbors (typically six or seven), regardless of how distant those neighbors are. For comparison, in metric-distance models, each bird interacts with all neighbors within a

well-defined region in space, no matter how many they are. Recently, Ginelli et al. proposed the model of the topological distance [64]. They defined neighbors as the Voronoi tessellation. In this model, each individual can interact with Voronoi neighbors each other. Thus, there is no metrical information, but only well-defined topological information. This model that is based on the topological distance showed that subgroups have a weak cohesion since each subgroup never becomes independently because of their Voronoi neighbors. However, there are still a few models and discussions that are based on the topological distance [64, 65, 66, 67].

2.2. Metric Distance vs. Topological Distance

In this section, we review the notions of metric and topological distances and spelling out the problem of models based on either of them.

A metric-distance model was proposed by Vicsek et al. [25, 26]. In this model, self-propelled particles (SPPs) are the individual individuals, which interact with other individuals within a fixed-radius neighborhood; the interactions encourage the individuals to align their direction. In other words, each individual has a range of perception (eyeshot) and attempts to emulate in the motion of other individuals within its eyeshot. The eyeshot gives a clear and consistent definition for all individuals of their interaction neighborhood. In the models of Vicsek et al. [25, 26, 57] and Couzin et al. [28], the eyeshot interaction distance is set the same for all individuals. Mathematically, the metric-distance model can be defined as follows. An individual labeled by the index i has a position $\mathbf{x}_i(t)$ and velocity $\mathbf{v}_i(t)$ at a time t. The next state of every individual is determined simultaneously at each time step. Specifically, the next state is given by the formula

$$\mathbf{x}_i(t+1) = \mathbf{x}_i(t) + \mathbf{v}_i(t)\Delta t \qquad (2.2.1)$$

The velocity of the individuals is determined to have an absolute value v and a direction that is given by the angle $\theta(t)$. This angle is updated according to the expression

$$\theta(t+1) = \langle\theta(t)\rangle_r + \Delta\theta \qquad (2.2.2)$$

where $\langle\theta(t)\rangle_r$ denotes the direction of the velocity averaged over all the individuals within a radius r of the given particle, which defines its neighborhood. The average of the directions is given by the angle $\langle\sin\theta(t)\rangle_r/\langle\cos\theta(t)\rangle_r$. Each individual aligns its direction with the direction averaged within its neighborhood radius r, but with a noise representing the uncertainty of its estimation of that average. The noise also represents the degree to which the individual is free of social restraint. In this paper, we fix the absolute value of velocity. Other metric-distance models add regions such as repulsion and attraction zones [28, 52, 53, 54, 55, 59, 60, 68, 69, 70], increasing the complexity of their behaviors; this is important in modeling the flocking of birds or the schooling of fish. However, because we wish to consider abstract models, we do not add such complexities in this section.

The metric-distance model provides a good explanation for collective, synchronized motions when the density of individual individuals is high. Such density-dependent synchronization is a common feature of collective behavior, e.g., in locust swarms [51] and fish schools [44]. In the metric-distance model, if the individual density is high, the neighborhoods of the individuals tend to overlap significantly with each other. Because of such overlapping neighborhoods, the individuals imitate one another, eventually synchronizing and aligning in the same direction. At the other extreme, if the individual density is low, their neighborhood rarely overlap; in such cases, groups may be formed but rarely synchronize.

Recently, another approach to the phenomenon of synchronization has been suggested. From their observations of bird flocking, Ballerini et al. proposed the idea that topological distance should be used to define the interaction neighborhood [32, 33]. Rather than assuming that an individual interacts with all other individuals within a given radius, they suggest that the individual interacts with only its 6-8 closest neighbors regardless of how distant they are. This model can be compared with the "magic number seven" hypothesis, which states that a limit of individual instant cognition is given seven objects, plus or minus two [71]. This hypothesis means that there is a cognitive limitation for the birds. Such limitation of the cognition also is

applied for the flocking models. Bode et al., for instance, constructed the model by a limited interaction and suggested that the limited interaction plays an important role in flocks [62, 63]. The difference between the metric-distance and topological-distance models lies in how they define the neighbors interacting with a given individual; the former model considers all individuals within an interaction range r, whereas the latter model considers only its six or seven nearest neighbors. Thus, each bird always interacts with its six nearest neighbors, regardless of their separation. Ballerini et al. carried out computer simulations of the metric-distance and topological-distance models of the attraction zone. They observed that topological-distance models were more robust against predator attack than were metric-distance models [32, 33]. Topological-distance models can be robust since individuals can interact with their flock-mates even when separated from their flock. In metric-distance models, the individual can no longer interact with its flock once separated by more than the interaction range.

The question remains, however, whether birds really interact with exactly six or seven neighbors. If there is a fluctuation to taking neighbors around 6-7, what scale this fluctuation would be? Such questions arise for the metric-distance model. Is the eyeshot range, i.e., the limiting distance of each individual's perception, correct? In other words, does the modeled neighborhood of each individual correspond to its true neighborhood? Such questions inevitably occur, and indeed were raised by Bajec et al [61]. They pointed out that the range of each individual's perception is never completely clear. We adapt their approach by considering uncertain neighborhoods of the individuals. We will, therefore, discuss the notion of the neighborhood and neighbors and then present a new model in the following section.

2.3. The Abstracted MTI model

2.3.1. Algorithm

In previous section, we discussed the difference between the metric distance and the topological distance. To apply the ambiguity of the metric and topological distance to our model, we re-evaluate these models, which leads to a hybrid metric-topological interaction (MTI) model. First, we point out that, when considering an individual's neighborhood, the notions of metric and topological distance are inseparable. Second, we describe the definitions of an interaction neighborhood in terms of the metric and topological distances, corresponding to identifying flock-mates as a class and a collection, respectively. By introducing these notions, it would become clear between the flocking model and the animal cognition. Finally, we propose the new model for collective behavior, namely the MTI model.

In a neighborhood defined by the topological distance, the individual can interact with its nearest 6-8 neighbors, no matter their distance. Thus, every individual has a unique limit to its perception defined by its neighbors' distances. This perception limit of the individual corresponds to its metric neighborhood. In other words, the notion of the topological distance implicitly admits a neighborhood defined analogously to the metric-distance model. Thus, in a certain sense, a topological-distance model can be construed as a type of metric-distance model. How about the metric-distance model? It may seem that topological distance plays no role in defining a metric-distance neighborhood. However, when defining the metric-distance neighborhood, the modeler creating a model always considers the mean density of individuals, i.e., how many individuals fit into such a neighborhood. But this latter notion corresponds to topological distance; thus, the topological distance is used to define the metric-distance neighborhoods. This is an important point for the collective behavior since we should give an appropriate neighborhood to individuals in advance. Therefore, the concepts of metric and topological distance are complementary.

An important point in topological-distance models is that the neighborhood of each individual is not fixed in advance. To put it another way, the neighborhood of each individual is elastic in terms of the metric distance. The topological distance depends on the notion of metric distance. Let us recall that a metric-distance neighborhood is determined in advance by the researcher making the model. Hence, we can consider that topological-distance models serve to make the metric neighborhoods uncertain, but in a way different from earlier fuzzy-logic approaches [61].

The topological-distance model can be considered as a metric-distance model with uncertain

neighborhoods but, conversely, a metric-distance model cannot be construed as a topological-distance model with uncertain neighborhoods. However, an analogous *uncertain-neighbor* problem pertains, corresponding to the uncertainty of whether a given individual will interact with another nearby individual. In a metric-distance model, an individual interacts with all other individuals within its neighborhood. The number of neighbors within its neighborhood fluctuates dynamically as nearby individuals enter and leave its neighborhood. Hence, we can interpret a metric-distance model as a topological-distance model in which the number of interacting neighbors is uncertain. Thus, the topological-distance and metric-distance models can be viewed as the other with added uncertainty. As shown above, the topological distance cannot be defined without the metric distance, and vice versa.

Next we re-interpret the neighborhoods in terms of class and collection cognition of an individual. The metric-distance neighborhood is defined by an individual's eyeshot (the limit of its perception); the individual determines its next direction by averaging the direction of the flock-mates in its neighborhood. In the averaging operation, the individual integrates over its whole neighborhood to obtain one direction; the neighborhood is an assembly that the individual wishes to imitate. We call such a cognition a class cognition. A class corresponds to uniting different objects (such as events, phenomena, etc.) into one type. In the case of the metric distance, all directions in the neighborhood are compressed into one direction.

The individual of a topological-distance model interacts with its 6-8 nearest neighbors. Seen as a neighborhood (not as a set of *neighbors*), the neighborhood of each individual expands and shrinks continuously. It is important for the flocking model that each individual has a different neighborhood. At each time step, the individual of a topological-distance model adjusts its eyeshot (the limit of its perception) so as to prevent interactions with neighbors further than the 7^{th}-9^{th} nearest neighbors. The individual in such a model behaves as if these further neighbors don't exist. Such an individual does not recognize an assemblage of a certain size around him, but rather decides its next action only from its particular 6-8 nearest neighbors. We call such a cognition a collection cognition. The notion of collection comes from gathering up similar objects, recognizing them as a set of objects.

We point out here the qualitative difference between class and collection cognitions. A class cognition compresses sundry individual information similar to the process of abstraction. By contrast, a collection calculation gathers up similar objects but does not compress their information. There is, thus, a qualitative difference between them. But we also note the interdependence between both types of cognition. To carry out a class cognition, one needs to identify similar objects from which to abstract; this identification corresponds to a collection cognition. Similarly, a collection cognition requires a criterion for identifying a set of similar objects, which corresponds to a class cognition. We consider this ambiguous but qualitative difference in cognition to be very important in the decision-making of animals. These notions are by no means strange. It has turned out that, for instance, fishes may have two systems to recognize conspecifics. One is the system that fishes can distinguish small number of objects [72], and another is the system that fishes can distinguish the numerical rate such as 1:2 or 2:3 [73]. These two systems would correspond to the collection (distinguishing small number) and the class cognition (distinguishing the numerical rate). Agllilo et al. suggested that a fish would have two mechanisms of the quantity, but it is hard to prove that there is no ambiguity between these two systems [72, 73, 74]. When we consider the animal's numerical cognition, these two systems have been discussed for many studies. From these perspectives, the class and the collection cognition would be enough possible on animals [72, 73, 74, 75].

Interactions based on metric and topological distance correspond to this distinction, and the ambiguity between these calculations corresponds to the ambiguity between the metric and topological distances. This cognitional ambiguity allows us to consider topological distance and metric distance as two aspects of a single model. This is why we use the terms, which are a collective and a class cognition.

We emphasized above that the metric distance and the topological distance can each be construed as the other with an uncertain neighborhood or uncertain neighbors. This concept is the motivation of our hybrid model. Roughly speaking, our model lies between the extremes of the metric-distance and topological-distance models. We describe our algorithm in Figure 2.1, and sketch our model here. First, we set $\mathbf{x}_i^t$ as a position vector and θ_i^t as an angle of each individual. i is an index of each individual. t is a time step, respectively. $<>_S$ means to take

average of directions in set S (for example, S is given as N-TOP or N-MET in Figure 2.1). We use this average to compute the result of individual's interaction such as metric or topological distance. Our model is characterized by two parameters: a, the threshold for class cognition, and b, the threshold for collection cognition. When the individual uses class cognition, its interaction neighborhood is defined by metric distance. On the other hand, when the individual uses collection cognition, its interaction neighbors are defined by topological distance. The main feature of our MTI model is that, at every time step, each individual updates its neighborhood, switching between class (metric) and collection (topological) cognition (Figure 2.2). Each individual, therefore, has a different interaction range and adjusts its neighborhood to the varying conditions in the flock. The flexibility of its neighborhood is determined by the parameters a and b for class and collection cognition. For example, if the difference in the direction between the individual of interest and his neighbours is under a ($\exists i \in$N-TOP, $|\theta_i^t - \langle\theta\rangle_{\text{N-TOP}}| < a$), the individual of interest changes his interaction domain to the metric distance, which means that the individual changes to the class cognition from the collection cognition when his neighbours seem to behave like himself. Or if the difference in the direction between his randomly selected two neighbours is over b ($\forall i, j \in$N-MET, $|\theta_i^t - \theta_j^t| > b$), then this individual uses the topological distance again.

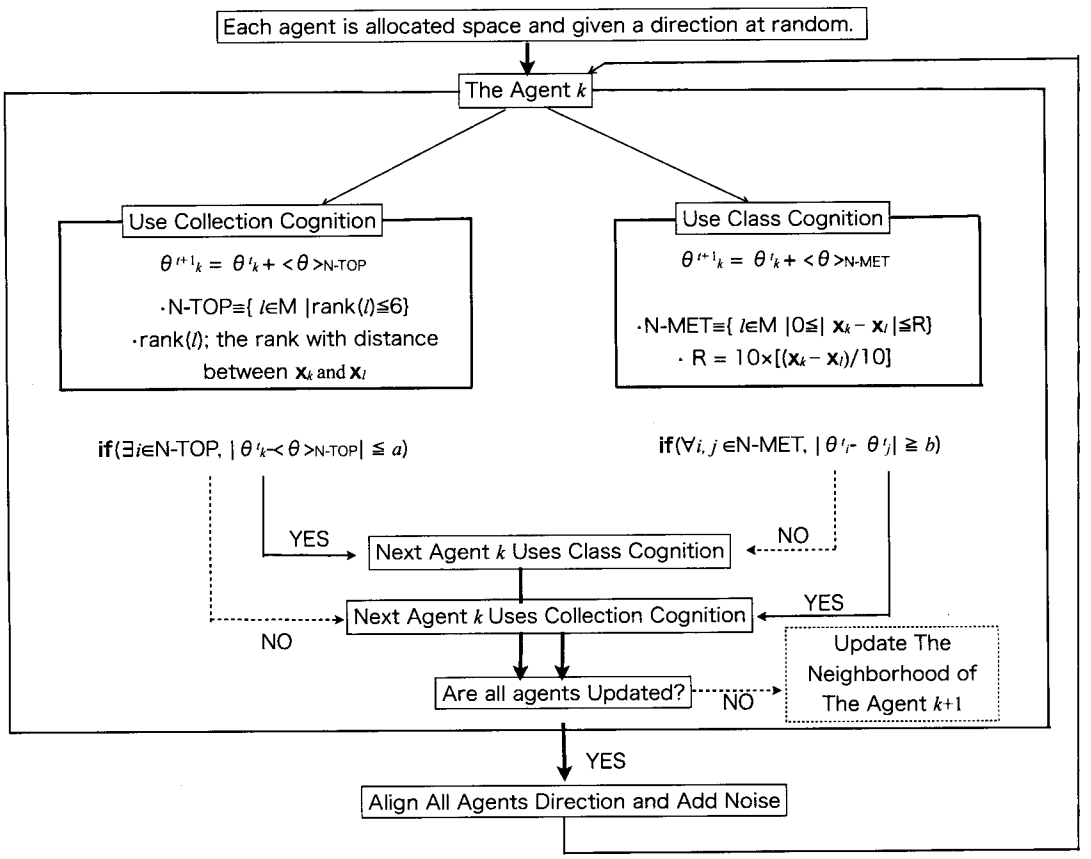

Figure 2.1. Algorithm of the metric-topological interaction model. $\mathbf{x}_i^t$ is a position vector and θ_i^t is a angle of each individual. i is an index of each individual. t is a time step. $\langle\rangle_S$ means to take average of directions in set S. The model has only two parameters: a (the threshold for collection calculation) and b (the threshold for class calculation). At each time step, each individual decides whether to define its interaction neighbors based on the metric or topological distance.

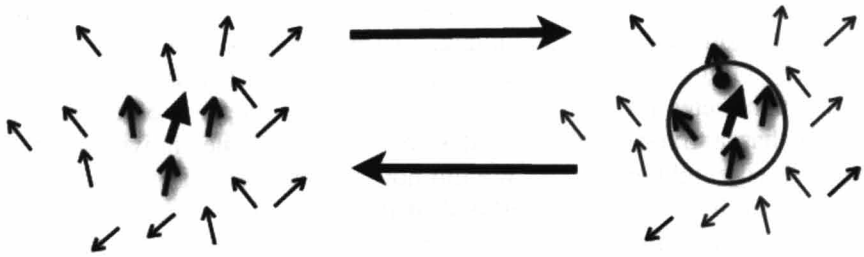

Figure 2.2. Depiction of the metric-topological interaction model. Initially, the center individual interacts with its 1^{st}-3^{rd} , for example, neighbors as defined by the topological distance (shown in shaded arrows). If the direction alignment of these neighbors is under a threshold a, the individual re-defines its neighborhood for next decision to be based on the metric distance. The right figure shows that the re-defined neighborhood, which contains new individuals (the arrow with circle). If the direction alignment of two individuals selected at random exceeds a second threshold b, the neighborhood is again re-defined, returning to the topological distance neighborhood shown in the left figure. Thus, an individual of the metric-topological interaction model can alternate between neighborhoods defined by the metric distance and the topological distance.

From this definition, we can consider that if a is higher, class cognition is favored over collection cognition. For example, the individual tends to use class cognition when a is high, meaning that individuals will behave like those of a metric-distance model. By contrast, if b is lower, then collection cognition is favored over class cognition, meaning that individuals will behave like those of a topological-distance model. Hence, these parameters are essential for the MTI model. The degree of ambiguity of the class (metric) and collection (topological) cognition is represented by these parameters and we can reproduce the behaviors of metric-distance and topological-distance models by tuning these parameters appropriately. For this reason, our MTI model can be considered as a hybrid of the metric-distance and topological-distance models. Here, we need to pay attention to the model that Hidenbrandt et al. proposed that treats the metric and the topological interaction. In their model, each individual can adjust its interaction range when its density of neighbors changes (Hidenbrandt et al., 2010). However, our hybrid model focuses on the degree of alignment (that is determined by the threshold parameter). We definitely distinguish two interactions that are the metric and the topological distance. The individual of our model can use only one interaction (the metric or the topological distance) in the same time, respectively.

2.3.2. Behavior of Abstract Flocking Model

Here we discuss the properties of our MTI model. First, we define the order parameter that estimates the degree of alignment of all individuals in the system

$$\varphi = \frac{1}{Nv}\left|\sum_{i=1}^{N}\mathbf{v}_i\right| \qquad (2.3.1)$$

The absolute value of each velocity is given by v, whereas N is the number of individuals in the system. The order parameter φ measures the degree of the alignment. If the directions of all individuals are nearly the same, φ is high. φ rises to 1.0 at a maximum when the directions of all individuals are perfectly aligned. At the other extreme, the order parameter is zero when the directions of the individuals are completely uncorrelated. Huth and Wissel call this order parameter "polarization" [59], a term we also adopt. φ decreases if the noise of each individual is high. We, therefore, define the noise parameter p as follows.

$$\Delta\theta = 2\pi p \qquad (2.3.2)$$

The individual behaves completely randomly if the noise parameter is set equal to 1.0. Using this definition, we compare the three models, that is, the metric-distance, topological-distance, and MTI models. Figure 2.3 shows the relation of the order parameters in these three models with the noise parameter for simulations of 20,000 time steps. We set the individual of the metric distance has a fixed neighborhood size of 100 and the individual of the topological distance has a fixed neighbors as six. We did not take the method of Voronoi neighbor for the topological distance [64]. The neighborhood of the topological distance is only determined by the rank of individual's distance [32, 33]. We set the parameters for the metric-topological interaction model as a=1.2 (radians) and b=1.2 (radians).

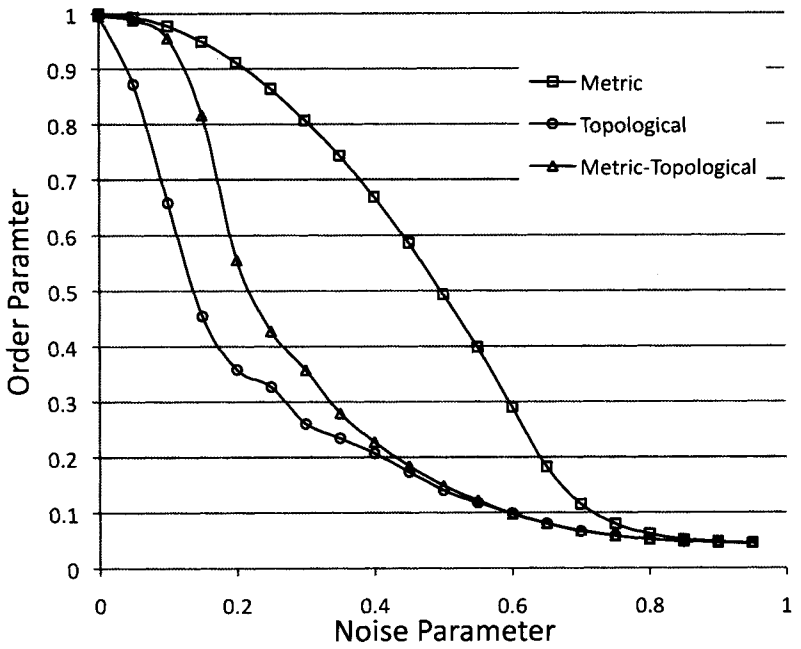

Figure 2.3. Dependence of the order parameter on the noise parameter in the metric-distance model (rectangular), the topological-distance model (circle) and the metric-topological interaction model (triangle). The number of individuals was 400 and the length of the space 1000. The order parameter of the topological-distance and metric-topological interaction models decreases more rapidly than that of the corresponding metric model.

In each model, the polarization tends to decrease as the noise parameter rises. Relative to the metric-distance model, both the topological-distance and the MTI model rapidly decrease. At high noise levels, the MTI model resembles the topological-distance model since the metric-distance neighborhood tends to break down in high noise. Next, we examine the behavior of each model at noise parameter 0.1.

Intermittency is a useful parameter to characterize the motion of the individuals as one flock, as done for the SPP model (metric distance) [76]. Intermittency corresponds to the sudden decay of polarization observed in a time series. When such a decay occurs, a flock of individuals divides into several flocks with different directions. However, after a certain time, the flocks rejoin into one flock and the system's polarization recovers. Intermittency, thus, is a measure of the collective motion in a single direction. Moving as one flock is an important property in understanding collective behavior.

(A)

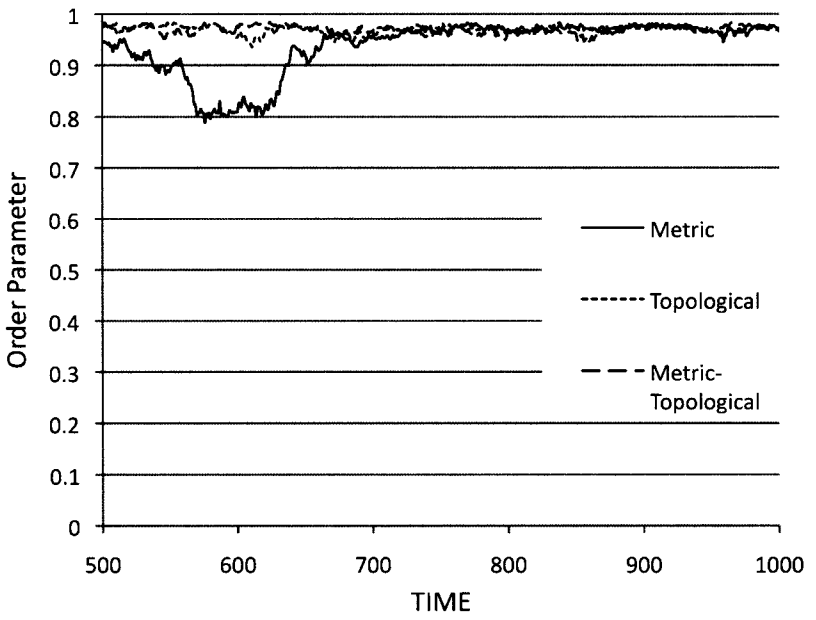
1
0.9
0.8
0.7
0.6
0.5
0.4
0.3
0.2
0.1
0
Order Parameter
500
600
700
800
900
1000
TIME
Metric
Topological
Metric-
Topological

(B)

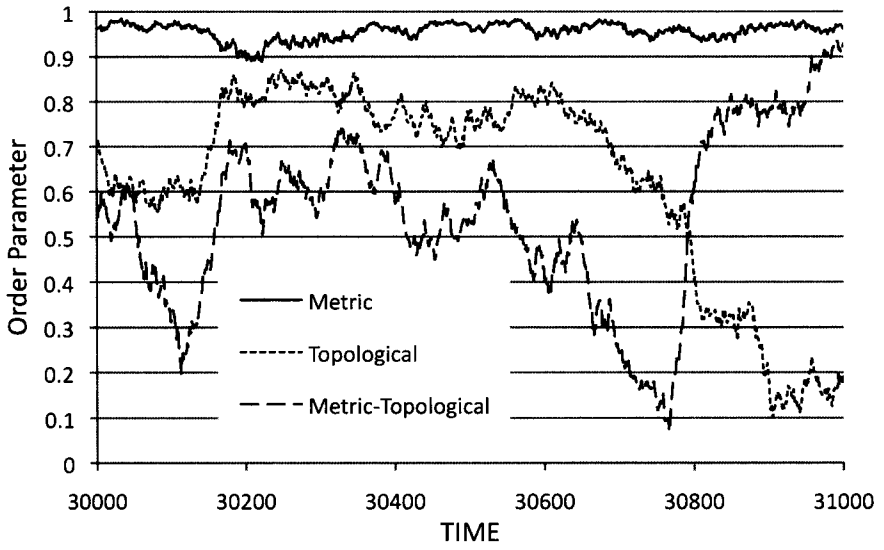
1
0.9
0.8
0.7
0.6
0.5
0.4
0.3
0.2
0.1
0
Order Parameter
30000
30200
30400
30600
30800
31000
TIME
Metric
Topological
Metric-Topological

(C)

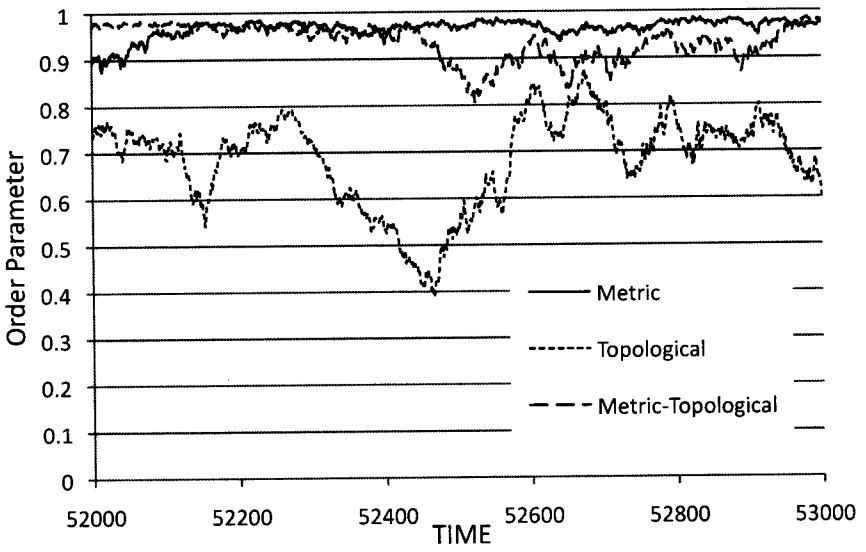

Figure 2.4. Time series of the polarization for the three models. The solid line corresponds to the metric-distance model, the dotted line corresponds to the topological-distance model, and the dashed line corresponds to the metric-topological interaction model. The neighborhood radius of the metric-distance model was set to 100, and the number of neighbors in the topological-distance model was set to six. The number of the individual is fixed 100.

The solid line in Figure 2.4 shows the time series of the polarization of the metric-distance model. The polarization shows a sudden decay and soon recovers from it. The individual of the metric distance has a fixed neighborhood size of 100, so the sum of neighborhoods for all individuals is significantly larger than the space (1000×1000). Hence, the metric-distance neighborhoods of the individuals overlap each other significantly, and for this reason, the polarization recovers quickly (Figures 2.4A, B, and C). Of course, the density of individuals plays an important role for the flocking behavior under the metric distance [25, 56, 57]. In this study, however, we focus on how to make flocks in a limited environment. We previously discussed the problem that a modeler adjusted a radius of the metric interaction when we used it. Therefore, what we should examine here is not the behavior of flocks under various densities, but the adaptability in a limited space.

By contrast, the flocks of the topological distance (dotted line in Figure 2.4A, B and C) align the same direction for the early steps, but the polarization hardly recovers over 0.9 even after 20,000 steps (Figure 2.4B). This lack of recovery stems from the neighborhood of topological distance. The individuals align their directions in early steps because of the interaction length is infinite (Figure 2.5A). The flock of the topological distance, however, cannot maintain this distance because the interaction range changes with the topological interaction. Once the individuals form small clusters, they are unlikely to decrease their density again (Figure 2.5B). These small but high-density clusters scarcely interact with each other because the interaction range of each individual is concentrated mostly within the cluster. Hence, these clusters rarely integrate into one flock. For comparison, clusters in the metric-distance model can easily interact with each other because every individual interacts with other individuals within its fixed neighborhood no matter how many individuals lie within. In a metric-distance model, a flock can have a high density and still interact with other flocks (Figure 2.5C); hence, it is easier to integrate the flocks of a metric-distance model into one flock compared with those of a topological-distance model.

(A) (B)

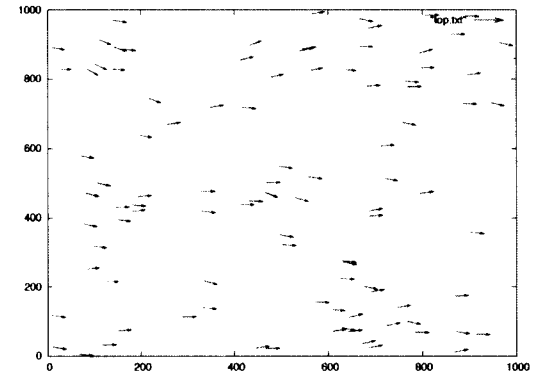

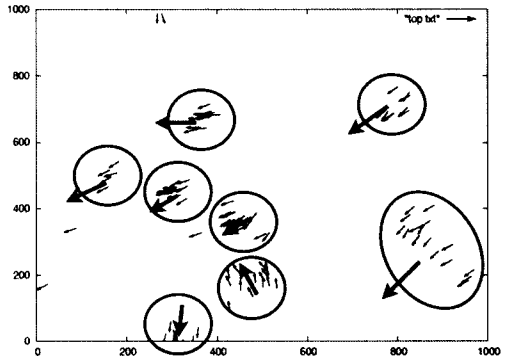

(C)

(D)

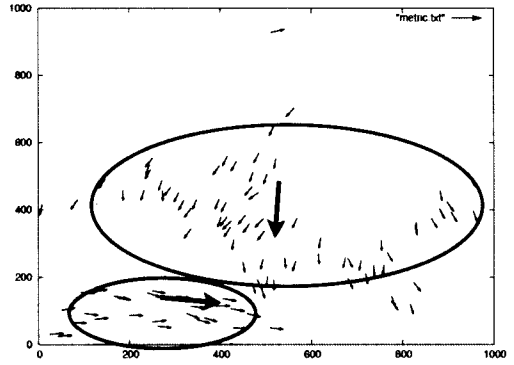

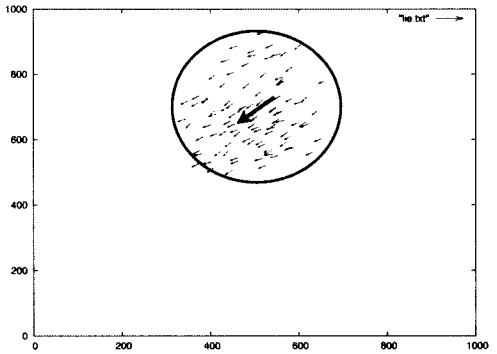

(E)

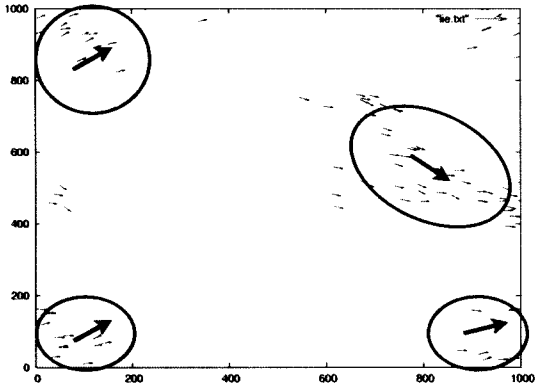

Figure 2.5. (A) State of a topological-distance system after 1,000 steps. In such early stages, all three models behave in nearly the same way. (B) State of a topological-distance system at 42,300 steps. The individuals form small clusters and their polarization is 0.725. (C) State of a metric-distance system at 27,775 steps. The polarization is 0.721. Despite having almost the same polarization as the previous topological-distance system, the individuals form only three flocks. (D) State of a metric-topological interaction system at 52,200 steps. The individuals move as one flock and maintain this flock by adjusting their neighborhood. (E) State of a metric-topological interaction system at 31,000 steps, showing several flocks.

The MTI model (dashed line in Figure 2.4) exhibits both behaviors of the metric-distance and topological-distance models. (We set the parameters a=1.2 (radians) and b=1.2 (radians), respectively, in Figure 2.1) Large and small intermittencies occur repeatedly (Figure 2.4C). Unlike the topological-distance model, clusters in the MTI model do interact significantly with other clusters. To see the detail of the MTI model, Figure 5D shows the individuals at 52,200 steps (Figure 2.4C); the individuals form one flock and move as one aggregation. In this case,

this flock lasts about 300 steps. The flock maintains its unity as in the metric-distance model by adjusting the interaction neighborhoods. For comparison, Figure 2.5E shows its state at 31,000 steps (Figure 2.4B) when the polarization is 0.2, indicating that there are several flocks moving in different directions. This state resembles the behavior of the topological-distance model. Hence, the MTI model exhibits both properties, that is, moving as one flock and dividing into several flocks. From this simulation, individuals of the MTI model show more dynamical flocks (dividing, uniting, keeping one collective) under a given space without determining each neighborhood in advance. The state of a MTI model is more dynamic than those of the metric- and topological-distance models.

Next we examine the changes in the flock behavior due to tuning the parameters, i.e., the thresholds for class and collection cognition. To characterize the integrating and dividing flocks, we define the "flocking duration" and the "recovery time". The duration time is defined as the mean time for which the polarization is over 0.9. If the polarization is over 0.9, almost of all individuals are aligned in a similar direction; thus, we deem the individuals to move as one flock when the polarization is over 0.9. The recovery time is defined by the mean time for which the polarization is under 0.9, which characterizes the time required for divided flocks to re-integrate into one flock. Figure 2.6A shows the relation among class cognition (metric distance), collection cognition (topological distance), and flock duration. Evidently, class cognition plays an important role in determining the duration time. As class cognition becomes more significant, the duration time becomes longer, because the system behaves like a metric-distance model when class cognition predominates. The same reasoning applies to the recovery time (Figure 2.6B). Flocks rarely divide into several flocks because the neighborhood of each individual overlaps so much with those of the other individuals in the flock. Both figures divide into three areas, which are colored white, gray, and black. In the black areas, the system behaves like a topological-distance model, whereas systems in the white area behave as metric-distance models. The distinctive behavior of the metric-topological interaction model discussed in Fig 2.4 is identified with white areas. Systems in this area have properties both of the metric- and topological-distance models. In this gray area, it observed the tendency that individuals never showed converging into one flock nor getting into several peaces, but supported both patterns at the same time in a given space. This is because of the ability of changing neighborhood for MTI model. By tuning the parameters of class and collection cognition, we can obtain behaviors of both the metric- and topological-distance models from a single hybrid model.

(A)

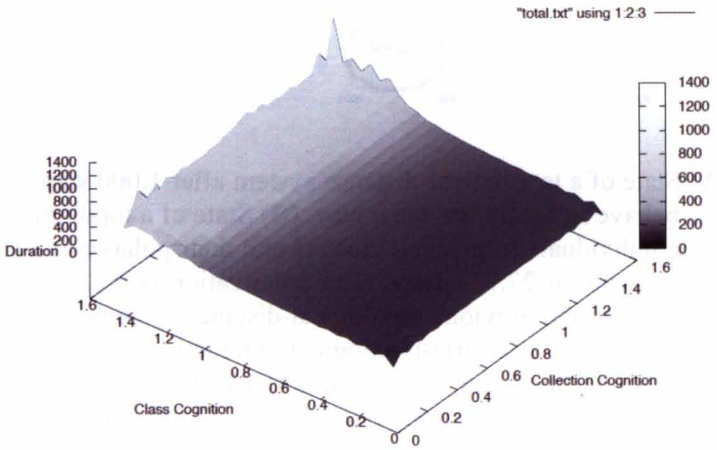

(B)

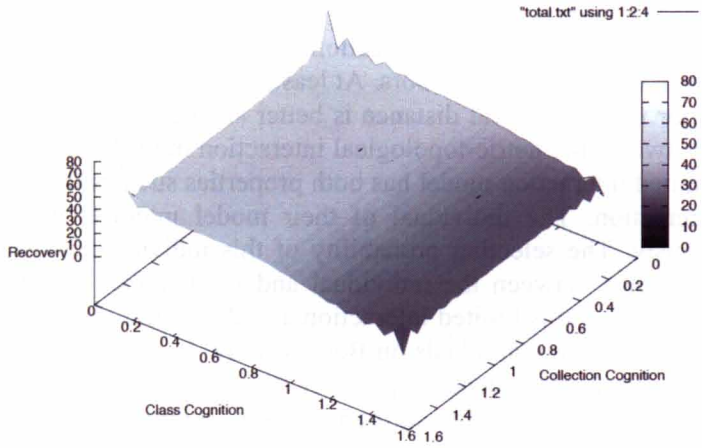

Figure 2.6. Relative effects of class and collection calculation on the duration (A) and recovery time (B). The system resembles a metric-distance model in the white area and a topological-distance model in the black area. The flock duration (A) and recovery time (B) show a tendency to increase and decrease, respectively, as class calculation becomes dominant, i.e., as the metric-distance model predominates. Systems in the white areas are intermediate, exhibiting properties of both limiting models. We take 100,000 steps for this simulation. The number of the individuals is fixed 100.

2.3.3. Discussion

Although we have pointed out the differences between the metric-distance and topological-distance models, we have also pointed out that these models have a strong connection in nature. In the metric-distance model, the individuals have a fixed limit of perception, corresponding to their interaction neighborhoods, which the researcher defines in advance. Outside of this neighborhood, individuals do not interact with each other. Analogously, in the topological-distance model, the perception limit is defined by the number of neighbors. We showed that the two models can be viewed as uncertain versions of each other, either as a metric-distance model with an uncertain neighborhood or as a topological-distance model of uncertain number of interacting neighbors. We pointed out that the researcher creating a model cannot avoid such uncertainties.

We took a positive evaluation against this problem of the uncertain neighborhood. Therefore, we adopted a different approach by re-casting this uncertainty in terms of class and collection cognition. To use these terms, we emphasize the aspect of the ambiguity of the cognitions, which is the class and the collection cognition, when the individual recognizes his environment. The interdependency of two cognitions makes individuals switch between the metric and the topological interaction. The individual of our hybrid MTI model decides the nature of its neighborhood "on the fly" at each time step, switching between the metric-distance and topological-distance. In the MTI model, neither the neighbors nor the neighborhoods are determined by the researcher in advance. Not to determine each neighborhood beforehand, each individual can adjust a size of his neighborhood where he is. The MTI model shows that the flock divides into several flocks or unites into one large flock because each individual can change his neighborhood flexibly against his environment. This behavior would not observed for the model of pre-determined neighborhood such as metric or topological distance.

Our hybrid model behaves like the metric-distance model when the individuals within a neighborhood are well-aligned; this corresponds to our notion of class cognition. By contrast, the hybrid model behaves like a topological-distance model when individuals differ significantly from their neighbors, i.e., when individuals exhibit less coherent motion than in the metric-distance model; this corresponds to our notion of collection cognition. The two limiting cases differ only in the relative balance between class and collection cognition. It should be also emphasized that the difference between the metric distance and the topological distance is relative; they represent only two limiting cases of the same perception. The MTI model, therefore, is a hybrid model, intermediate between the metric-distance and topological-distance

models on taking account of previous studies [25, 28, 32, 33, 61].

Constant switching between class and collection cognition makes the individuals possible to overcome the problem of uncertain neighbors. At least, we can suggest one approach of whether the metric distance or the topological distance is better should be tabled. It is a worth to point out the difference between the metric-topological interaction model and the model of Bode et al [62, 63]. Bode's limited interaction model has both properties such as the metric interaction and the topological interaction. The individual of their model interacts with one neighbor and updates asynchronously. The selecting probability of this individual is decreased in inversely proportional to a distance between the individual and its neighbor [62, 63]. The topological interaction is represented by this limited interaction and the metric interaction is represented by the selecting probability of the individuals on Bode's study. In contrast, the interaction range of the MTI model is not purely this stochastic property (the interacting individual is determined by the probability) but is determined by surrounding his environment. The randomness only emerges in the checking the neighborhood (class congnition) of the individual. Moreover, we confirmed that an individual took one set from several individuals or he differentiated independent individuals from one aggregation. The MTI model never only mixed the metric distance with the topological distance, but also deeply related to the animal's cognition. These attitudes, which are the randomness of the interaction and the cognition of the individual, are a main difference between Bode's model and our model.

2.4. MTI model in Two-Dimension

2.4.1. To approach a real collective behavior

In this section, we consider more realistic case for the collective behavior. See Figure 2.7A and 2.7B, which show the rough sketches of the MTI model. An individual using the MTI model determines its neighborhood by switching between two different but related neighborhoods, defined by the metric distance and the topological distance. Figure 2.7A shows the topological neighborhood, and Figure 2.7B shows the metric neighborhood. When the green individual uses the topological distance, the central individual aligns its direction to coincide with the average of the directions of the yellow individuals. The yellow individuals comprise the topological neighborhood around the central individual. On the other hand, the metric neighborhood (Figure 2.7B) is quite different. This is the main different point from previous section (abstracted model). We added more two zones, the attraction zone (colored blue) and the repulsion zone (colored red), to the alignment zone (colored yellow). We chose these interaction zones based on the model that was proposed by Huth et al. and other researchers [28, 55, 59, 60]. The attraction zone is shown in blue, meaning that the central individual is attracted to the blue individuals who are in the blue area. A blue individual, in other words, is a target of the central individual, who tries to approach him. The alignment zone is shown in yellow, meaning that the central individual aligns himself with the yellow individuals who are in the yellow area. Although these two interactions, which are the metric and the topological interaction, are quite different, an individual of the MTI model can switch between the two dependent on the behavior of its neighbors. In this section, we firstly give the explanation for the way of the computation of two interactions. Next, we discuss the switching algorithm of MTI model and the variation of speed for each individual.

(A) (B)

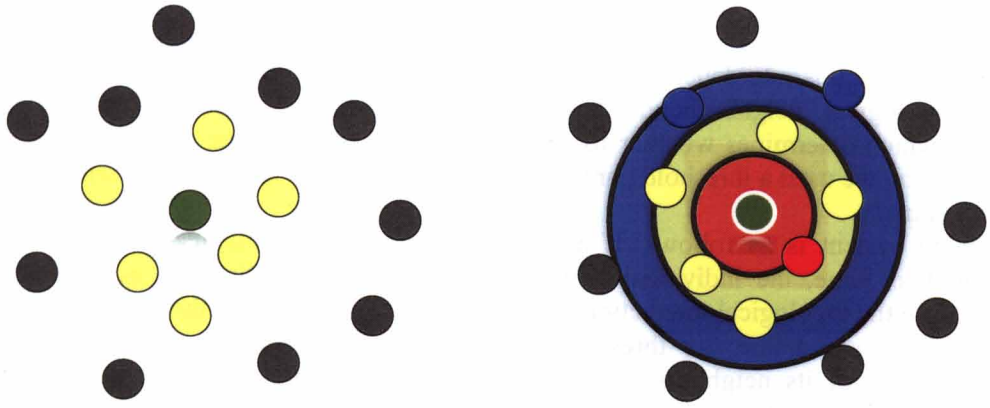

Figure 2.7. The image of the metric-topological interaction model. A corresponds to the topological distance, and B corresponds to the metric distance. The red zone of Figure 2.7B corresponds to the repulsion zone, the yellow zone of Figure 2.7B corresponds to the alignment zone, and the blue zone of Figure 2.7B corresponds to the attractive zone. Each individual of the MTI model switches between these two interactions, which are shown in Figure 2.7A and 2.7B, based on the behavior of its neighbors.

First, we consider the topological interaction (Figure 2.7A). The definition of the topological interaction is not yet settled. Ginelli and Chaté, for example, define the topological neighbors as Voronoi's tessellation [64], whereas Bode et al. interpreted the topological interaction as the limited interaction [62, 63]. Sometimes, the density-dependent interaction is also regarded as the topological interaction [68, 69]. In this study, we use the simple rule that each individual can interact with the nearest six neighbors when that individual is using the topological interaction. Thus, the direction of the individual for the next step is given by the following equation:

$$\hat{\mathbf{v}}_k^{t+1} = \hat{\mathbf{v}}_k^t + \frac{1}{(n_T)_k^t} \sum_{l \in N\text{-}TOP_k^t} \hat{\mathbf{v}}_l^t \qquad (2.4.1)$$

In this equation, k is the index of each individual, and t is the time step of the simulation. We described this condition as the symbol $(\text{-})_k^t$. $\hat{\mathbf{v}}_k^t$ is the unit velocity vector of individual k when the time step is t. $N\text{-}TOP_k^t$ is the set of individual k's topological neighbors, which are its six nearest neighbors at time t. $(n_T)_k^t$ is the number of elements of the set $N\text{-}TOP_k^t$. In this paper, we set $(n_T)_k^t = 6$, and we define (2.4.1) as the topological interaction.

Next we consider the metric interaction (Figure 2.7B). In Figure 2.7B, there are three layers of interactions, which are the repulsion, the alignment and the attraction zones. We add up all directions that are determined by these three zones. Thus, the direction of the individual for the next time step is given by the following equation:

$$\hat{\mathbf{v}}_k^{t+1} = \hat{\mathbf{v}}_k^t + \frac{1}{(n_{Rep})_k^t} \sum_{l \in (N-MET_{Repulsion})_k^t} \frac{\mathbf{x}_k^t - \mathbf{x}_l^t}{\left\|\mathbf{x}_l^t - \mathbf{x}_k^t\right\|} + \frac{1}{(n_{Align})_k^t} \sum_{l \in (N-MET_{Alignment})_k^t} \hat{\mathbf{v}}_l^t + \frac{1}{(n_{Attra})_k^t} \sum_{l \in (N-MET_{Attraction})_k^t} \frac{\mathbf{x}_l^t - \mathbf{x}_k^t}{\left\|\mathbf{x}_l^t - \mathbf{x}_k^t\right\|} \qquad (2.4.2)$$

In this equation, k is the index of each individual, l is the index of each interacting neighbor of the individual k, and t is the time step of the simulation. $\hat{\mathbf{v}}_k^t$ is the unit velocity vector of individual k when the time step is t. $\mathbf{x}_k^t$ is the position vector of individual k when the time step is t. $\|\text{-}\|$ represents the norm of the vector. The expressions $(N\text{-}MET_{Repulsion})_k^t$, $(N\text{-}MET_{Alignment})_k^t$, and $(N\text{-}MET_{Attraction})_k^t$ are the sets of the individuals in the repulsion, alignment, and attraction interaction zones, respectively, and $(n_{Rep})_k^t$, $(n_{Align})_k^t$, and $(n_{Attra})_k^t$ are the number of elements for these each set.

Next, we discuss the timing of switching between the metric and the topological interaction. An individual using the MTI model can choose only one type of interaction, either topological

or metric, per time step. The switching operation is based on the class-collection (metric-topological) interdependence of the MTI model that we discussed in the previous section. We can relate this interdependency to the individual's ability to transition between the metric and topological neighborhoods because the individual is affected by its past neighborhood, which determines whether its interaction range is the metric or the topological distance. Therefore, we used a threshold parameter to determine when an individual will change its interaction domain.

The switching system is as follows. If an individual uses the topological distance for a sufficient length of time, the individual will have almost the same direction as its nearest neighbors because the topological interaction always leads him to align with them (see Equation (2.4.1)). Therefore, we define the threshold parameter, a. If the difference between the individual directions of its neighbors and the average of neighbors' direction is under the threshold parameter, the individual of interest changes its interaction domain to the metric distance. Thus, the condition for switching from the topological to the metric interaction is;

$$\forall\ i \in N\text{-}TOP_k{}^t,\quad \cos^{-1}(\langle \hat{\mathbf{v}}_i^t, \langle \hat{\mathbf{v}}_l^t \rangle_{l \in N\text{-}TOP_k^t} \rangle) < a \qquad (2.4.3)$$

$\langle\ \rangle_{N\text{-}TOP_k^t}$ indicates the mean value for elements of a set $N\text{-}TOP_k{}^t$, while <, > signifies the operator of the inner vector. This equation represents the individual transitions to the class cognition from the collection cognition when its neighbors seem to behave almost identically. This transition is consistent with the definition of the class cognition.

When an individual switches to metric interaction, that individual must prepare the sizes of its interaction domains for the metric interaction. These domains, which are the repulsion, alignment, and attraction zones, are determined by the distance between the individual of interest and its topological neighbors. First, we check the distance between the furthest neighbor, the sixth neighbor in this case, and the individual of interest. The distance between them determines the three interaction domains. Concretely, each individual takes three interaction zones as follows.

$$\#_k^t = \begin{cases} [(\|\mathbf{x}_k^t - \mathbf{x}_s^t\| - \mathrm{R}^2_{\min})/5] & \text{when } \|\mathbf{x}_k^t - \mathbf{x}_s^t\| - \mathrm{R}^2_{\min} > 0 \\ 0 & \text{otherwise} \end{cases} \qquad (2.4.4)$$

$$\begin{aligned} (\mathrm{R}_1)_k{}^t &= \mathrm{R}^1{}_{\min} + r \times \#_k^t \\ (\mathrm{R}_2)_k{}^t &= \mathrm{R}^2{}_{\min} + al \times \#_k^t \\ (\mathrm{R}_3)_k{}^t &= (\mathrm{R}_2)_k{}^t + at \times \#_k^t \end{aligned} \qquad (2.4.5)$$

$\#_k^t$ is a positive integer that is determined by the distance between the individual of interest (indexed k) and the furthest neighbor (indexed s). [] is the floor function. $\mathrm{R}^1{}_{\min}$ and $\mathrm{R}^2{}_{\min}$ are the minimum range when $\#_k^t$ is zero. r, al, at are the parameters of the proportional constant. All parameters are listed on Appendix A. Equations (2.4.5) correspond to the three interaction zones. In other words, the interval $[0, (\mathrm{R}_1)_k{}^t]$ is the repulsion zone, $[(\mathrm{R}_1)_k{}^t, (\mathrm{R}_2)_k{}^t]$ is the alignment zone, and $[(\mathrm{R}_2)_k{}^t, (\mathrm{R}_3)_k{}^t]$ is the attraction zone. There is no attraction zone when # is zero.

Next, we consider the switching property for the metric interaction. The individual always verifies whether or not the metric interaction is well defined by considering two of its neighbors who are randomly selected from among other individuals in its metric neighborhood. Then, individual assesses the difference of the directions between these two neighbors. Here, we recall the definition of the class cognition. The class cognition was defined as the abstraction of a single notion from the differences of objects. The abstraction, however, never fits its definition anymore when objects in the notion conflict with each other. Thus, an individual who uses the class cognition must always check its neighbors to verify whether the class cognition is being used appropriately. Conflict between the class and the collection cognition corresponds to large differences in direction between the neighbors that are being compared. Therefore, we set the threshold parameter b in the case of the class cognition. The individual switches its neighborhood to the topological neighborhood when the difference between the directions of

two randomly selected individuals within its metric neighborhood is over the threshold parameter b or, in other words, when the individual cannot keep the class cognition under the threshold parameter any longer. Thus, the switching condition from the metric to the topological interaction is given as follows;

$\forall i, j \in (N\text{-}MET_{Repulsion})_k^t \cup (N\text{-}MET_{Alignment})_k^t$
(i and j are randomly selected from the set $(N\text{-}MET_{Repulsion})_k^t$ or $(N\text{-}MET_{Alignment})_k^t$)
$\cos^{-1}(\langle \hat{\mathbf{v}}_i^t, \hat{\mathbf{v}}_j^t \rangle) > b$ (2.4.6)

The individual, after switching to the topological neighborhood, aligns its directions with the nearest six individuals to construct the metric neighborhood again (using the Equation (2.4.1)). We can tune these parameters to observe the various flocking behaviors. Tuning these threshold parameters is equivalent to determining whether the individual prefers to use the collection or class cognition. In this paper, we set these two parameter as one parameter, that is $a=th$, $b=th$ for two dimension and $a=th$, $b=2*th$ for three dimension. We set these parameters to fit experimental results for following section.

Finally, we also add velocity variation to the three-dimensional MTI model. If we consider the flocking behavior in two dimension, we fixed the speed as the constant. However, most fascinating collective behaviors, such as flocking birds or schooling fish, are in three dimensions. By adding velocity variation, we hope to gain deep insight into this collective behavior. The definition of the velocity variation is very simple and is given as follows:

$$v_i^{t+1} = V_0 - V_+ \cos(\theta) \quad (2.4.7)$$

θ_i^t is the angle for the polar coordination (v_i^t, φ_i^t , θ_i^t) for an individual i when the time is t. Each velocity (scalar quantity) v_i^{t+1} is determined by the angle for the perpendicular axis. This means that the speed of each individual is affected by the gravitation. V_0 shows the velocity when the individual moves horizontally. The minimum speed of each individual is given as $V_0 - V_+$ when the individual goes up perpendicularly. The maximum speed of each individual is given as $V_0 + V_+$ when the individual descends perpendicularly. This formula indicates that the velocity changing of the individual is always connected to its direction. Thus, it is natural to define the intensity of speed in a way that has some connection with the direction changing. Some researchers consider this gravitational effect to the individual in the flock [68, 69].

Therefore, from (2.4.1) - (2.4.7), the direction vector of each individual is given as the following:

$$\mathbf{v}_k^{t+1} = v_k^{t+1} \hat{\mathbf{v}}_k^{t+1} \quad (2.4.8)$$

In this way, the next state of all individuals is determined. We summarize the algorithm in the Appendix A section. We set the boundary condition is periodic one. However, there is no essential difference of our results between them (for example, reflection one).

2.4.2. Role of Two Interactions in the MTI flock

Simulations of this model show that the spontaneous direction can change without noise (Figure 2.8). The direction change is used to show that the noise of each individual causes the flock's direction to change. Couzin's model also included noise for each individual [28]. Most models of flocking or schooling behavior have used individual noise that is unrelated to explain the various formations and the various motions of collective behavior [28, 55, 59, 60, 78]. It is worth pointing out that the rapid direction changing of the metric-topological interaction model is not explained by the external noise model because the external noise model states that each individual has a different direction for the external noise but almost all of the differences in each direction are cancelled by averaging their directions. The rapid direction changing does not only require a difference in the direction of each individual, but it also requires a certain consensus of the whole direction. Each individual of the metric-topological interaction model has a different

neighborhood. In other words, the differences in the range of the repulsion, alignment, and attractive zones makes the entire motion change directions. This difference in the neighborhood ensures both of the requirements; that is, the differences in each individual's direction and a certan consensus of the whole direction. This phenomenon cannot be explained by the model that has randomly distributed areas for each individual, that is, for the repulsion zone, the alignment zone, and the attractive zone. Therefore, this result shows that the flock as a one whole should be effected for its past neighborhoods. This fact is consistent with the results of Couzin et al. in 2002 [28].

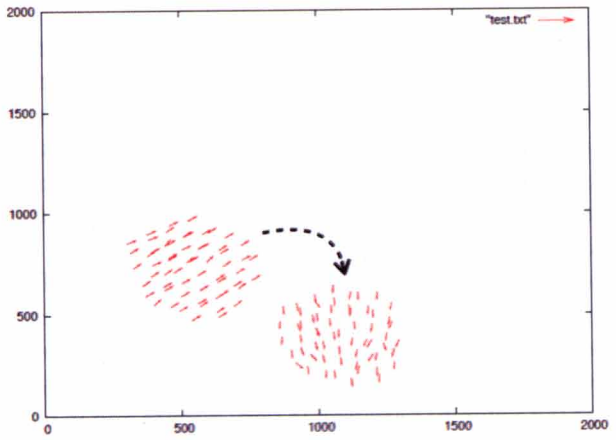

Figure 2.8. The flock of the MTI model rapidly changes their direction (nearly 90°) in 200 steps.

Next we examined the contribution of switching behavior of each individual to the flocking behavior as one collective. In other words, each individual stops switching between the metric and the topological interaction and keeps using the metric interaction, which is obtained by Equation (2.4.4) and Equation (2.4.5), when they move as one collective. Figure 2.9 shows the lifetime of moving one flock for the normal MTI model and the MTI model which stopped adjusting its interaction (only using the metric interaction). Blue bars correspond to the normal MTI model and red bars correspond to the MTI model without adjustment. Clearly, we can observe that there is a difference between them. The flock of the MTI model without adjustment collapses within 7,000 steps. About 70% of the flocks never survive if each individual stops switching two interactions on the way. On the other hand, the lifetime of the MTI flock is longer than the MTI flock without adjustment. Switching behavior between two interactions prevents the flock collapsing.

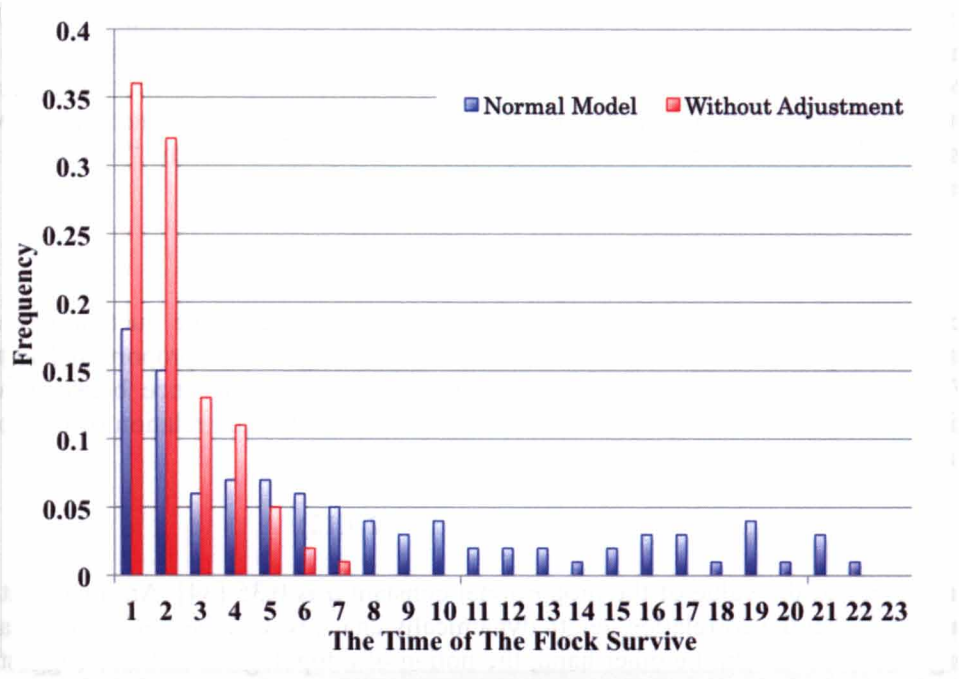

Figure 2.9. A comparison of the MTI model and the MTI model without adjustment between the class cognition and the cognition as a collection. The number of the individuals of the flock is fixed at 100.The horizontal axis is the number of steps for which the flock does not collapse. The vertical axis is the frequency. The red bar is the MTI model without adjustment between the class cognition and the collection cognition. The blue bar is the MTI model. We observed one flock that was moving and rounding as a single aggregate up to 22000 steps. We examined this simulation 500 times for each case and made a histogram every 1000 steps. The flock of the MTI model without adjustment collapses before 2000 steps have passed. On the other hand, for the normal MTI model, there is a flock that survives up to 22000 steps.

2.4.3. Scale-free Correlation in Real flocks

Next, we examine the scale-free correlation of the MTI model. The scale-free correlation is measured by using the correlation function defined by Cavagna et al. [34]. We define the fluctuation vector before we define the correlation function. The fluctuation vector $\mathbf{u}_i$ is given by subtracting the average of the whole velocity vector from each individual's velocity vector $\mathbf{v}_i$ (i is the index of each individual).

$$\mathbf{u}_i = \mathbf{v}_i - \frac{1}{N}\sum_{k=1}^{N}\mathbf{v}_k \qquad (2.4.9)$$

where N is the number of individuals in the flock. To compute each fluctuation vector, we obtain more interior information for the flock. In other words, the fluctuation vector shows the direction of the bias of each individual in the flock to which they belong. Next, we define the correlation function $C(r)$.

$$C(r) = \frac{\sum_{ij}\mathbf{u}_i \cdot \mathbf{u}_j \delta(r - r_{ij})}{\sum_{ij}\delta(r - r_{ij})} \qquad (2.4.10)$$

The distance between each individual is given by r_{ij}. The delta function is defined by $\delta(r\text{-}r_{ij})=1$ if $r=r_{ij}$; $\delta(r\text{-}r_{ij})=0$, otherwise. Based on the research of Cavagna et al. [34], a real flock

with a finite size has a correlation function with a value of one at short distances, which decays with increasing r, and at last, the value of the correlation function becomes negative at large distances. This shows that the flock always has a correlation domain at short distances and an anti-correlation domain at large distances. The value of the correlation function monotonously decreases, so there is a distance of the noncorrelation. They called this the "correlation length". In other words, the equation must be satisfied as follows.

$$C(r = \xi) = 0 \qquad (2.4.11)$$

By calculating the value of ξ, we can see the distance over which the fluctuation vectors are correlated. Cavagna et al. showed that this "correlation length" was proportional to the flock size. Flock sizes are calculated by determining the maximum distance between two birds belonging to the flock. We represent the "flock size" as L; then the relation of the correlation length and the flock size must be satisfied;

$$\xi = aL \qquad (2.4.12)$$

For a real flock, the value of the proportional constant a is 0.35 [34]. An important point of this equation is that the correlation length dynamically changes with the flock size, regardless of how large the flock is. On the other hand, the notion of a topological distance suggests that an individual only interacts with its nearest seven neighbors. It seems that the notion of a topological distance has a gap with the correlation domain. Despite each individual only interacting with seven neighbors, each individual has larger domains of information sharing than that obtained using a topological distance. Figure 2.10 shows that the flock of the MTI model has a correlation domain corresponding to the fluctuating vectors. The flock can be divided into two parts, that is, the top domain of the flock points in the left direction and the bottom domain of the flock points to the right. The middle area of the flock corresponds to the un-correlated area because this area changed continuously for a series of steps. The metrc-topological interaction model shows these inclinations for flocks of other sizes and numbers of individuals. The SPPs model does not show that the correlation domain is clearly observed for one type of flock.

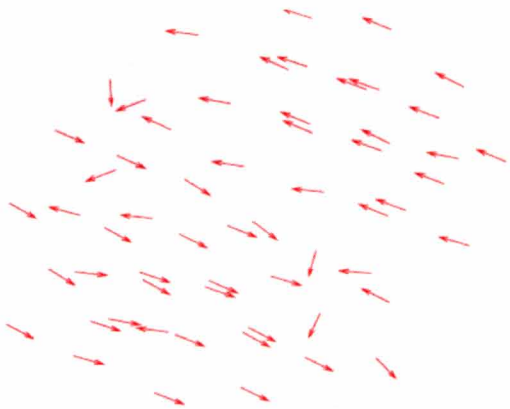

Figure 2.10. The fluctuation vector of the flock of the MTI model. The flock number is 60. The flock clearly has a correlation domain. The flock can be divided into two parts. The center of the flock is the area of non-correlation

We examined the relation between the correlation length and the flock size of the MTI model. We used periodic bounded conditions for all simulation, and the size of the space was set at 2000×2000. One example of the relationship between the correlation function and the distance is shown in Figure 2.11A. It confirms that the value of the correlation function gradually decreases in relation to the distance. The correlation function is obtained by checking where the correlation function first intersects with zero. In this case, the correlation length is 270 when the number of individuals is 100. We varied the number of the flock at n= 30, 40, 60, 80, 100 and

ran 100 simulations for each fixed number. Figure 2.11B shows the results of 500 simulations. The horizontal axis is the size of the flock, and the vertical axis is the correlation length. Figure 2.11B shows that the flock of the MTI model has a correlation between the correlation length and the flock size. It should be noted that the gradient that is given by using the method of least squares is 0.352. This value is almost the same value given in the empirical work of Cavagna et al. [34], that is, $a = 0.35$. The two dimensional MTI model, therefore, is considerably close to the behavior of a real flock in terms of the correlation of the fluctuation vectors. The method used for calculating the correlation function follows the method of Cavagna et al. The correlation length was examined for one flock. In other words, we did not take account separate flocks, as did Crizok et al. [57]. We also examined the scale-free correlation in a time series of a flock. The number of individuals in the flock is 100. The value of the correlation length is obtained from the average of the value of the correlation function for 1,000 steps. The flock lasted for 8,000 steps of the simulation, so we were able to collect 8 data points. We plotted the data in Figure 2.11C this way. The horizontal axis corresponds to the flock size and the vertical axis corresponds to the correlation length. The correlation length and the flock size are clearly correlated. The value of the proportional constant, a, is 0.35. This value is in good agreement with empirical results. It is worthwhile to point out that the flock size widely varies from 780 to 900. The individuals of the type-token model always make their neighborhood along with their environment. It may be that these properties of the MTI model are reflected in the scale-free correlation. We simulated other cases where we changed the numbers of individuals and obtained similar results from 100 times simulations, that is, 0.353±0.022.

(A)

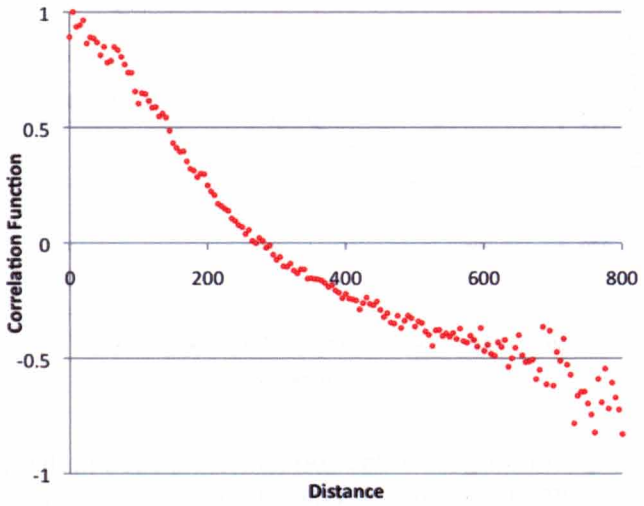

(B)

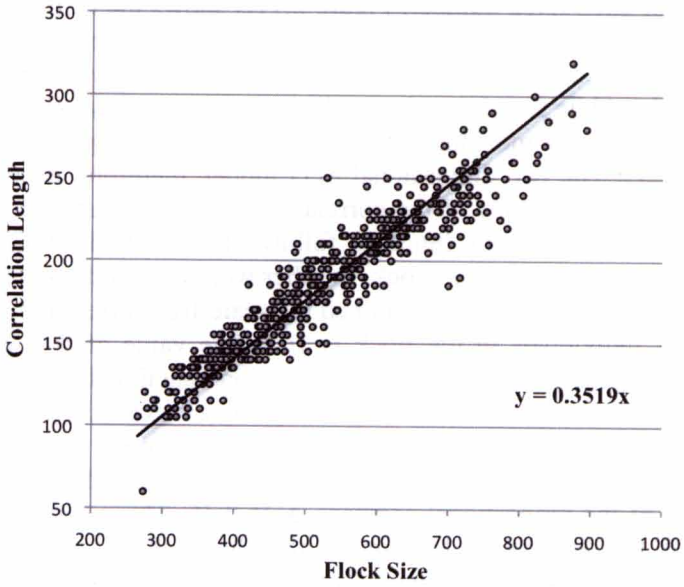

(C)

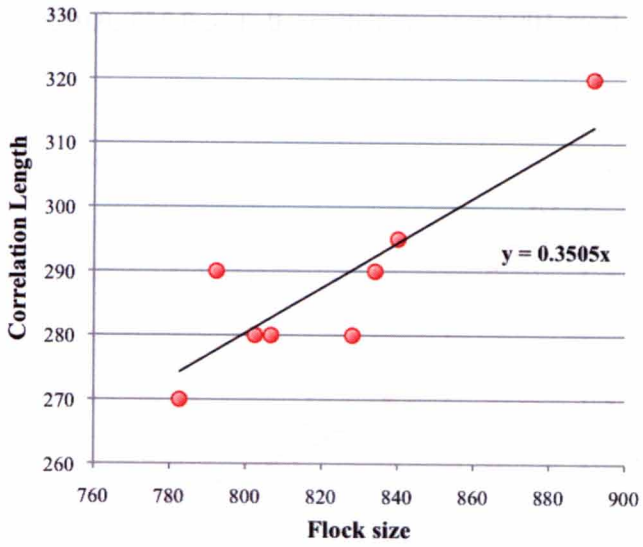

Figure 2.11. (A) Example of a figure of the correlation function in the flock. The number of individuals is 100. The correlation function gradually decreases its value and corresponds to the distance. The correlation length is given when the correlation function crosses 0 on the x-axis. In this case, the correlation length is 270. (B) The relation between the correlation length and the flock size. We ran 100 simulations for the number of the individuals n = 30, 40, 60, 80, 100, and the results are plotted on the above graph. The correlation length and the flock size are clearly correlated. It is remarkable that the proportional constant is 0.352 for the MTI model. This value is coincident with the empirical value. (C) The scale free correlation of the type-token model when the number of individuals is 100. The horizontal axis corresponds to the flock size and the vertical axis corresponds to the correlation length. The type-token model shows a correlation of 0.89 between the correlation length and flock size.

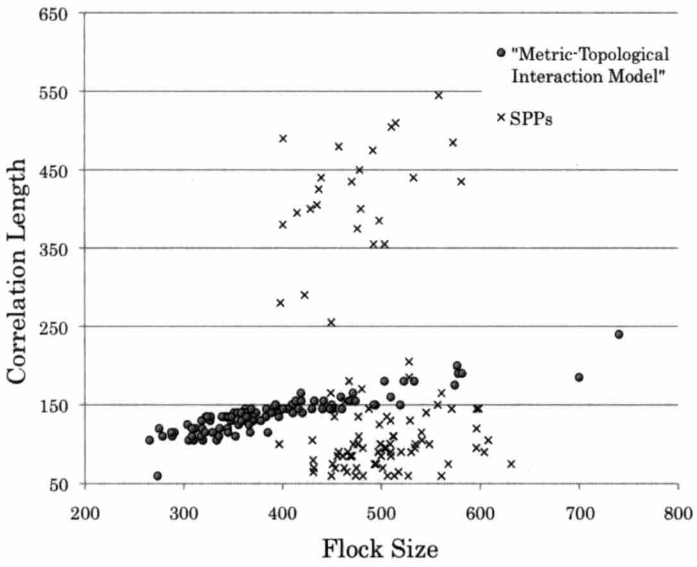

Figure 2.12. A comparison of the SPPs model and the MTI model for the relation between the correlation length and flock size. The number of the individuals of the flock is fixed at 30. The SPPs model has no correlation between the correlation length and flock size (its correlation value is -0.15). On the other hand, the MTI model shows correlation between the correlation length and flock size (its correlation value is 0.89). Furthermore, for the SPPs model, the size of the flock is restricted to a small region (400-600). The invariant interaction range does not allow for various flock sizes.

On the other hand, we want to consider the SPPs model. We compared the MTI model with the SPPs using the same conditions. The neighborhood of each individual in the SPPs model, which is the metric distance, is 100. The number of individuals is fixed at 30 for both models. The results are shown in Figure 2.12. The horizontal and vertical axes are the same as those in Figure 2.11B, C. The MTI model is well correlated. The SPPs model, however, shows that there is no correlation between the correlation length and the flock size. It can also be seen that the flock size of the SPPs model stays within a certain range, that is, 400-600. This occurs because the individuals of the SPPs model have an interaction range that is fixed. The fixed neighborhood cannot vary with the flock size. On the other hand, the flock size of the MTI model has a 2.5-times larger range than the flock size of the SPPs model. The individual of the MTI model continuously switches between the class cognition that is metric distance and the cognition as a collection that is the topological distance. Therefore, each individual has a different repulsion zone, alignment zone, and attractive zone; these differences in the neighborhood result in various flock sizes. Additionally, the gradient of the MTI model is 0.349. The MTI model, thus, has a scale-free correlation when the number of individuals is fixed.

2.4.4. Critical Property in the MTI model

2.4.4.1. Renormalization of the Fluctuation

The scale-free correlation suggests that high correlation domains of fluctuations always exist in flocks. Additionally, the range of the correlation domains is not dependent on flock size. In other words, the larger the size of correlation domains, the larger the flock size is. In a previous study, we showed that the MTI model succeeded in explaining the scale-free correlation in two- and three-dimensional simulations. From our simulation, there are always two highly correlated domains in the flocks.

A self-similarity, or fractal, is considered to be an important property when discussing the relation between parts and whole. The self-similarity suggests that a part of the structure contains the information about the whole structure. Therefore, it can sometimes be considered as a bridge between parts and whole. If we confirm that correlation domains in flock have this

kind of self-similarity, it could allow us to suggest that the tuning direction that is seemingly random to external observers, has a global meaning in flocks and results in large correlation domains such as scale-free correlation.

To evaluate this idea, we analyzed a flock with the MTI model by using a fluctuation vector. The fluctuation vector can be obtained by subtracting the average velocity vector from each individual velocity vector. In this section, we only consider the directional variance inside the flock. In other words, we only consider the direction of the fluctuation relative to the motion of the flock. This discrete information, left or right, is not an unnatural definition. Analogously, critical phenomena of a spin glass are constituted from up and down spin. In fact, collective phenomena are discussed in the context of statistical dynamics.

Figure 2.13 shows an example of renormalization for a flock under the MTI model. We apply renormalization five times for this flock. The upper-left of the flock in Figure 2.13 is represented by a velocity vector. The number of individuals is 300. The size of space is 2000×2000. The Unit length of this space is equal to a unit vector of an individual. We take the unit fluctuation vector (upper center in Figure 2.13) and divide this flock into three colors: red, green and blue. Red represents the largest correlated sub-domain in the flock. Green represents the second largest sub-domain in the flock. Blue corresponds to the rest of the flock.

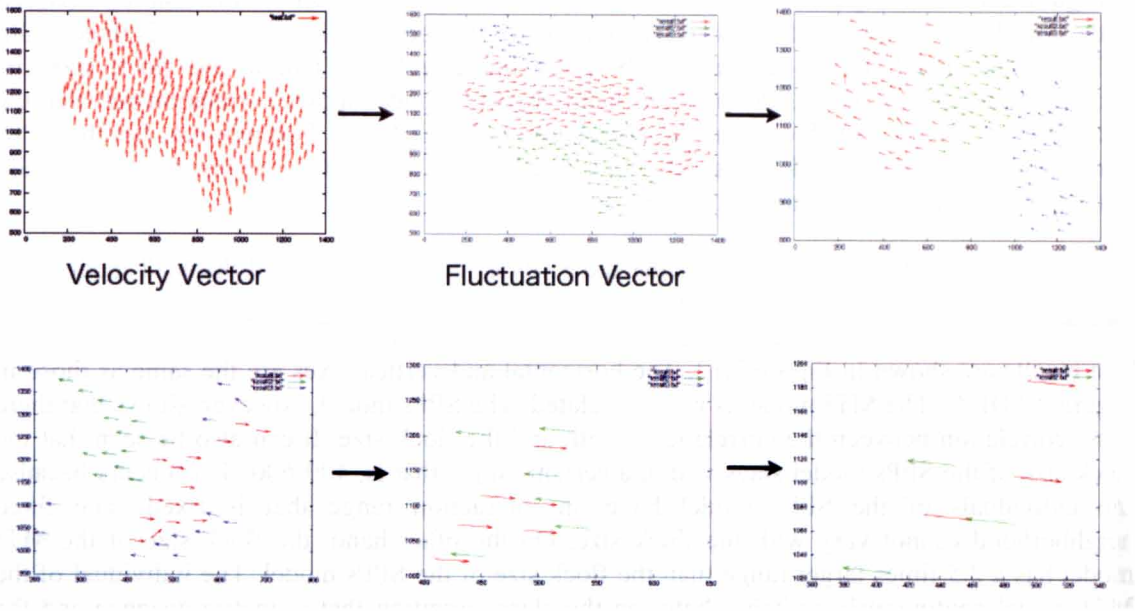

Figure 2.13. Successional renormalization for the MTI flock. The number of individuals is 300. Solid black arrows indicated application of one time renormalization. The red cluster is the largest correlation cluster; the green cluster is the second largest cluster, and blue represents the rest of the flock. The self-similar structure of correlation domains can be observed.

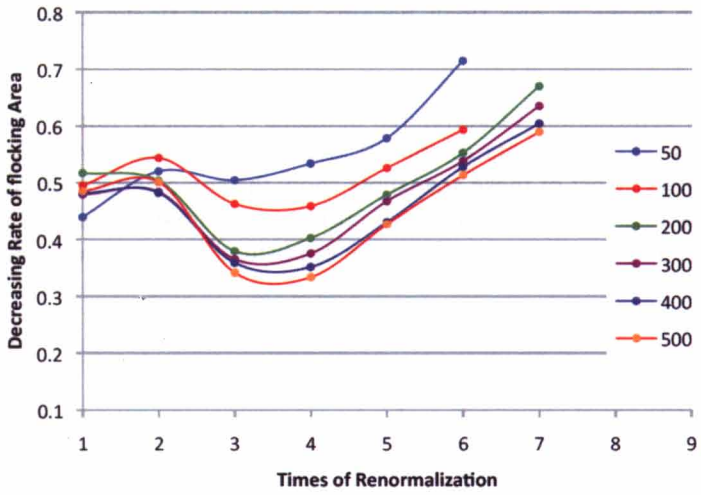

Figure 2.14. Decreasing rate of flocking as a function of renormalizations. Each color corresponds to the number of individuals (50, 100, 200, 300, 400, 500). For the first and second renormalizations, the rates of decrease show half the degree of flocking present before applying renormalization. For the third and fourth renormalizations, the rate of decrease drops to one-third.

We define clusters recursively: An individual belongs to a cluster C, which is colored red, for example, if it is within a certain radius (80 in our analysis) of any other individuals belonging to C. We focus on the red colored individuals, which are the largest cluster, and take the fluctuation vector again, which yields the data in the upper-right panel of Figure 2.13. It can confirm that there are large correlation domains inside of the red cluster of the upper-center in Figure 2.13. This fact suggests that the sub-flock of the red cluster shares different directional information, although it seems to have the same information for a single renormalization. Repeating this method five times, we reach the lower right of Figure 2.13. Large coherences never vanish until the last renormalization. This reveals a nested structure of correlated domains in a flock. Figure 2.14 shows a decreasing rate of a red cluster's area as a function of renormalizations. The flock's area is measured by using 25×25 lattices on a moving space of dimension 2000×2000. The number of individuals is 50, 100, 200, 300, 400 and 500. We selected a non-dividing flock and took an average rate of decrease in area, over 1,000 step intervals. The horizontal axis represents the number of instances of renormalization. There is the same tendency for all cases to display a rate of decrease of one half from the 1st to 2nd instances of renormalization, which suddenly decreases to 0.35 at upon a 3rd renormalization. Tails of the graph increase after the 4th renormalization because the relative number of individuals becomes large for the last few renormalizations. However, the size of the correlation domains is always greater than one third of the correlation domain before renormalization. Thus, the scale-free correlation is also applicable to correlated sub-flocks. This suggests that there is a self-similar structure of fluctuations in flocks.

2.4.4.2. Fluctuation induces split of flocks

In the previous section, we observed that flocks in the MTI model show a self-similar structure of fluctuations. This self-similarity suggests that directional tuning of each individual who tries to adjust its neighborhood results in global correlation domains such as scale-free correlation. Perpetual local alignments of each individual seem to behave randomly. However, each alignment always connects to the global correlated fluctuation, such as scale-free correlation. In this section, we will discuss the functionality of internal fluctuations contributing to flocking movements. We observed that MTI flocks showed scale-free correlation and that flocks were often divided into two highly correlated parts (colored red and green clusters) as shown in Figure 2.13. From many simulations, we observed that when flocks of the MTI model divided into two parts, splitting lines of flocks were mostly on line between two large correlated areas, which are colored as red and green individuals in Figure 2.13. In other words, these

highly correlated sub-flocks in one flock become individual flocks after the large flock has collapsed. If so, it is possible to consider that these correlated sub-flocks in one flock may have a partial impact on movements as independent flocks.

We investigate the contribution of correlated domains to flock dividing. We report the timing of flock dividing and take snapshots of the 30 steps before flock division. We consider 100 snapshots of MTI flocks. Most of these snapshots show the same pattern as Figure 2.15. In other words, the division is located between the two correlation domains which sizes are two largest domains respectively. These two clusters have the opposite direction of one another.

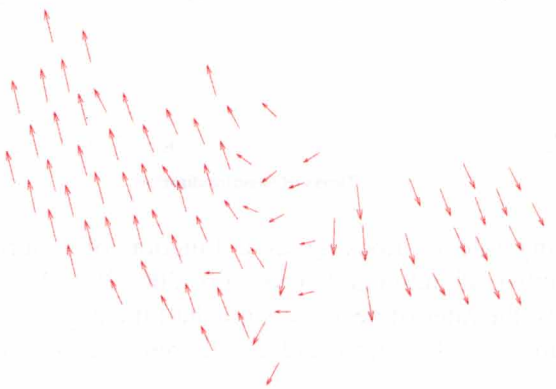

Figure 2.15. The state of fluctuation vectors for 30 steps before the flock divides.

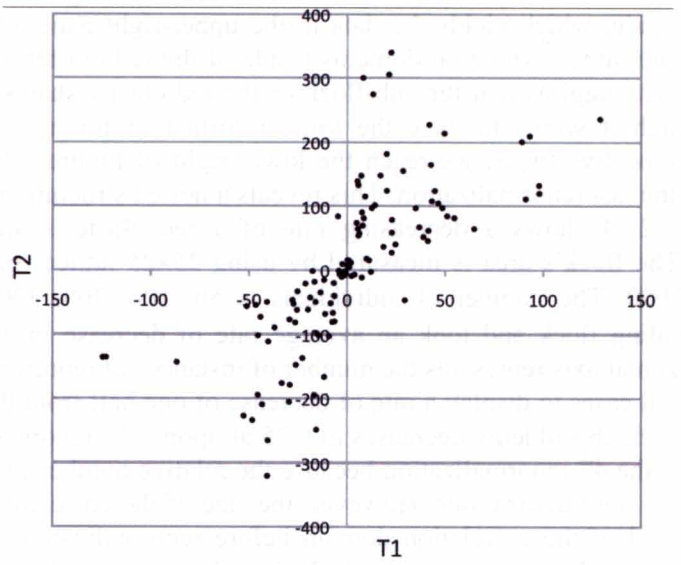

Figure 2.16. The relation between T_1 and T_2. T_1 is the torque of the largest cluster and T_2 is the second largest cluster. There is a positive correlation between (0.71) T_1 and T_2. This means that each sub flock rotates the same direction

Next, we investigated the torque between two correlated fluctuation vectors. Torque is one of the moments in physics that measures the tendency of a force to rotate an object. The magnitude of a torque is determined by three quantities, the force applied, the length of lever arm that connects an applied force to a basing point, and the angle between two. In this case, the force (F) corresponds to an average of an absolute value of fluctuation vectors in a cluster of interest. A lever arm length (r) is the distance between the center of mass of the whole flock and the cluster of interest. The angle (θ) is determined automatically after these procedures. Then, the torque (T) is

$$T = rFsin(\theta) \qquad (2.4.13)$$

The value of T indicates the strength of turning, and the sign of T indicates the direction of rotation. We take a torque for two correlated areas whose sizes are the largest and second largest clusters that are indexed 1 and 2. If the signs of T_1 and T_2 are the same, each sub flock rotates in the same direction. Figure 2.16 shows the relation between these two quantities (T_1 and T_2). There is a positive correlation (0.71) between T_1 and T_2. This suggests that the coordinated torques of correlated subparts leads to the flock dividing. These subparts become new flocks after flock dividing. This is another aspect of scale-free correlation that is not suggested by Cavagna et al. Scale-free correlation in the flock suggests that a flock continues to coordinate with these correlated sub domains that can be split away.

2.4.4.3. Oscillation of the strength of fluctuation

In this section, we investigate the amplitude of the fluctuation vector inside of flocks. Figure 2.17 shows how the amplitude of the fluctuation vector oscillates with time. We estimate the amplitude of the fluctuation vector as the absolute value of the average of fluctuation vectors that belong to the largest correlated domain. For example, these members correspond to red individuals in the upper center of Figure 2.13. Rate of these members always is above 0.35 (data not shown). One-third of individuals have the same direction for their fluctuation vector. The oscillation shown in Figure 2.17 shows how these members tune the strength of the fluctuations as a small flock. We compare the oscillation of the largest cluster with the second largest cluster, which is constituted by the green colored individuals in Figure 2.13. In the inset of Figure 2.17, the green line corresponds to the oscillation of the second largest cluster. The green line shows the same shape as the red line. As the amplitude of the red line increases, the amplitude of the green line also increases. The green cluster, as we observed in Figure 2.13, moves in a direction opposite to the red cluster. The green cluster compensates for the strength of fluctuation of the red cluster. This role-sharing tendency is observed throughout our simulation.

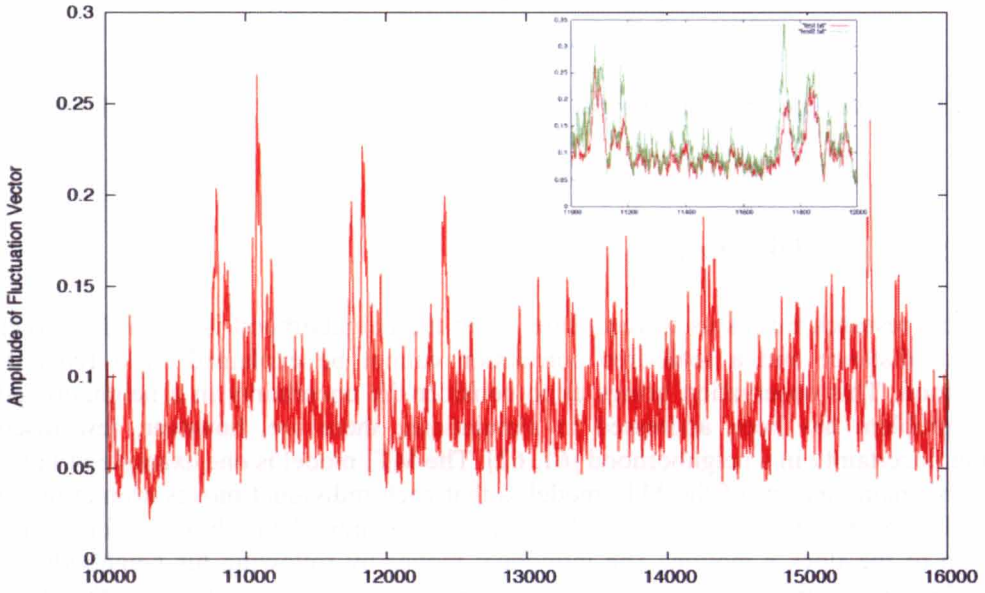

Figure 2.17. Oscillation of the average absolute value of fluctuation vector in the largest cluster. Inset: the green line is the oscillation of fluctuation vectors in the second largest cluster. Both lines are highly correlated.

As we discussed previously, fluctuations in the flock had the potential power to split the flock in some cases. Thus, flocks must suppress increases in fluctuation amplitude to prevent division. As a result, the absolute value of the fluctuation vector shows temporal fluctuations. To investigate this detail, we take the power spectrum of the time series in Figure 2.17. We define $S(f)$ as a power spectrum for the fluctuating representation in Figure 2.17. The mathematical expression is;

$$S(f) \sim f^{-\alpha} \qquad (2.4.14)$$

Figure 2.18 shows the power spectrum of Figure 2.17. It shows a $1/f$ power law over a wide rage of time scales with $\alpha \approx 1.5$. Emergence of this kind of power law is considered to be the characteristic property of critical phenomena such as self-organization criticality (SOC). This fact is consistent with several interpretations, one of which is the collective behavior on critical phenomena. Cavagna and others, who discovered scale-free correlation, suggest that some kind of criticality might in fact be present in starling flocks. Our simulation showed that it is also observed being criticality on a continuous time scale.

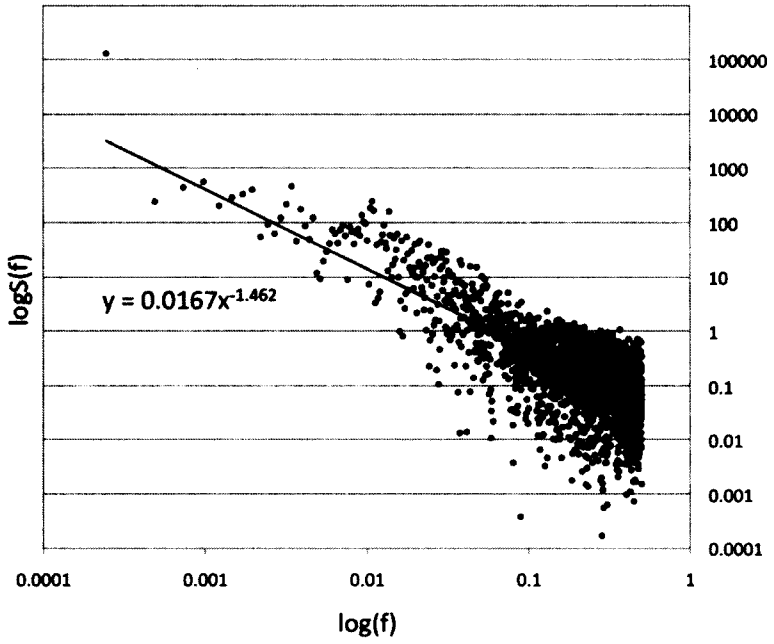

Figure 2.18. Power spectrum $S(f)$ for the oscillation in Figure 2.17. The graph shows $1/f$ power law.

2.4.5. Discussion

Empirical research makes us to reconsider what the neighborhood is for each individual. A topological distance and a scale-free correlation cannot be explained by a fixed distance neighborhood. This observation brings us to consider the uncertainty in a neighborhood. This kind of problem has been addressed in simulations; there are, however, few discussions regarding uncertainty in a neighborhood [61, 62]. The MTI model is one example of this kind of model. The main concept of the MTI model is that each individual moves around in checking whether his own neighborhood is well-defined. The individual, thus, performs a double evaluation of the flock's motion. The individual moves by following his neighborhood while also checking its neighborhood as an evaluation of the whole. Our results show that this double evaluation is needed to produce scale-free correlation without giving external noise for each individual.

Previous studies of flocks (or schools of fish) have involved fixed neighborhoods or neighbors for each individual with the addition of external noise. The external noise introduces a degree of freedom that is irrelevant to the various situations. This means that each individual can move and select its direction if its flock will follow. The external noise that is irrelevant to their wholeness gives rise to the problem of interpreting the critical phenomena for tuning the noise parameter. The SPPs model does not show scale-free correlation unless the degree of freedom of each individual is irrelevant for his position and the relation with its neighbors. In other word, the main problem of the flock is not what kind of noise should be given, but how each individual makes intrinsic noise in a certain environment. The question as to what kind of

noise should be given leads to a trade-off, that is, the flock never shows a variety of formations if the noise is low but the flock loses its coherence if the noise is high. This trade-off relation cannot be solved by the SPPs model. In the end, this trade-off has caused researchers to consider a "soft degree of freedom" [34].

The MTI model, by contrast, does not require this kind of external noise. The noise arises from adjusting between the class cognition and the cognition as a collection. Our model shows that the different evaluations of the neighborhood for each individual cause the flock to change direction, to keep the flock stable, and to collapse the flock. In particular, the gradient of the relation between the correlation length and the flock size is in good agreement with empirical studies. The concept of a collective memory can be thought of as an uncertain neighborhood. It has been shown that there is a antisymmetric relation when the range of the neighborhood (metric distance) of each individual gradually increases or decreases with uniformity. Cousin suggested that this is important to understanding collective behavior, that the neighborhood should expand to share information with a larger domain, but he never demonstrated how this works [28]. The MTI model suggests that three properties (that is, changing directions, adjusting between the class and the cognition as a collection, and collapsing the flock) are closely connected with each other for constructing flocks. We suggest that these relationships can emerge only through using double evaluations, that is, each individual makes a movement and simultaneously checks the evaluation of the whole (in this case, the whole flock). Our approach is not a highly complex system, but exhibits various properties in its behavior. We consider, thus, that the MTI model also sheds light on the different interpretations of scale-free correlation and collective behavior.

2.5. MTI model in Three-Dimension

2.5.1. Behavior in three dimension

Figure 2.19A and Figure 2.19B are snapshots of a set of individuals using the MTI model. We fixed the threshold parameter at 0.05 radians. The arrow in both figures represents the velocity vector, which is projected onto a two-dimensional plane. The length of each velocity vector represents the amplitude of the individual's speed. Figure 2.19A shows a typical formation of the flocks observed using the MTI model, in which individuals move in a straight line as one collective. Another aspect of flocking behavior is direction changing. In Figure 2.19B, an MTI flock is going to change its direction. We observe that high-speed individuals who have long vectors are outside of the flock and low-speed individuals who have short vectors are inside of the flock. This means that each individual tunes its speed to change the flock's direction clockwise, which is represented by the solid line in Figure 2.19B.

(A) (B)

Figure 2.19. Two examples of formations for the MTI model's flock. The individual number is fixed 100. The distribution of the velocity vectors is projected onto a two-dimensional plane. (A) The flock moves one direction. The directions of individuals align are nearly uniform. (B) The flock shows a hard direction change. The individuals on the outside have high velocities, and the individuals on the inside have lower velocities. The threshold parameter is 0.05 radians. The black thin arrow shows the flock's directions several steps later.

A common feature of both figures is that each individual using the MTI model shows noise-like behavior without any external noise. Individuals never maintain one direction stably but always show a small deviations from their travelling direction. This noise-like behavior emerges from frequent switching between the topological and the metric distance. We examined the switching frequency is about 0.11(±0.04) in one step. This means that 11% of individuals change their neighborhood for every step. In other words, each individual makes the different interaction. This variety of different interactions in the flock gives a fluctuation to each individual. We also note that the randomness, in the MTI model, only emerges from an individual checking the class cognition to determine whether its metric neighborhood is being used under the proper conditions (satisfying the Equation (2.4.6)). The results would be very different if the MTI model were to add external noise to each individual because the intensity of the external noise cannot spontaneously change its value and thus may not be consistent with its environment.

Next, we observed a time series showing an MTI flock changing directions. We set the threshold parameter as th=0.05 (radians) for the following simulations unless otherwise noted. Figure 2.20A is the time series of a flock's absolute direction-changing rate per 10 steps for a single simulation. This graph shows that the changing rate sometimes rises to 0.22 radians (in other words, approximately 12 degrees). This graph shows that a flock using the MTI model sometimes rapidly changes its direction. Furthermore, we ran this simulation 100 times and averaged the highest value of each time series (Figure 2.20B). We discovered that an MTI flock changes its direction up to 0.27±0.09 radians within 10 steps. This value is about twice the mean value (0.15±0.03 radians).

(A)

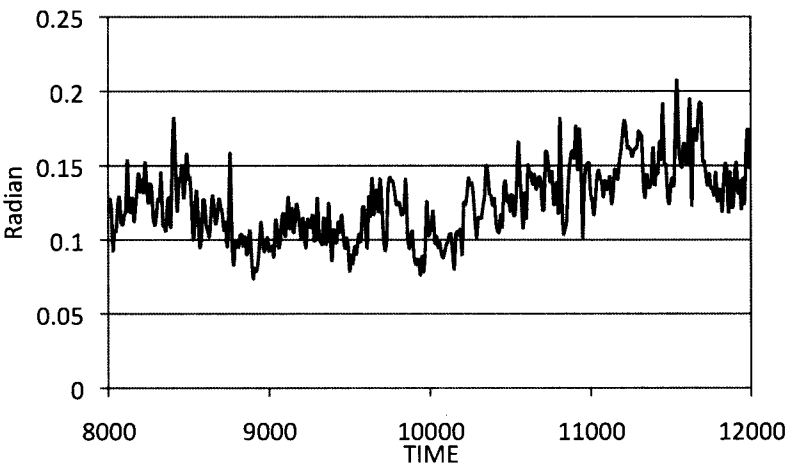

(B)

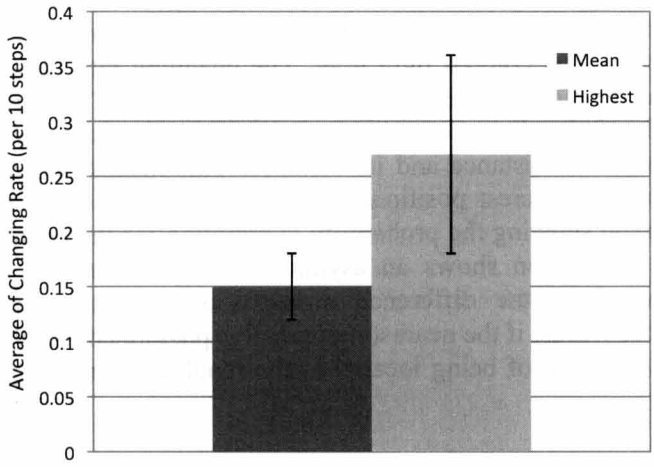

(C)

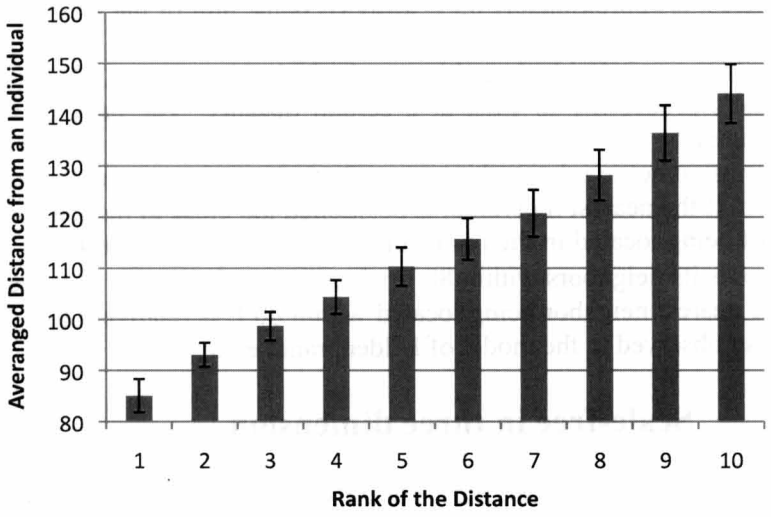

(D)

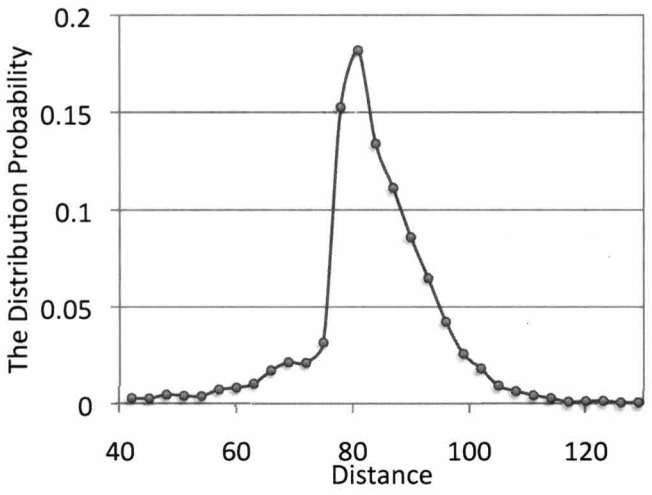

Figure 2.20. We set the number of individuals to 100. The graphs in Figure 2.20B, 2.20C and 2.20D show an average of 100 simulations, where each simulation consists of 4000 steps. (A) The graph shows an example of a time series for changing directions. We take the absolute value of the rate of change and plot its evolution over time. The vertical line corresponds to a rate change (radian) within 10 steps. In this graph, the flock changes its direction up to 0.21

radians. (B) A comparison between the mean direction changing rate and the highest direction-changing rate. The mean direction-changing rate is colored gray, and the highest direction-changing rate is colored light gray. The changing rate becomes roughly twice the mean value when the flock makes a hard direction change. (C) A graph of the relationship between the rank of the distance and the distance. We plotted the graph of the relation between the rank of the distance and its distance. This means that most nearest individual from the individual of interest positions about 85L away. There is a roughly proportional relation. (D) A graph showing the probability distribution for the nearest neighbor's distance. The probability distribution shows an asymmetric relation around its center, 80 L. This asymmetry comes from the difference property between the repulsion of the metric interaction. In other words, if the nearest individual is positioned too close to the individual of interest, it has a high risk of being located in the repulsion zone ($(R_1)_k' \geq 80$ L, see Equation (2.4.5)).

Figure 2.20C and 2.20D show the positional relationship between individuals in MTI flocks. Figure 2.20C shows the average distance between individuals graphed against the ordinal position. This relationship demonstrates that the nearest individual from the position of the individual of interest is approximately 85 L away (L is the unit of the length, and 1 L indicates the length of the unit velocity vector in the space). There is a linear dependence between the average distance between individuals and its topological order. Figure 2.20D is the graph of the nearest individual's probability to exist at a certain distance. The peak of the probability is found at approximately 80 L. This figure also shows that there is an asymmetric existing distribution. This asymmetric relationship comes from the property of the repulsion zone of the metric interaction. If the nearest individual is positioned too close to the individual of interest, it has a high risk of being located in the repulsion zone ($(R_1)_k' \geq 80$ L from Equation(2.4.5)). Thus, an individual avoids its neighbors within 80 L when it uses the metric distance. As a result, the possibility of the nearest neighbor being located within 80 L is relatively low. This asymmetric relationship is also observed in the model of Hildenbrandt et al. [79].

2.5.2. Scale-free in three dimension

In the case of three-dimension, we must not only examine the scale-free correlation for the direction, but also the scale-free correlation for the speed. In fact, Cavagna et al. not only defined the correlation function of the direction but also that of the speed. First, we defined the fluctuation speed with the fluctuation vector;

$$\phi_i = \|\mathbf{v}_i\| - \frac{1}{N}\sum_{k=1}^{N}\|\mathbf{v}_k\| \qquad (2.5.1)$$

ϕ_i is the fluctuation speed that is obtained by subtracting the average of all individual's speeds from each individual's speed; i is an index of each individual; and ||-|| indicates the norm of the velocity vector. Thus, $\|\mathbf{v}_i\| = v_i$ for our simulation. Then, we obtain the correlation function of the speed:

$$C_{sp}(r) = \frac{1}{c_0}\frac{\sum_{ij}\phi_i \cdot \phi_j\, \delta(r - r_{ij})}{\sum_{ij}\delta(r - r_{ij})} \qquad (2.5.2)$$

Similarly, the correlation length for speed is the point when the speed's correlation function becomes zero. For the mathematical expression, the speed's correlation length is ξ_{sp} when $C_{sp}(\xi_{sp}=r)=0$.

(A) (B)

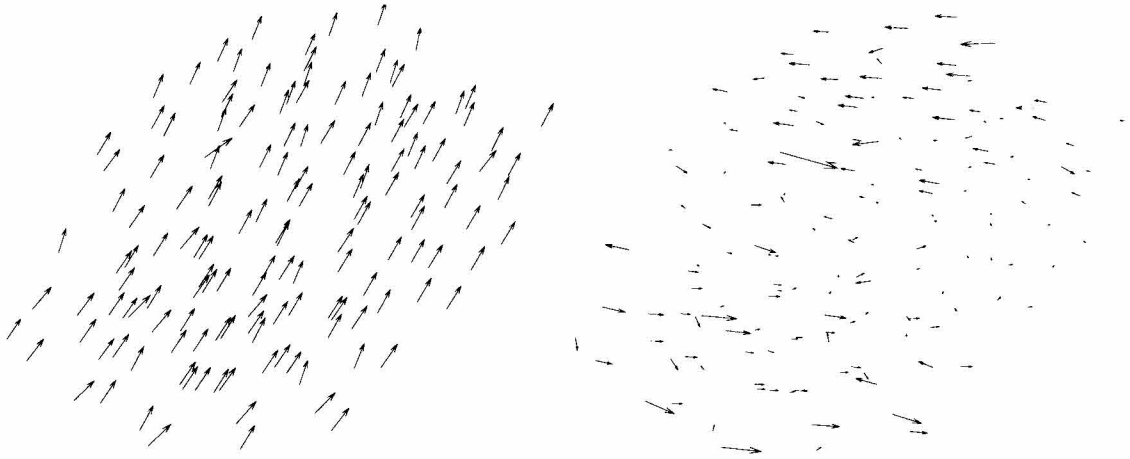

Figure 2.21. The distribution of the velocity vectors (Figure 2.21A) and the fluctuation vectors (Figure 2.21B) projected onto a two-dimensional plane. The number of individuals is 150. It appears that the individuals that are represented by the velocity vector align in nearly the same direction as the upper side. However, if we take the fluctuation vector from Figure 2.21A, then we discover two large correlation domains in the flock (the upper and lower halves). The shape from these two large subdomains is very similar to the distribution of the fluctuation vectors in a real flock.

(A)

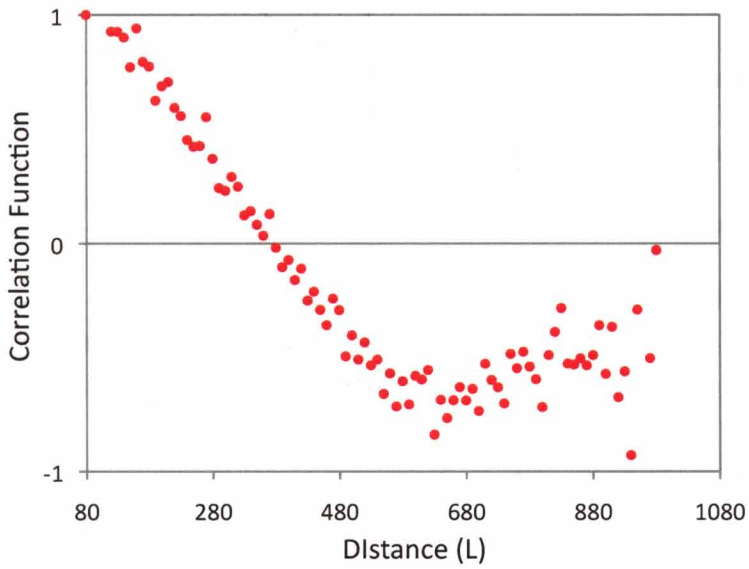

(B)

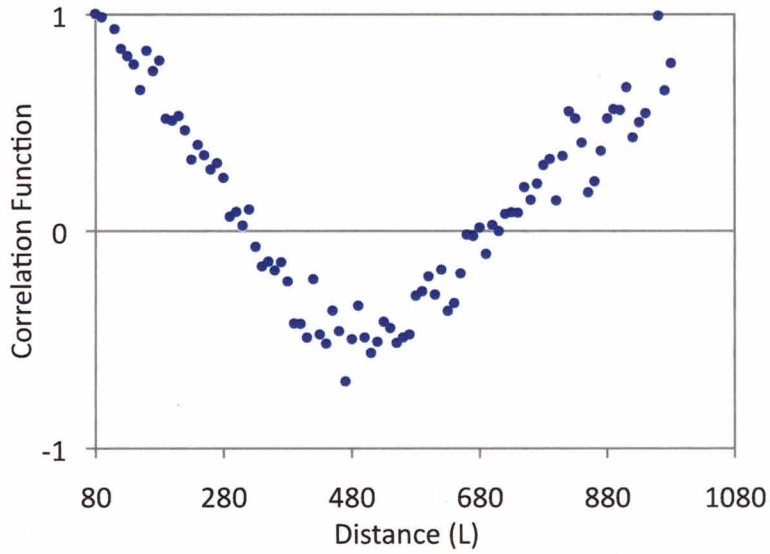

(C)

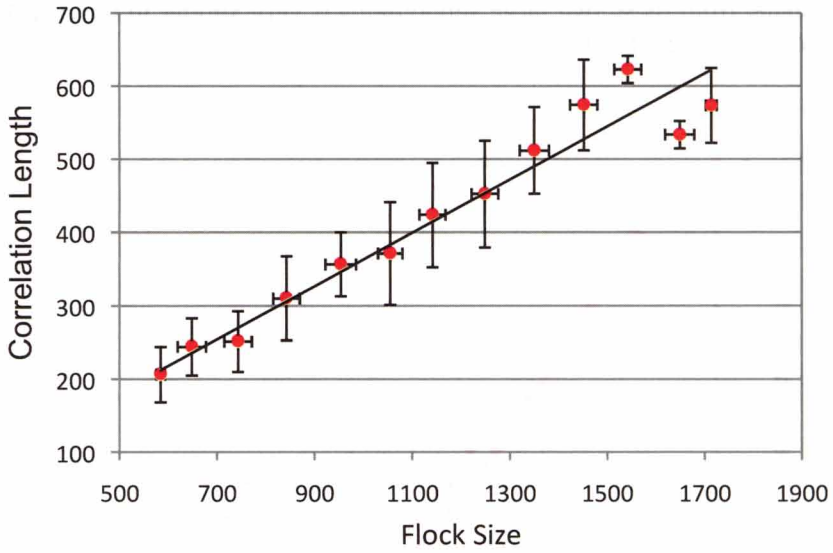

(D)

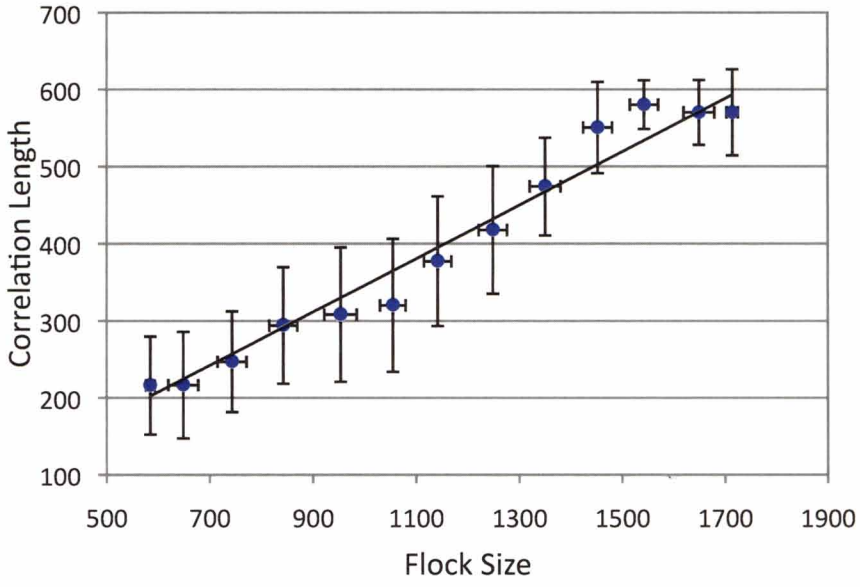

Figure 2.22. Figures 2.22A and 2.22B show the relationship between the correlation function

and distance. The number of individuals is 200, and the threshold parameter is 0.05 radians. The blue dots show the correlation function for the direction (using Equation (10)). The red dots show the correlation function of the speed (using Equation (12)). Both values gradually decrease as the distance becomes large. Especially the value of the correlation function suddenly rises up to positive values in speed. In this case, both of the correlation lengths are ξ=370 L (direction) and ξ_{sp}=320 L (speed). Figures 2.22C and 2.22D show the relationship between the flock size and the correlation length. The number of individuals is set between 100 and 300, and the threshold parameter is fixed at 0.05 radians. We made 300 simulations and averaged the results over a certain interval (100L on the horizontal axis). The error bars indicate the SD. The three-dimensional MTI model shows a scale-free correlation in both cases. The red dots correspond to the direction in Figure 2.22C, and the blue dots correspond to the speed in Figure 2.22D. Both are well correlated (correlation coefficients of 0.87 for the direction and 0.78 for speed). The gradients of both graphs are given as 0.36 (direction) and 0.35 (speed). The gradient for the speed matches Cavagna's result.

We can also observe scale-free correlation in a flock using the MTI model. Figure 2.21A shows the distribution of the velocity vector projected onto a two-dimensional plane. In this picture, the flock moves to the upper side, and it seems that each individual has almost the same direction. Now, we derive the fluctuation vector from this picture. By subtracting the mean velocity vector from each velocity vector, we obtain the distribution of the fluctuation vectors of this flock (Figure 2.21AB). Obviously, this flock has some correlated sub-domains within itself, although each velocity vector has a similar direction in the flock (the upper side and the lower side of the flock). These correlated sub-domains always exist inside of the flock and flexibly change their shape at every time step. Next, we examine the relationship between the correlation length and the flock size (the flock size is given as the largest distance between flock members). In the previous study, we only showed the direction of the scale-free correlation in two-dimensional cases (Section 2.3). In this study, we investigate scale-free correlation of both direction and speed with Equations (9) – (12). Figure 2.22A and Figure 2.22B are the graphs of the relationship between the correlation function and the distance. Both graphs have a tendency to decrease the correlation value when the distance becomes large. This is a reasonable finding compared with the empirical result. Furthermore, the correlation function of the speed (Figure 2.22B) shows its value abruptly rising up to the positive value when the distance becomes sufficiently large (not for all cases). This property has also been observed empirically, so it appears that the simulation result of the correlation function matches with the empirical result. We list other graphs under Supporting Information. Figure 2.22C and 2.22D show the proportional relationships between the correlation length and the flock size. The red points show the correlation with the direction (Figure. 2.22C), and the blue points show the correlation with the speed (Figure. 2.22D). We ran simulations 100 times for flocks with 100, 200, and 300 individuals, respectively. Both characteristics examined (speed and direction) exhibit scale-free correlation. The gradients of these graphs are 0.36 (direction) and 0.35 (speed). This result almost matches with the experimental result (the experimentally derived slopes are 0.35 for the direction and 0.36 for the speed) []34. It turns out that, even without knowing the whole shape of the flock to which individual belongs, each individual in the three-dimensional MTI model constantly adjusts its fluctuation vector to make the correlation sub-domains maintain the proper size.

2.5.3. Storing and Releasing Fluctuation

In the previous section, we observed that flocks using the MTI model displayed scale-free correlation of both qualities (direction and speed). If we take this fluctuation vector as noise, we can show that the noise has a structure inside the flock. This finding suggests that the noise-like behavior of the MTI individual is always limited to the structure of the scale-free correlation in the flock even though the noise-like behavior of the MTI individual appears random.

Do the fluctuations inside the flock have another aspect? We extended our approach to look at the whole concept of fluctuation in the flock. So far when discussing the MTI model we have fixed the threshold parameter *th* for the whole simulation. In this section, we tune this parameter's value through a simulation series. For example, the parameter value gradually

decreases when all of the individuals in a given space move as a single flock.

To clarify the meaning of the parameter tuning for the flock, we need to return to the notion of class and collection cognition. When the threshold parameter is high, the probability of exceeding *th* is very small (see Equation (2.4.3)). Thus, it is difficult for an individual to switch from the metric interaction to the topological interaction (see Equation (2.4.6)). In the same way, it is easy for an individual using the topological interaction to switch to the metric interaction. Therefore, the metric interaction (i.e. class cognition) is dominant when the threshold parameter is high, so each individual tends to neglect the differences between individuals within its neighborhood.

On the other hand, when the threshold parameter is small, individuals tend to use the collection cognition (i.e. topological interaction). Specifically, for an individual using the metric interaction, it is easy to switch to the topological interaction because the probability of exceeding *th* is high (see Equation (2.4.6)). Conversely, it is hard for an individual using the topological interaction to switch from the topological interaction to the metric interaction (see Equation (2.4.3)). Therefore, the topological interaction (i.e. collection cognition) is relatively dominant when the threshold parameter is small.

What happens to the individual when the threshold parameter gradually decreases or increases in the simulation? Before we begin this simulation condition, we must estimate the degree of the noise-like behavior of the MTI individual. We cannot estimate the noise-like behavior in advance because our model never introduces external noise. Therefore, we use the method that is described in Figure 2.24. The idea behind this method is that the noise is considered in the context of the SPP method. In other words, the degree of the noise estimates how the direction from the MTI model is different from the direction determined by the SPP method. Recall that alignment in the SPP model is determined by the average of the directions within the individual's neighborhood plus external noise. We therefore interpret the difference between this averaged direction and the determined direction from the MTI method as the noise contribution. Figure 2.24 shows our method for computing the fluctuation degree. First, we set the imaginary fixed neighborhood (blue dotted circle) for each individual, as in the SPP model. The radius of this imaginary circle is set to 100 L. We then determine the direction from the SPP model (blue colored arrow). Each individual has a direction that is determined by the MTI model (red colored arrow). We calculate the angle between the red and the blue arrow for each individual, and we refer to this value as the "fluctuation degree". We define a set for an individual k as $N\text{-}IM_k^t \equiv \{l \in N \mid 0 < \| \mathbf{x}_k^t - \mathbf{x}_l^t \| < 100\}$, and the number of elements of $N\text{-}IM_k^t$ is $(n_{im})_k^t$. Therefore, if we define each individual's next state as $\hat{\mathbf{v}}_k^{t+1}$, then the fluctuation degree (FD) would be given as follows:

$$FD_k^t = \cos^{-1}\left(\left\langle \hat{\mathbf{v}}_k^{t+1}, \frac{1}{(n_{im})_k^t} \sum_{l \in N-IM_k^t} \hat{\mathbf{v}}_l^t \right\rangle\right) \tag{2.5.3}$$

$$AFD^t = \frac{1}{n} \sum_{k=1}^{n} FD_k^t \tag{2.5.4}$$

We define (2.5.3) as the fluctuation degree (*FD*). In addition, we can compute the average of all of the fluctuation degrees (Equation (2.5.4)). We call this the average fluctuation degree (*AFD*).

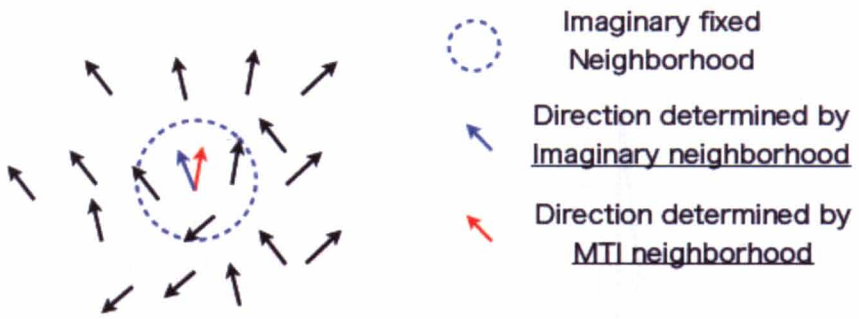

Figure 2.24. An image for computing the "fluctuation degree". The blue, dotted circle is an imaginary neighborhood, and the blue arrow is the direction that is determined by using the interaction of SPP model on the imaginary neighborhood. The red arrow indicates the direction that is determined by the MTI neighborhood. We take the absolute value of the difference between the red and blue directions. The fluctuation degree can be computed by using Equation (2.5.3).

The fluctuation degree (*FD*) asymptotically approaches zero when all individuals use the topological distance. Recall that an individual using the topological interaction aligns only its direction. Therefore, the difference between the two directions determined by the topological interaction and the imaginary SPP interaction becomes small because the direction determined by the imaginary neighborhood also only uses alignment. As a result, the *AFD*, which is the average of all *FDs*, also becomes small. Therefore, when the threshold parameter is small (nearly all individuals are using the topological interaction), the *AFD* is very small value.

Figure 2.25A shows the result when the threshold parameter is tuned. We began tuning the threshold 1,000 steps after the point at which the individuals formed a single flock. The number of individuals is fixed at 100. The threshold parameter *th* goes up or down by 0.1 radians every 100 steps. We started by tuning the threshold parameter from 1.0 radians to 0 radians and then reversed the process and tuned the threshold parameter from 0 radians to 1.0 radian. We do this in a single simulation. The red dots in Figure 2.25A correspond to the increasing threshold parameter, while the blue dots correspond to the decreasing threshold parameter. The arrows in Figure 2.25A indicate the direction of the process, and the numbers above the arrows indicate the order of the process. The simulation began by decreasing the threshold parameter from 1.0 radians to 0 radians for each individual (colored blue) and then began increasing the threshold parameter from 0 radians to 1.0 radians for each individual (colored red). We observed an asymmetric relationship (i.e., hysteresis) between the increasing phase of the threshold parameter and the decreasing phase. The discrepancy in the *AFD* when *th*=1.0 (radians) will disappear when enough time has passed. In particular, there is a point at which the *AFD* suddenly rises in as the threshold decreases. At this point, the flock explodes (see Figure 2.25B). Several flocks in our simulations exploded and divided completely into different flocks. Such explosions have been observed empirically, for example, in schools of fish [34]. Previously, there was no model that could replicate this property. This explosion was not observed when the threshold was increasing.

(A)

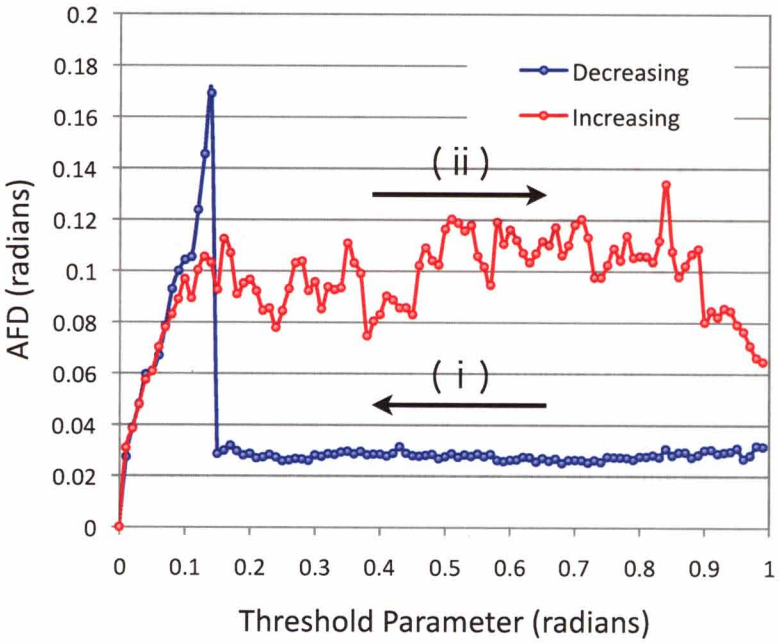
0.2
0.18
0.16
0.14
0.12
0.1
0.08
0.06
0.04
0.02
0
AFD (radians)
Decreasing
Increasing
(ii)
(i)
0
0.1
0.2
0.3
0.4
0.5
0.6
0.7
0.8
0.9
1
Threshold Parameter (radians)

(B)

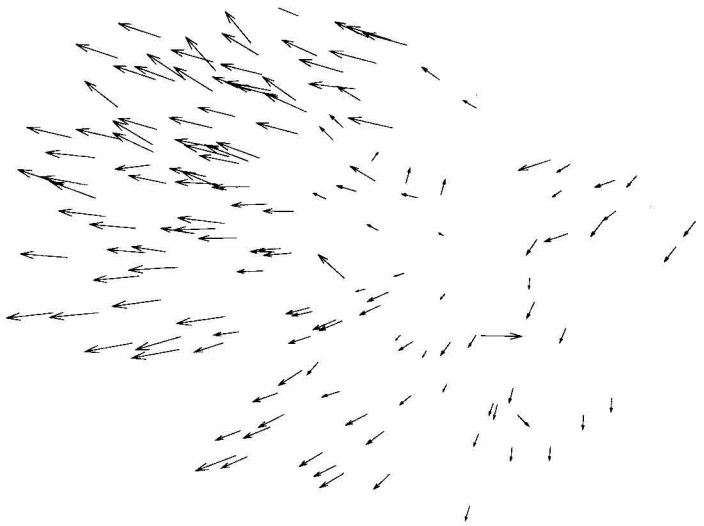

(C)

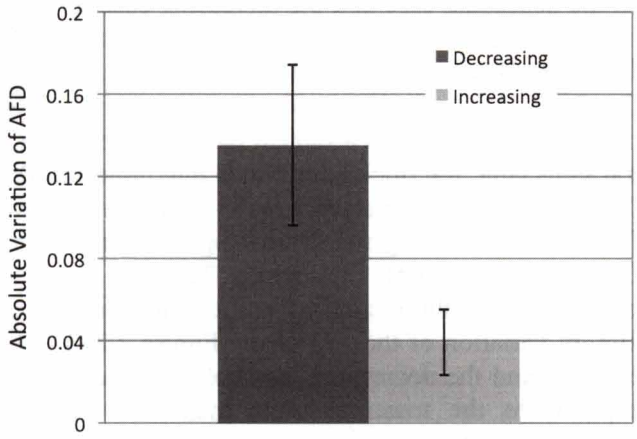

(D)

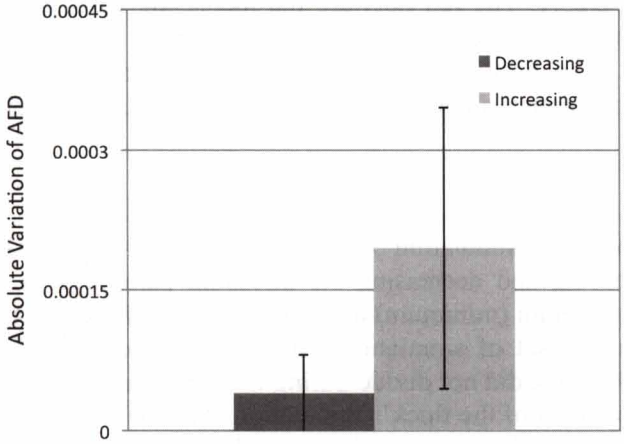

(E)

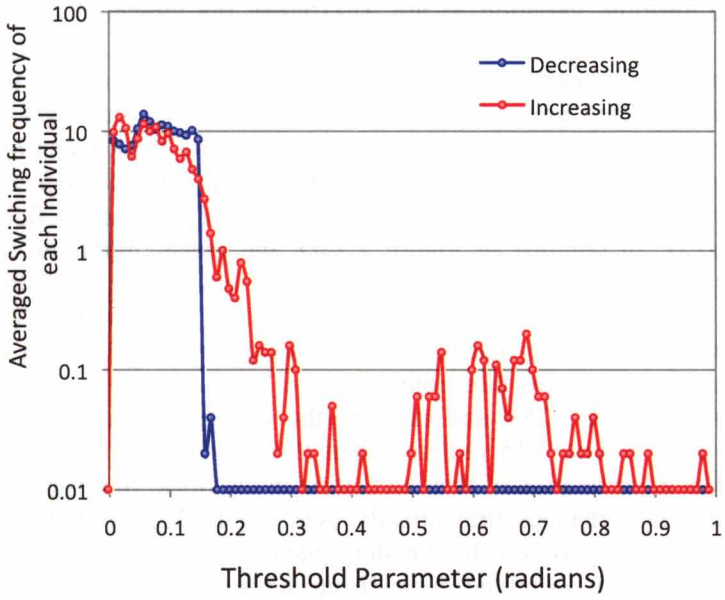

Figure 2.25. (A) The graph shows the value for the average fluctuation degree as the threshold parameter changes. The number of individuals is fixed at 100. The threshold parameter, *th*, decreases or increases 0.01 radians every 100 steps. The red dots are the increasing case, and the blue dots are the decreasing case. The arrows indicate the direction of the change. The numbers indicate the order of the processes. There is an asymmetric

relationship between the deceasing case and the increasing case. In the decreasing case, there is a point at which the average fluctuation degree increases suddenly to 0.15 radians. The flock explodes at this point. However, this explosion never occurs in the increasing case. (B) The explosion of the flock. An explosion is obtained by changing the threshold parameter gradually. Each individual spreads out in a radical pattern. The center of the explosion is on the right side. Several steps later, the flock has divided into three sub-flocks.

In Figure 2.25C and 2.25D, We selected a pair of the maximum (minimum) absolute variations of the *AFD* for the increasing and decreasing cases from one set of simulations. To do this, we took 50 data points from 50 simulations. The data would show the difference of variance of *AFD* for each step in the increasing and the decreasing case. (C) A graph of the mean absolute maximum variation of the *ADF* from Figure 2.25A. The increasing threshold parameter is colored gray, and the decreasing threshold parameter is colored light gray. The vertical axis corresponds to the mean absolute maximum variation of *ADF* from 50 simulations. (D) A graph of the mean minimum absolute increment of the *ADF* from Figure 2.25A. The increasing threshold parameter is colored gray, and the decreasing threshold parameter is colored light gray. The vertical axis corresponds to the mean minimum variation of *ADF* from 50 simulations. (E) The average switching frequency for each threshold parameter in Figure 2.25A. The red dots are the increasing case, and the blue dots are the decreasing case. The vertical axis represents the average switching frequency for each threshold parameter. The horizontal axis indicates the threshold parameter. The variation when the threshold parameter is decreasing around 0.15 radians is much steeper than when it is increasing.

We repeated this type of the simulation 50 times. One replicate of the simulation includes the entire process of increasing and decreasing the threshold parameter as in Figure 2.25A. We selected a pair of the maximum (minimum) absolute variation of the *AFD* for the increasing and decreasing cases from one set of simulations. In this way we took 50 data points from 50 simulations in which the flock did not divide during the simulation as we wanted to estimate the internal or inherent properties of the flock's fluctuation. All flocks in our simulation showed the same tendency when faced with *AFD* variation. We observed the same tendency for hysteresis even when the speed of each individual is fixed. Furthermore, all of the flocks in our simulation exploded. However, the timing of the flock's explosion was different in each simulation. We therefore take the absolute variation of the *AFD* when the threshold parameter increases or decreases by 0.01 radians, which corresponds to one step in Figure 2.25A. Figure 2.25C (2.25D) is the mean maximum (minimum) absolute variation obtained by tuning the threshold parameter. The increasing *th* is colored gray, and the decreasing one is colored light gray. Both figures suggest that there will be differences in the fluctuation of the flock when *th* is increasing and decreasing. In Figure 2.25C, the mean maximum of the *AFD* when *th* is decreasing is 3.5 times larger than when it is increasing (t-test: $p < 0.001$). The explosion of the flock causes this high variance of the *AFD*. In contrast in Figure 2.25D, the mean minimum of the *AFD* of the decreasing *th* is 0.2 times than the increasing one (t-test: $p < 0.001$). This small variance in the *AFD* comes from the first stage when *th* decreases from 0.5 to 1.0 radians (see Figure 2.25A). From these results, we conclude that there is an essential difference in a flock's fluctuation based on the tuning direction of its threshold parameter.

Next, we return to Figure 2.25A and examine the switching behavior around 0.15 radians. There is a sharp peak around 0.15 radians when *th* is decreasing that indicates "explosion". Then, we provide an interpretation of this fluctuation in the flock. In this region, the interactions between each individual changes dramatically (see Figure 2.25E). Figure 2.25E shows the average switching frequency versus the threshold parameter. This graph corresponds to Figure 2.25A. In Figure 2.25E, the switching event (from the metric to the topological interaction in this case) does not occur until the *th* reaches 0.15 radians. In other words, all of the individuals in the flock use the metric interaction. The switching event, however, suddenly becomes active when *th* reaches 0.13 radians. This means that the individuals nearly simultaneously switch from the metric interaction to the topological interaction. This event triggers the flocks' explosion. Nearly all individuals in the flock then repeatedly switch to the topological interaction and back to the new metric neighborhood. This switching behavior makes the flock

explode at 0.13 radians.

This process of decreasing *th* can be replaced with the following story. Based on the example shown in Figure 2.25A, we observe that this flock under the MTI model contains six to seven individuals that have a high *FD* (greater than 0.20 radians) when it reaches a high threshold parameter. In this case, the metric neighborhood of each individual is barely disrupted because this value is sufficiently small enough compared to high *th*, such as 0.8 radians. In fact, there is no individual who switches its interaction in the closed interval $th \in [0.18, 1.0]$ in Figure 2.25E. However, when the threshold value gradually decreases, the probability of disrupting the metric neighborhood, or the probability of exceeding *th* (satisfying Equation (2.4.6)), increases. Once the metric neighborhood of an individual is disrupted by its fluctuation exceeding *th*, the individual will reform a new metric neighborhood under the MTI method. Therefore, this individual fluctuates vigorously to create a new neighborhood. This behavior increases the fluctuation of other, nearby individuals. These adjacent individuals then break their metric neighborhoods and perpetuate the fluctuation of other individuals. In this way, the neighborhood disruption process instantly spreads through the flock, causing an explosion. It therefore appears that a small fluctuation in the flock has the power to break the entire flock. However, by neglecting the difference between individuals, or continuing to use the metric interaction, the flock can restrict its fluctuation inside itself. Storing fluctuations means that each individual never switches to the topological interaction but instead keeps using the same metric interaction. If all individuals in the flock do this, no fluctuation emerges from switching between the two interaction types. In this regard, it can be considered that the entire flock stores its fluctuation, which is caused by a switching event, because the fluctuation would make the flock explode if the switching event occurs.

However, the flock with an increasing *th* never explodes as it does when *th* decreases. In the increasing case, the *AFD* first gradually rises as the threshold parameter becomes large. The *AFD* variation keeps its high value after *th* reaches 0.2 radians. All individuals tend to use the topological distance and continue to switch from metric to topological interaction or from topological to metric interaction when the flock with an increasing *th* starts out with a small *th* (see Figure 2.25E). Each individual always tries to resolve differences in direction with the topological interaction as they occur. The fluctuation is not neglected as in the decreasing case but instead is released by each individual. Nearly all individuals use the metric interaction after 0.3 radians, but several individuals switch to the topological interaction and back a new metric interaction. We observed that this process continues even when *th* exceeds 0.5 radians in Figure 2.25E. This robust switching process becomes difficult as the degree of fluctuation scales down. That is why the *ADF* never becomes consistent at high *th*. In contrast to the decreasing *th*, a high *ADF* after 0.3 radians means that the flock releases its fluctuation. Releasing the fluctuation means that each individual never keeps using the same metric interaction but that some individuals can switch between two interactions. The flocks cannot store the fluctuation when they release it.

We also point out that variations in speed never affect our results, including explosions. All events in the model without speed variation are the same as in the model with speed variation. Therefore, we can apply these results to both flocking behavior and fish schooling.

2.5.4. Discussion

We showed that this inherent noise revealed a special property, called scale-free correlation, with respect to direction and speed when the threshold parameter is set in an appropriate manner. Furthermore, the shape of the correlation function for both the direction and speed fit with experimental data despite the inclusion of several noisy graphs (such as Supporting Information Example 3). This indicates the correlation function shows slow decay in the flock. Scale-free correlation requires the individuals to change their behavior (direction and speed) in context. To explain this flexibility, spontaneous judgment of direction and speed is needed for each individual. If we provide the noise externally, the model has to find the proper noise intensity for every case. Several researchers consider this type of inherent noise to be an important issue when studying collective behavior [31, 80]. Although Hemelrijk's model can also explain scale-free correlation, it only applies a scale-free correlation to the direction [24]. The scale-free correlation for the speed and shape of the correlation function had not previously been

demonstrated. Our model satisfies all properties (scale-free correlation to the speed, direction and shape of the correlation function). This is the main achievement of our study.

In the previous section, we observed that various flocking behaviors (including explosion) were obtained by tuning the threshold parameter. Let us interpret this in the context of the class and the collection cognition. In our model, we correspond the metric interaction to the class cognition and the topological interaction to the collection cognition. Recall that the class cognition means the cognition of "sameness" (or neglecting the differences) and that the collection cognition means the cognition of "difference" (or distinguishing the differences). Switching between the class and the collection cognition means that each individual checks "the difference" and re-constructs "the sameness" of its neighbors' behavior. This switching operation makes each individual fluctuate, and this fluctuation is not sufficient to collapse the flock. However, if the class cognition is dominant, "the difference" never disappears but instead continues to exist inside of the flock because the switching event never occurs. We observed that the flock exploded if these neglected difference were recognized simultaneously. In this sense, it can be thought that the flock stores the fluctuation and that the power of these fluctuations collapses the flock. In contrast, the difference would never be neglected and is eliminated by each individual if the collection cognition is dominant. The difference cannot be maintained inside of the flock. In this sense, the flock never stores the fluctuation but always releases it.

The biological significance of the difference between the class and the collection cognition emerges as a sense of the quality (class) and quantity (collection) [34, 35]. However, distinguishing between quality and quantity is very difficult in principle [29, 36]. Our model suggests that this difficulty in distinguishing the two cognitions has a great effect on the collective movement. Storing and releasing the fluctuation never emerges through only one side of the two cognitions but is released by both cognition states. This also means that the difficulty of distinguishing both cognitions may sometimes make the flock continue to use the same cognition. We considered the case when the class cognition was maintained and observed that this is the cause for an explosion. Our switching model provides an interpretation of fish school explosions from this cognitive perspective.

Our model can induce inherent noise, which shows scale-free correlation, for each individual from the perspective of switching between the class and collection cognitions. Some flocking models include noise without considering the individual's context [25, 26 28, 52, 53, 55, 59, 60, 78]. Therefore, the origin of the noise remains vague. Compared with this type of model, our model shows that switching between the two cognitions inevitably generates noise. Other models have too many biological or environmental restrictions [62, 63, 66 , 79]. In this type of model, it becomes difficult to focus on what is important for the collective behavior because there are too many parameters. Our model is constructed based on a minimal assumption that each individual uses two cognition states and adjusts between them according to the environment. We believe that this cognitive perspective will play an important role in understanding the collective phenomena.

3. Evolving Lattice Model in Ecological Systems

3.1. Background

Adaptation is one of the intriguing issues for vast biological events such as evolution and ecology [81, 82]. Each species must survive in various environments. Generally, we consider fitness to explain that species adapts to an environment. "Survivor of fittest", proposed by Darwin [82], is the most famous theory for the adaptation and the evolution. Many evolving model, therefore, have applied the concept of fitness whether we like or not [81, 83, 84, 85]. The celebrated model of Bak and Sneppen explained the biological evolution by using a fitness landscape [83, 84]. Their model has very simple construction. Each species has own fitness among species and connects each other on the periodic one-dimensional line. A selected least fit species flips its value of fitness randomly. Then two connected species also flip their value of fitness at random. Bak and Sneppen explained biological evolution of an ecology such as power laws for extinction's distribution by using this simple model [83, 84].

The evolutional model of Bak and Sneppen provides many suggestions when we consider the species' adaptation in fitness landscape. The problem of their model, which we take up here, is their assumption of perfect information of the fitness because the model needs the knowledge of all fitness value to decide a least fit species. This assumption seems unnatural. The concept of fitness landscape, however, implicitly requires the knowledge of global fitness information. In the living world, it is very hard to ask perfect information for an environment because an environment would dramatically change with time and the relation between species also changes with their environment. Therefore, we must admit this incomplete information for the environment when we construct the model of adaptation.

If we accept changing environment, we change the consideration to adapting process as a whole species from particular species [86, 87, 88, 89]. It could become disadvantage for only increasing population of fittest species. Let consider the genetic example. In the genetics, there are two types of allele that are wild type and mutant [90, 91]. The wild type is most common in the population of allele. If the proportion of the wild type becomes too large, it would make easy to become extinct when the environment changes. To avoid such extinction, it never needs to produce wild type, but also some mutations. However, too many mutations make allele's fitness fall. Therefore, it needs the balance between the selection and mutation in the population. The balance between selection and mutation also appears as the balance between selection and variation in the ecological evolution [81, 92]. However, we generally must find fine-tuning of the mutation rate for gene reproduction to obtain optimal variety of mutants for the adaptation. We confirm here that the problem of incomplete information for the environment would shift into the statistical property in the population. This statistical property emerges as probabilistic parameters in many models [91, 92, 93, 94, 95, 96, 97, 98]. The problem, which we suggest for the model of Bak and Sneppen, comes back again here. To determine the optimal degree of variation, we need the complete global information of the population.

The assumption of complete global information would erase the essential problem for adapting individuals to their environment. The problem of incomplete information, which we have discussed, imposed on modelers who decide fine-tuning between selection and variation. Apparently, this incomplete information in the living world should not reduce to the modeler, but adapting individuals. If we try to discuss the adapting process of species, we never easily have to start with the assumption of complete globality. Therefore, we must pay attention to not losing the incomplete information when we construct the model of adaptation to an environment.

In pervious study, we suggested that the importance of incomplete observation (information) for the adapting process [99, 100, 101]. We insisted that the dynamic relation between incomplete locality and globality would be needed if we want to understand the adapting process. The relation between locality and globality, however, tends to replace the relation between parts and a whole on the context of self-organization. The concept of self-organization is the global emergence property through the local interaction without any central control. The ecological model of Bak is also sorted by one kind of the model of self-organization. Unfortunately, most of these models require complete global information such as the threshold

value, least fit species and parameter turning [83, 84, 86, 87]. The balance between globality and locality is assured by these factors in advance. Therefore, there is no dynamical relation between them in the model of the self-organization.

Returning to the definition of the word "self-organize", we point out that the word must contain two levels, which are "self" (parts) and "making self" (whole), at least. However, the word "self" would contain other elements, which never have belonged to "self", because the "self" can make progress by actively taking in unknown factors when he adapts to changing environment. "Self" itself must be defined as incomplete in the self-organization. Changing "self" also requires changing "making self" as a whole. Therefore, we cannot avoid the problem of the incomplete information when we consider the relation between locality and globality. Considering self-organization, faithfully, suggests that the relation between parts and whole must progress by containing such incompleteness [100, 101]. That is why it needs to consider the dynamical relation between locality and globality in adapting process.

In this paper, we use the lattice theory to represent the incompleteness of locality in adapting process. The lattice structure in the lattice theory also provides us dynamical changing globality. Each species can observe only parts of environment. This local incomplete information represents as block information. Each species construct the dynamical globality by using block information. In our evolving lattice model, local incomplete information drives the constructed lattice evolving. Then constructed global information re-estimates incomplete local information by using a quotient lattice. The quotient lattice plays a role of identifying a set of connected block information as representative block information. Using identification by a quotient lattice, we show that species can obtain variation without any parameter tuning.

3.2. Basic Notion

To construct our model, we use a lattice theory. The lattice theory has widely used in the computer science such as an automaton theory [102, 103]. Here we review the basic definitions and notion, which are used in our model for unfamiliar readers of the lattice theory.

Definition 2.1 (*Partial Order*) Let P be a set. An order on P is a binary relation $\leq$ on P such that, for all $x, y, z \in P$

(i) $x \leq x$

(ii) $x \leq y$ and $y \leq x \Rightarrow x = y$

(iii) $x \leq y$ and $y \leq z \Rightarrow x \leq z$ □

We denote a partially ordered set by the pair, $(P, \leq)$. For example, a set of bit (binary) strings can construct a partial order. A bit string $a_1a_2a_3\ldots a_n$ is a finite sequence of zero or one ($a_i \in \{0, 1\}$). An order between two bit strings such as $a_1a_2a_3\ldots a_n$ and $b_1b_2b_3\ldots b_n$ is defined by $a_1a_2a_3\ldots a_n \leq b_1b_2b_3\ldots b_n$ if $a_i \leq b_i$ for all i. We use a set of bit strings in this study. However, A partial order is not a lattice. Then we define the *meet* and the *join*. We define the join "$\vee$" and the meet "$\wedge$" of two elements x and y in P. The join can be defined by $x \vee y = sup\{x, y\}$ when it exists. The join can be defined by $x \wedge y = inf\{x, y\}$ when it exists. The notation of *sup* (*inf*) means the lowest (greatest) upper bound of $\{x, y\}$ in P.

Definition 2.2 (*Lattice*) Let $(P, \leq)$ be a non-empty partially ordered set.
If $x \vee y$ and $x \wedge y$ exist for all $x, y \in P$, then $(P, \leq)$ is called for a lattice. □

To distinct a partially ordered set, we denote a lattice as $(L, \leq, \wedge, \vee)$. In this paper, there are often-used sets that are an ideal and a filter. An ideal is used when we construct the congruence on a lattice.

Definition 2.3 (*Ideal*) Let $(L, \leq, \wedge, \vee)$ be a lattice. A non-empty subset of J is called an *ideal* if
(i) $x, y \in J$ implies $x \vee y \in J$,
(ii) $x \in L$, $y \in J$ and $x \leq y$ imply $x \in J$. □

Definition 2.4 (*Filter*) Let $(L, \leq, \wedge, \vee)$ be a lattice. A non-empty subset of F is called an *ideal* if
(i) $x, y \in F$ implies $x \wedge y \in F$,
(ii) $x \in L$, $y \in F$ and $y \leq x$ imply $x \in F$. □

The typical example of an ideal is a down set on a lattice. The definition of a down set is a subset $J = \{y \in L \mid y \leq x\}$ when $x \in L$. We denote a down set of x as $\downarrow x$. It can easily be rerified that a down set satisfies the condition of ideal. In a similar way, we can define an upper set on a lattice such as $F = \{y \in L \mid x \leq y\}$ when $x \in L$. We denote an upper set of x as $\uparrow x$. We can also rerify that an upper set satisfies the condition of a filter. Next, we consider congruence on a lattice to define a quotient lattice. A congruence is an equivalence relation which is restricted by a certain condition.

Definition 2.5 (*Congruence on a Lattice*) Let $(L, \leq, \wedge, \vee)$ be a lattice. Let an equivalence relation on L be $\theta = \{\langle x,y\rangle \in L \times L\}$ such that any $x, y, z \in L$,
(i) $\langle x,x\rangle \in \theta$
(ii) $\langle x,y\rangle \in \theta \Leftrightarrow \langle y,x\rangle \in \theta$
(iii) $\langle x,y\rangle \in \theta$ and $\langle y,z\rangle \in \theta \Rightarrow \langle x,z\rangle \in \theta$

We also denote $\langle x,y\rangle \in \theta$ as $x \equiv y \pmod{\theta}$. Then an equivalence relation is a congruence on L, if for any $x, y, z, w \in L$, $(x \equiv y \pmod{\theta}$ and $z \equiv w \pmod{\theta}) \Rightarrow (x \vee z \equiv y \vee w \pmod{\theta}$ and $x \wedge z \equiv y \wedge w \pmod{\theta})$ □

Then we can make a quotient lattice by using a congruence.

Definition 2.6 (*Quotient Lattice*) Let θ be a congruence on a lattice $(L, \leq, \wedge, \vee)$, then a set L/θ is defined by

$$L/\theta = \{[x]_\theta \mid x \in L\} \text{ with } [x]_\theta = \{y \in L \mid x \equiv y \pmod{\theta}\}$$

The join and the meet on L/θ are defined by

$$[x]_\theta \wedge [y]_\theta := [\, x \wedge y \,]_\theta, \quad [x]_\theta \vee [y]_\theta := [\, x \vee y \,]_\theta$$

Then we call $(L/\theta, \leq, \wedge, \vee)$ the quotient lattice of L modulo θ. □

In this study, we construct a quotient lattice from a given ideal. First we introduce the equivalence relation derived from an ideal.

Definition 2.7 (*Equivalence Relation Derived from an Ideal*) Let J be an ideal on a lattice L. The equivalence relation derived from an ideal J is;

$$\theta(J) := \{\langle x, y\rangle \in L \times L \mid \exists z \in J \; x \vee z = y \vee z\}$$ □

We can easily rerify that Definition 2.7 satisfies Definition 2.5 and that $\theta(J)$ is well-defined to be a congruence relation. Then next proposition ensures the ideal as a block of the partition derived by a quotient lattice. This proposition would be used when we discuss the existence of the lowest block information.

Proposition 2.8 Let $\theta(J)$ be an equivalence relation derived from an ideal J on a lattice L. Then J is a block of the corresponding partition of L.

Proof. J is a block of the corresponding partition of L iff $\forall x \in J$, $[x]_{\theta(J)} = J$ (*)
Therefore we must prove (*).
(i) $\forall y \in [x]_{\theta(J)} \Leftrightarrow (\exists z \in \theta(J))\; x \vee z = y \vee z \Rightarrow x \vee z = y \vee z \in J$ (Definition 2.3) $\Rightarrow y \leq y \vee z$, $y \in J$ (Definition 2.3)

(ii) Supposing $y \in J$, for $[x]_{\theta(J)}$, it is trivial that $x \in J$, then $x \vee y \in J$. Clearly, $x \vee (x \vee y) = y \vee (x \vee y)$. It entails $y \in [x]_{\theta(J)}$

From (i) and (ii), we proved $[x]_{\theta(J)} = J$. □

We also point out that a quotient lattice is deeply connected to a map between lattices, which is called a *homomorphism*.

Definition 2.9 (*Homomorphism*) Let L and K be a lattices. A map $f : L \rightarrow K$ is said to be a homomorphism if for any $x, y \in L$,

(i) $f(x \wedge y) = f(x) \wedge f(y)$ (*meet-preserving*)

(ii) $f(x \vee y) = f(x) \vee f(y)$ (*join-preserving*)

Especially, f is called isomorphism when f is a bijective homomorphism. □

Proposition 2.10 (*Homomorphism between a Lattice and a Quotient Lattice*) Let θ be a congruence on a lattice L. Then $(L, \leq, \wedge, \vee)$ is a lattice and a natural quotient map $f : L \rightarrow L/\theta$, defined by $f(x) := [x]_\theta$, is a homomorphism.

Proof. We check that a natural quotient map f satisfies Definition 2.5.

$f(x \vee y) = [x \vee y]_\theta = [x]_\theta \vee [y]_\theta = f(x) \vee f(y)$

$f(x \wedge y) = [x \wedge y]_\theta = [x]_\theta \wedge [y]_\theta = f(x) \wedge f(y)$ □

The next theorem is often used in this paper. The theorem is used for constructing a quotient lattice from an ideal. Using this theorem, we can determine a quotient lattice from a given lattice.

Theorem 2.11 (*Reconstruction of a Lattice from a Quotient Lattice*) Let L be a lattice and f be a natural quotient map such as $f : L \rightarrow L/\theta$. For the binary relation derived from an ideal $J \subseteq L$, there exists a filter $K \subseteq L$ such that $[x]_{\theta(J)} = f^{-1}(x)$, where for any $x \in K$, $f^{-1}(x) := \downarrow x - \cup_{y \in K,\, y < x} \downarrow y$

Proof. See [99]. □

3.3. The detail of Evolving Lattice model

There are many individual differences in species, but there are many common properties in species. In our model, the different and the common properties in species apply to bit strings. Bit strings represents species. Bit strings are constructed from a series of zero and one sequence such as 010011. Formally, n-bit string can represent $a_1a_2a_3 \ldots a_n$ and $a_i \in \{0, 1\}$ for all $i \in \{1, 2, \ldots, n\}$. We briefly denote $a_1a_2a_3 \ldots a_n$ as $[a]_n$. We can replace the resemblance or the differences between species to the resemblance or the differences between bit strings.

In a set of bit strings, we can make an order between two bit strings is defined by $[a]_n \leq [b]_n$ if $a_i \leq b_i$ for all $i \in \{1, 2, \ldots, n\}$. Therefore, a set of n-bit strings constructs a partial order. We also define the meet and the join in n-bit strings.

Definition 3.1 (*Meet and Join of n-Bit String*) Let $[a]_n$ and $[b]_n$ be a n-bit strings.

(*meet*) $[a]_n \wedge [b]_n := \min\{a_1, b_1\}\min\{a_2, b_2\} \ldots \min\{a_n, b_n\}$

(*join*) $[a]_n \vee [b]_n := \max\{a_1, b_1\}\max\{a_2, b_2\} \ldots \max\{a_n, b_n\}$ □

The notation of $\max S$ (or $\min S$) means taking the largest (or smallest) value in a set S.

In our model, we provide two types of bit strings. One is a bit string that represents an environment (or a *target*). Another is a bit string that represents a species. We denote $[t]_n$ and $[s]_n$ for a target bit string and a species bit string, respectively. We consider a group of species, which are represented by n-bit strings, as a set $M = \{[s^1]_n, [s^2]_n, \ldots, [s^m]_n\}$. The number of elements in a set M is fixed at m. Each species tries to adapt a target bit string $[t]_n$. An adaptation in our model means that each species tries to imitate a target bit strings. In other words, we presume that a bit string of a species has high fitness from the evolutional perspective when it

resembles a target bit string.

To raise fitness, a species has to decide what is important or what is not important for the adaptation. Or this proposition would replace the following question such as "which should be changed in a part of a bit string to raise fitness?" However, we point out that there are two problems for the adaptation between an environment and a species. First, a species generally never can have a perfect knowledge for an environment. Many models of the adaptation to an environment take account into this point. Second, an interaction between a species and an environment never would be independent for the other species. The model of adapting to an environment must satisfy at least these two conditions.

Imperfect knowledge for an environment is expressed by concealing a part of a target bit string. Each species can only observe n-1 bit from a target n-bit strings. The concealed position in a target bit string is randomly selected for each time step. If a concealed position is k ($1 \leq k \leq n$) at time t, each species can observe a target bit string $t_1 t_2 \ldots t_{k-1} t_{k+1} \ldots t_n$.

Here we consider block information. Block information means a part of unchanging bit string by species' adaptation. Each species hold the part of block information in its bit string. The residual part of block information would change its value randomly. The definition of block information is as following.

Definition 3.2 (*Block Information*) Let $[s]_n$ and $[t]_n$ be a n-bit strings. $[s]_n$ is a species and $[t]_n$ is a target. k is a concealed point of a target.

For $1 \leq j \leq n$,

$$b_j = \begin{cases} 1 \text{ (if } a_j = t_j \text{ and } j \neq k) \\ 0 \text{ (if } a_j \neq t_j \text{ and } j \neq k) \\ 0 \text{ or } 1 \text{ (otherwise)} \end{cases}$$

□

From the definition 3.2, we observe that block information $[b]_n$ is also n-bit string. One in block information means unchanging positions by species' adaptation. Zero in block information means changing positions by species' adaptation. In doing this way, we obtain all block information for all species which is a set $B=\{[b^1]_n, [b^2]_n, \ldots, [b^l]_n\}$. The number of elements of a set B is less than the number of elements of M ($|B| \leq |M|$, we denote $|\text{-}|$ as a cardinality) because it contains some block information is the same. For example, consider 3-bit strings. A target, which is the case of no concealed point, is 011 and species are {010, 111, 010}. Then a set of block information is {110, 011}. We also use a set of block information that contains the same block information (the case of above example {110, 011, 110}). We denote this set as $\overline{B}$.

A set of block information constructs a partial set, but not a lattice. A lack of a lattice structure means that there is no unified structure that connects block information each other. Therefore, we need to construct a lattice structure from a given set of bit strings. In this study, we use a topped-intersection structure to construct a lattice. Next definition is the topped-intersection structure for bit strings.

Definition 3.3 (*Topped-Intersection Structure in Bit Strings*) Let L be a set of bit strings. If L is a topped-intersection structure, L satisfies the conditions (a) and (b).

(a) For any $S \subseteq L$, $\wedge S \in L$,

(b) $\vee L \in L$ □

The definition 3.3 means that a topped intersection structure is closed under the meet. In other words, a topped intersection structure contains any pair of elements for the meet operation. We consider 3 bit strings again. A target, which is the case of no concealed point, is 011 and species are {010, 111, 010}. Thus a set of block information is {110, 011}. The topped intersection structure of {110, 011} is {010, 110, 011, 111}. Obviously, {010, 110, 011, 111} makes a lattice. We denote a lattice, which is constructed from block information, as L. By using a

topped intersection structure, we obtain global information between block information.

We defined block information as a required block to raise fitness for each species. However, the decision of block information would involve a contextual constraint. We can correspond this contextual constraint to a quotient lattice because equivalence relations on a lattice are restricted by the global structure. Making a quotient lattice plays a role of an interface between local and global information. Before we discuss how to determine an ideal in the lattice, we define block information being induced by a quotient lattice. The block information, which is induced by a quotient lattice, is as follows.

Definition 3.4 (*Block Information Being Induced by a Quotient Lattice*) Let L be a set of bit strings and θ be a congruence on lattice L. For $1 \le i \le |B|$,

$[b^i]_n \leftarrow \vee \{[x] \in L \mid [x] \in [a]_\theta \text{ such as } [b^i]_n \in [a]_\theta\}$ □

Therefore, we can determine a unique element, which is induced by a quotient lattice. A determined element corresponds to a top of the congruence to which it belongs. The reason of this directly is confirmed from Definition 2.7. Figure 3.1B shows an example of the process from obtaining block information to new block information.

Determining an ideal, which means a down set for a lattice, is important for our model because the result would change by the selection of an ideal. Here we consider a "reference point" to determine an ideal in a lattice L. The meaning of a reference point will be discussed latter. If a reference point is determined, an ideal determines as a following rule.

Rule 1 (*Determining an Ideal*) Let L be a lattice and $[r]_n \in L$ be a reference point. Then an ideal is $\downarrow [x]_n$. $[x]_n$ is randomly selected from a filter $\uparrow [r]_n$. □

Rule 2 (*Determining a Reference Point*) Let L^t be a lattice, $[r]_n^t$ be a reference point and $\overline{B}^t$ be a set of block information, which contains the same block information, at time t. Then a reference point at time $t+1$ is,

$$[r]_n^{t+1} = \begin{cases} [r]_n^t \quad (\text{if } [r]_n^t \in L^{t+1} \text{ and } [r]_n^t \neq [0]_n^t) \\ \text{randomly selected } [x]_n^{t+1} \in \{[r]_n^t \wedge [y]_n^{t+1} \mid [y]_n^{t+1} \in L^{t+1}\} \\ (\text{if } [r]_n^t \notin L^{t+1} \text{ and } [r]_n^t \neq [0]_n^t \text{ and } \{[r]_n^t \wedge [y]_n^{t+1} \mid [y]_n^{t+1} \in L^{t+1}\} \neq \phi) \\ \text{randomly selected } [b]_n^{t+1} \in \overline{B}^{t+1} \ (\text{otherwise}) \end{cases}$$ □

Rule 3 (*Checking a Reference Point*) Let L^t be a lattice, $[r]_n^t$ be a reference point and $\overline{B}^t$ be a set of block information, which contains the same block information, at time t. Then next rule for the reference point is,

$$\begin{cases} \text{Use Rule 2 for next step if}([b^k]_n^t \in \uparrow [r]_n^t) \\ \text{randomly selected } [b]_n^{t+1} \in \overline{B}^{t+1} \text{ for next step (otherwise)} \end{cases}$$

$[b^k]_n^t$ is randomly selected from $\overline{B}^t$ to check a reference point. □

$[0]_n$ means an all zero n-bit string 00...0 in a lattice L. Rule 2 and 3 is how to determine a reference point in a lattice. The reference point is randomly selected from a set $\overline{B}^t$. Therefore, a reference point reflects the proportion of population of block information (4^{th} line of Rule 2). A reference point is created by the intersection operation when the reference point of time t does not exist on a lattice L^{t+1} (2^{nd} line of Rule 2). The reference point plays an important role for the adaptation of species as a whole (see **Results**). Rule 3 suggests we check whether a reference point reflects the proportion of block information in a set $\overline{B}^t$ because the origin of a reference point comes from a set $\overline{B}^t$.

Here we consider the meaning of a reference point in the model. A reference point means the finest information for the resemblance to the target bit strings. From the definition 3.4, we confirm that $[x]_n$ would be substituted by $[r]_n$ if an ideal is $\downarrow[r]_n$ and $[x]_n \leq [r]_n$. The lower elements would be identified by the upper element of the congruence to which they belong. There is no finer block information than a reference point (see Proposition 2.8). Rule 1 means, thus, that the lowest block information in a lattice becomes coarser than a reference point when we construct an ideal.

This strong identification of block information by a quotient lattice would provoke mistakes of block information (see the example of Figure 3.1B). This errant block information, however, contributes to generate a diversification in species without any mutate parameter. We point out that all error of block information are restricted by a reference point and a lattice structure. Errors induced by strong identification are not simply random. The error contains a history of the evolving lattice structure.

We summarize the algorithm of our model.

(A)

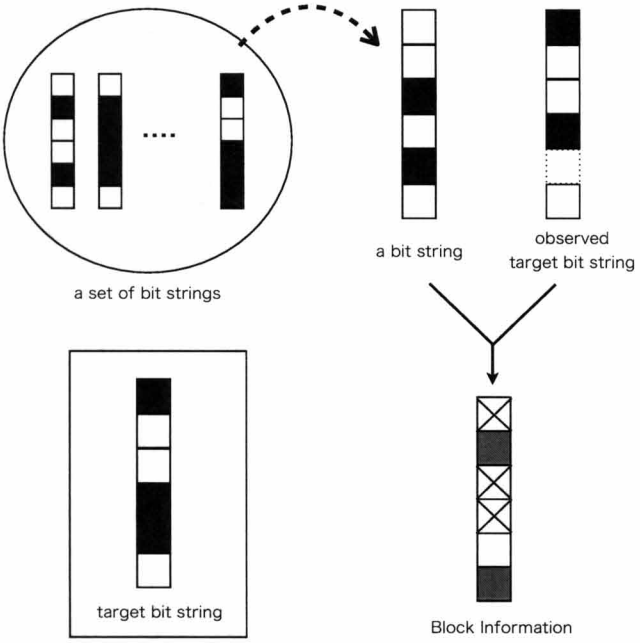

(B)

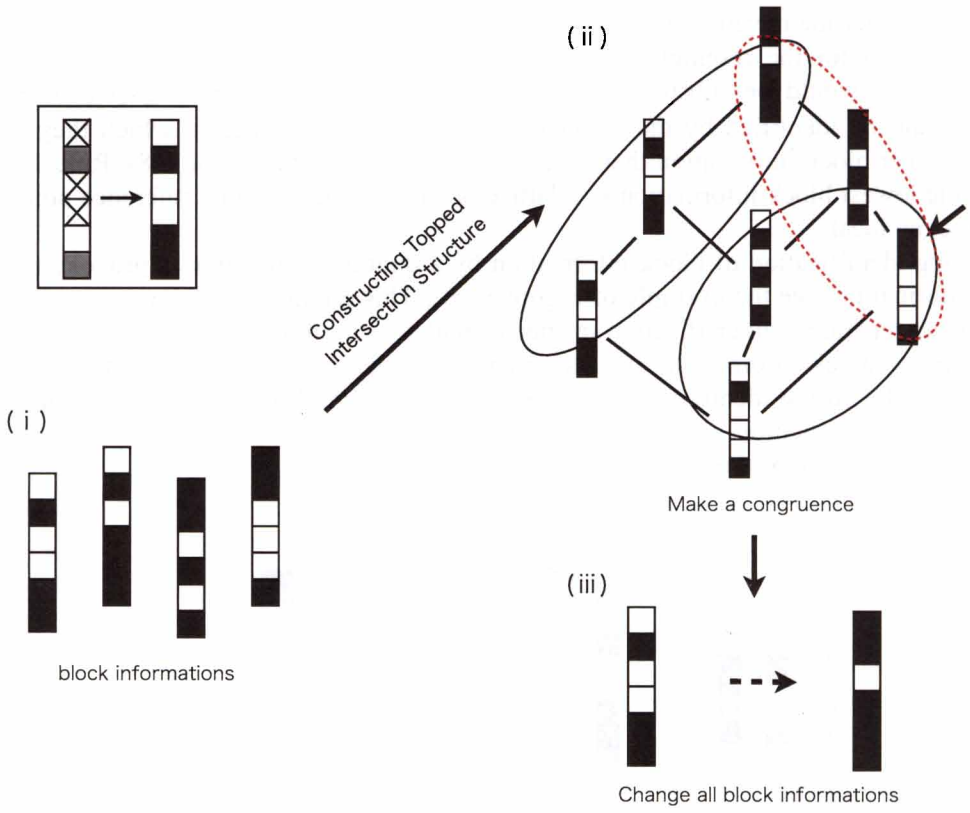

(C)

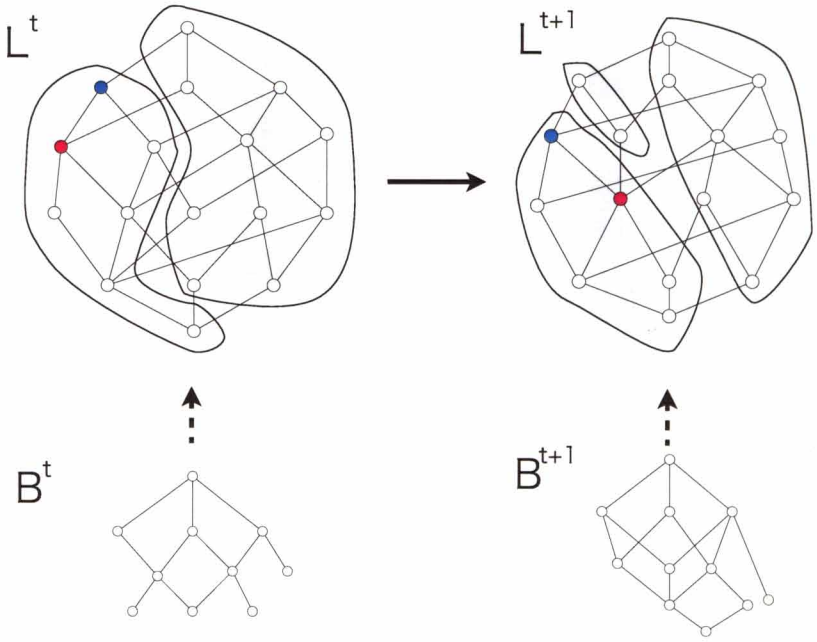

Figure 3.1 (A) Constructing block information from a set of species M. A concealed position corresponds to the dotted rectangle. We color black (one) and white (zero) to each bit string. Block information is represented by gray, white and cross. Grays correspond to unchanging positions. Crosses correspond to changing positions. A white corresponds to undetermined position by Definition 3.2. (B) Image of constructing a topped intersection structure and changing block information from a quotient lattice. Above rectangle shows that block information change its color in this figure. (i) corresponds to a set of block information. (ii) corresponds to a topped intersection structure by using (i). The solid arrow means a reference point. A red dotted circle is a filter of the reference point. Black circles are the congruence. (iii) shows an example of changing block information by using a quotient lattice. (C) Example of the evolving lattice. A set of block information corresponds to B. The constructed lattice

corresponds to L. It can be observed that B is not still a lattice. Red elements mean a reference point. Blue elements mean a selected ideal. The structure of the lattice changes through time step but the reference point is succeeded by into next lattice L^{t+1}.

Algorithm

(1) Generating m n-bit strings $[s^1]_n^0$, $[s^2]_n^0$, ..., $[s^m]_n^0$ and a target $[t]_n$ string randomly.

(2) Determining a concealed position of the target is randomly selected from $\{1, 2, \ldots, n\}$. Making block information from a set of n-bit strings $M^t = \{[s^1]_n^t, [s^2]_n^t, \ldots, [s^m]_n^t\}$ by using Definition 3.2. A set of block information is denoted $B^t = \{[b^1]_n^t, [b^2]_n^t, \ldots, [b^{lt}]_n^t\}$.

(3) Making a lattice L^t by using a topped intersection structure of B^t (Definition 3.3).

(4) Determining a reference point $[r]_n^t$ in a lattice L^t by using Rule 2 and checking a reference point by using Rule 3.

(5) Making an ideal $\downarrow[x]_n^t$ from a reference point $[r]_n^t$ by using Rule 1. Constructing a quotient lattice from the ideal $\downarrow[x]_n^t$.

(6) Substituting new block information by using Definition 3.4.

(7) Changing each n-bit string by using block information. For $1 \le j \le n$ and $1 \le i \le m$,

$$s_j^{i,t+1} = \begin{cases} s_j^{i,t} \ (\text{if } b_j^{i,t} = 1) \\ 0 \text{ or } 1 \ (\text{otherwise}) \end{cases}$$

(8) And constructing new set of species $M^{t+1} = \{[s^1]_n^{t+1}, [s^2]_n^{t+1}, \ldots, [s^m]_n^{t+1}\}$.

□

We define the time step as (2)-(7) as one step. Repeating (2)-(7), we can observe the evolution of species and the lattice. Figure 3.1C is an example of evolving lattice by using our algorithm. We constructed a lattice (L) from the partial order (B), which we called block information. Red elements correspond to a reference point in a lattice and blue elements correspond to a selected ideal by using Rule 1. The reference point is succeeded by into next lattice. Therefore, the identification through a quotient lattice never changes so dramatically, but affects next lattice through the reference point.

3.4. Results

We set the number of species as 2^n for n-bit string. 2^n is the total number of n-bit strings. For example, there are 4 for 2-bit stings, which are {00, 01, 10, 11}. This number setting means that one n-bit string in all kind of n-bit string potentially has one niche. We tried a half and a double of 2^n. However, there was no essential difference between them. Therefore, we fix the number of species as 2^n. There is no additional parameter to our model.

We examine the time series of the evolving lattice model. In this simulation, we consider a set of 8bit strings. Figure 3.2A is the time series of the number of element in the evolving lattice. It can be observed that the number of element in a lattice dynamically changes for every step. This suggests that the global structure, which is constructed from incomplete information, is not static. Therefore, the relation between globality and locality keeps changing through negotiation. Figure 3.2B shows the time series of the averaged distance to the target bit string. The averaged distance d can be computed by using following mathematical expression.

$$d^t = \frac{1}{m}\sum_{i=1}^{m}\sum_{j=1}^{n}\frac{\left|t_j - s_j^{i,t}\right|}{n} \qquad (3.3.1)$$

We point out that the averaged distance also has information of fitness of total species. A bit string has the highest fitness when it is consistent with the target bit string. The averaged distance, thus, is the degree of fitness of total species. Figure 3.2A shows that the averaged distance oscillates around d=1.1. Although d is large for early interval, the value soon shows an oscillation around low d. This oscillation keeps persisting for long time steps. The graph shows that each species tries to adapt the target, but sometimes many species fail to adapt its target. Therefore, the process of the adaptation to the target is far from equilibrium.

Next we discuss Figure 3.2C. The vertical line of Figure 3.2C is bit flip rate per bit. It can be express by using following mathematical expression.

$$flip^t = \frac{1}{m}\sum_{i=1}^{m}\sum_{j=1}^{n}\frac{\left|s_j^{i,t+1} - s_j^{i,t}\right|}{n} \qquad (3.3.2)$$

The time series of bit flip rate shows like white noise (indeed, the slop of the power spectrum is -0.22). The bit flip rate never stays positive, sometimes becomes zero, which means that no bit flip event occurs in a certain interval. No bit flip event can occur when an ideal fully covers a lattice. The degree of the bit flip rate roughly depends on the structure of the quotient lattice, constructed by block information because the way of selecting ideal affect changing or unchanging positions for each bit string. Generally, it tends to become larger the number of elements of a quotient lattice when bit flip rate becomes larger. Figure 3.2D shows the correlation between bit flip rate and the log scale of number of congruence in a quotient lattice. The number of congruence is the number of the partition in a lattice. For example, the number of congruence is two for Figure 3.1B (ii). It can be observed zero bit flip rate occurs only when the number of congruence is one from Figure 3.2D. The correlation coefficient in Figure 3.2D is 0.68. The correlation relationship between them suggests the bit flip is not merely random. The structure of the evolving lattice affects the value of bit flip rate. The bit flip rate temporally changes without any parameter tuning.

(A)

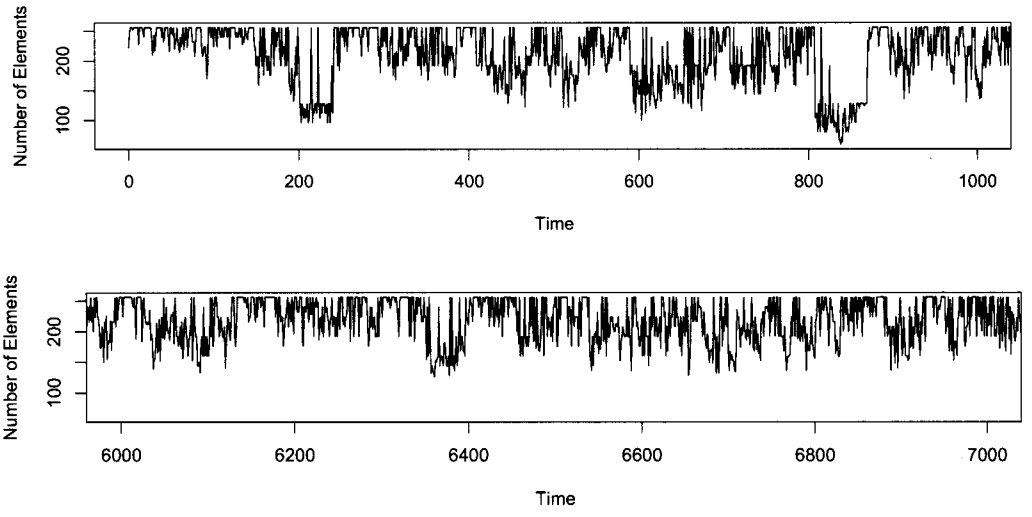

(B)

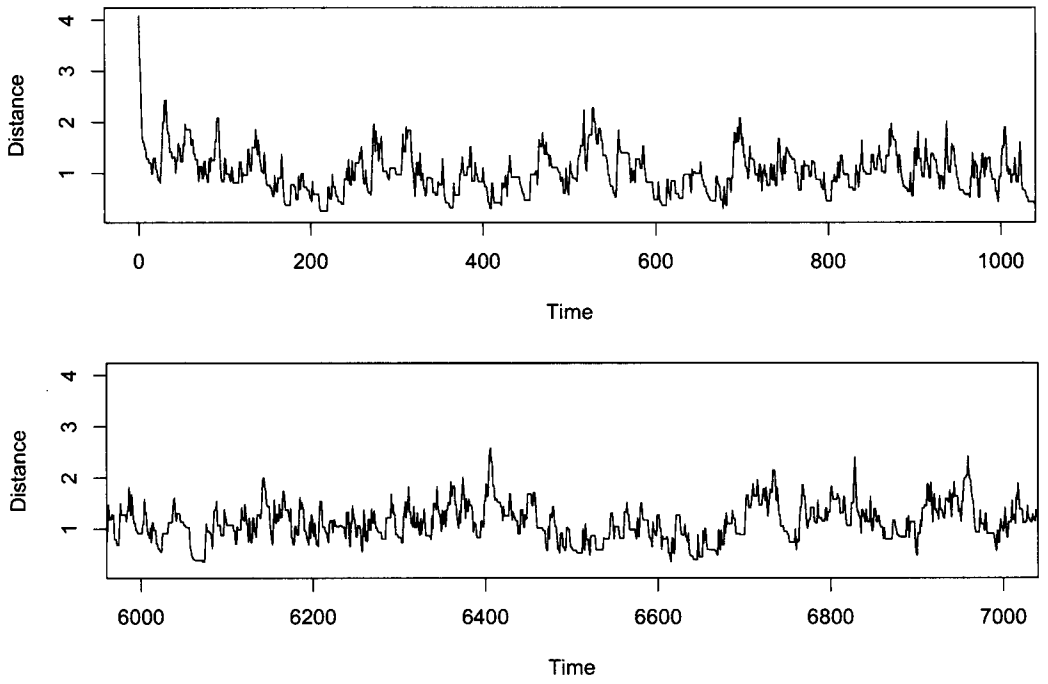
Distance
1
2
3
4
0
200
400
600
800
1000
Time
Distance
1
2
3
4
6000
6200
6400
6600
6800
7000
Time

(C)

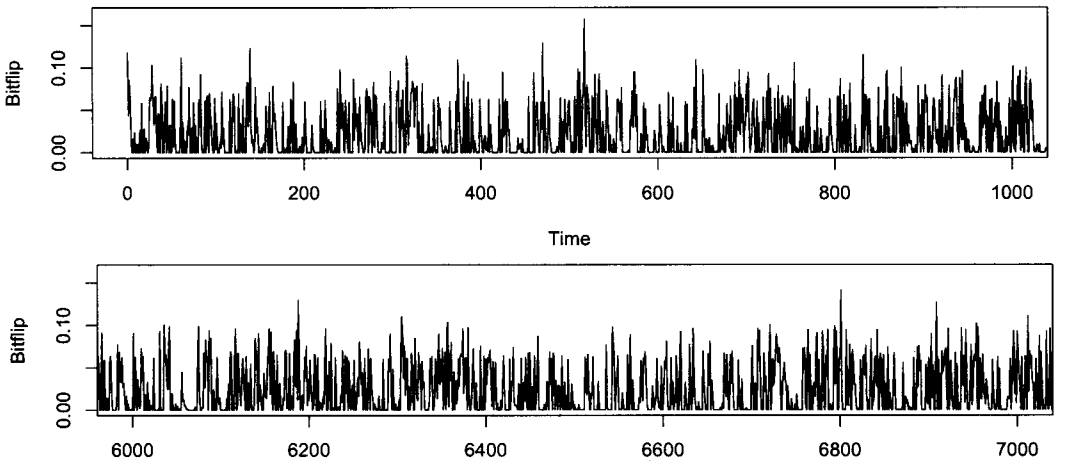
Bitflip
0.00
0.10
0
200
400
600
800
1000
Time
Bitflip
0.00
0.10
6000
6200
6400
6600
6800
7000

(D)

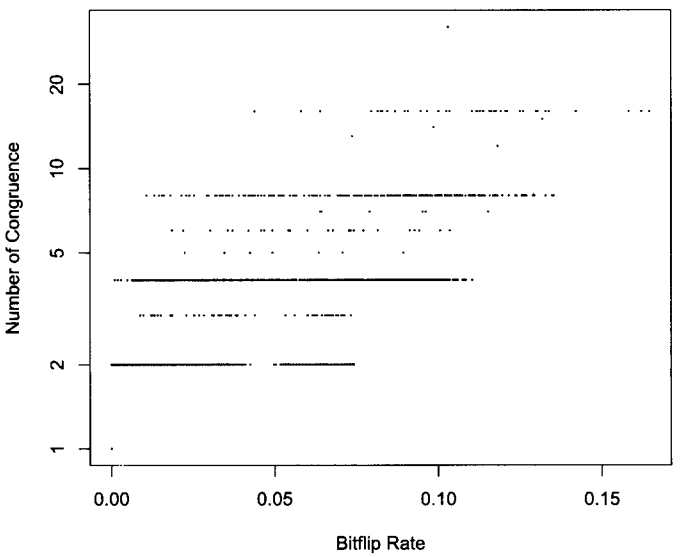
Number of Congruence
1
2
5
10
20
0.00
0.05
0.10
0.15
Bitflip Rate

Figure 3.2 (A) The graph shows a time series of the number of elements of a lattice. The constructed lattice never behaves static but dynamical. (B)The graph shows a time series of the averaged distance between a target and species. Smaller distance means higher fitness of total species. We can observe an oscillation in this graph. The mean averaged value is about 1.1. (C) The graph shows a time series of the averaged bit flip rate per one bit. The bit flip rate is determined by block information and a quotient lattice for each step. (D) The relation between the bit flip rate and log scale of number of congruence in a quotient lattice, which is constructed from block information. There is a roughly correlation relation between them. The correlation coefficient is 0.68.

To estimate the lifetime distribution is very important when we consider the evolutional or ecological system [104]. Especially, the power law whose slop is -2 is universally observed by many biological events such as fossil records [105, 106, 107]. Figure 3.3 shows that our model also has -2 power law for the lifetime distribution for 7-bit, 8-bit and 9-bit strings, respectively (we simulated 100,000 steps, respectively). The lifetime, in this study, is the length of time steps whose one kind of n-bit string exists in the population. Bit strings, which are far from the target, would become extinct for high probability and bit strings, which are near by the target, would survive for high probability. Showing power law distribution means that there is no characteristic scale for extinction events of species. The power law suggests that species never behave independently, but interact each other through incomplete information. In our model, we construct a lattice from disjoint block information. The bit flip rate, which determines extinction events, is regulated by an evolving lattice. This regulation of our model inserts the global information to the population dynamics.

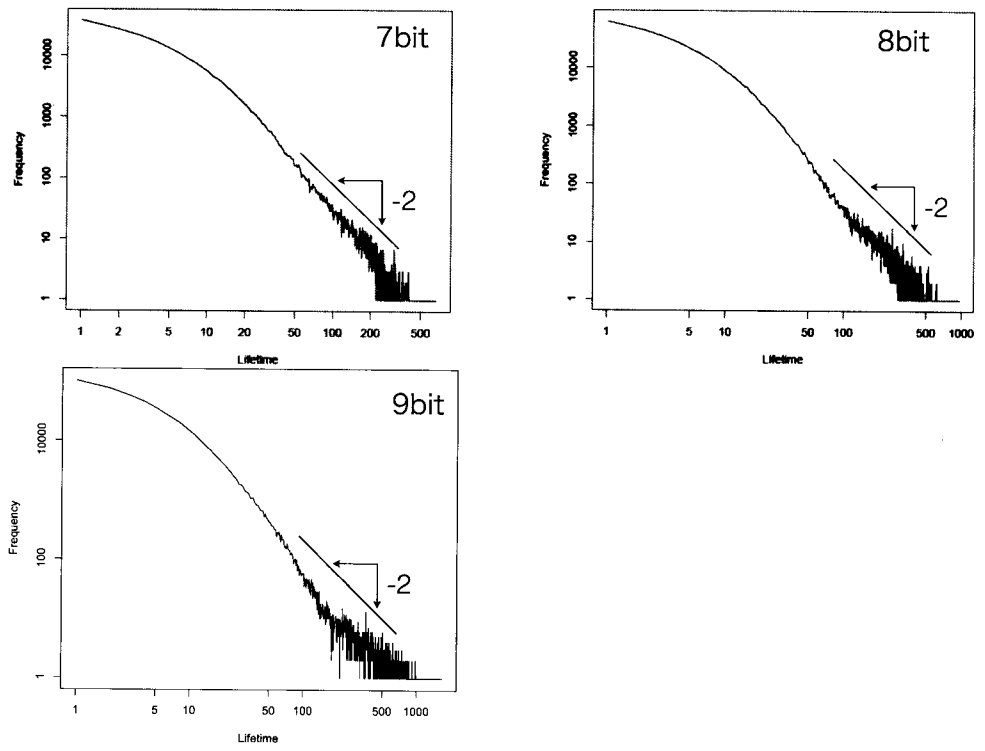

Figure 3.3 Both figures show the distribution the lifetime of each species for 8bit strings and 9bit strings. The vertical line is the frequency and the horizontal line is the lifetime of each species. We plotted them as log-log plot. Both bit strings shows the power law. The slopes of each graph are -2.17±0.15 (7bit), -2.18±0.07 (8bit) and -2.04±0.03 (9bit), respectively. We simulated 100,000 steps for each case.

Evolving lattices also affect oscillations for the averaged distance from the target. Figure 3.4 shows a power spectrum for Figure 3.2B. We define f as a frequency and $S(f)$ as a power spectrum. Then we get the mathematical expression as $S(f) \sim f^{-\gamma}$. The slope of the graph is γ

= -1.36±0.02. In other words, Figure 3.4A obeys $1/f$ fluctuation. This relation indicates that adapting target bit string at different times correlates for the very long time scale. Here we discuss the importance of a reference point for $1/f$ fluctuation. We examined what would happen to the power spectrum without a reference point. Recall a reference point takes in local information. In other words, an element, which constructs an ideal, is randomly selected from evolving lattice without a reference point. If the model lacks a reference point, the distribution of power spectrum shows Figure 3.4B. Obviously, the graph becomes flat for high frequency. We examined both slopes in high frequency region (0,0.05] for these two figures. Then we get both slopes were -1.08±0.02 (Figure 3.4A) and -0.45±0.05 (Figure 3.4B), respectively. The difference of value between them is more than double. Figure 3.4B contains two essential suggestions for our model. One is that there is a distinction between short time scale and long time scale for our evolving lattice model. The slop of low frequency region purely depends on the evolving structure of lattices. Adaptive behavior of long time scale is mainly performed by evolving lattices without the reference point. Another is that divided two regions in power spectrum suggest that $1/f$ fluctuation results from the collaboration between the evolving lattice structure and the way of choosing its reference point. Adding a reference point in a lattice, species also can adjust in short time scales.

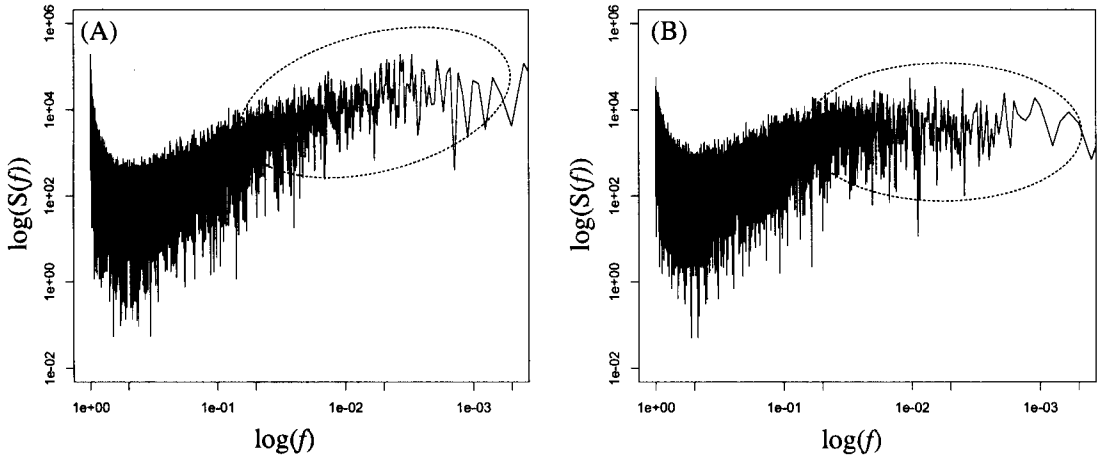

Figure 3.4 Power spectrum $S(f)$ for the oscillation in Fig. 3.2B. The slope of Figure 3.2B is -1.36±0.02. The graph shows $1/f$ noise for species' adaptive behavior. Power spectrum $S(f)$ for the oscillation like Fig. 3.4A without a reference point. The graph becomes flat for high frequency. Species without the reference point never shows the high intensity for short time scales. This suggests that the low intensity for long time scales purely result from global constraints, which correspond to a series of lattice structure. The slopes in the dotted region are -1.08±0.02 (Figure 3.4A) and -0.45±0.05 (Figure 3.4B), respectively.

Next we compared with the model, which we called a "mutation model", to argue the characteristic property of evolving lattice model. The detail of algorithm is listed on Appendix. Here we present the main concept of the mutation model. The mutation model shares the common feature using block information. Each species (n-bit string) constructs block information from the target and divides into two regions, which are unchanging and changing positions. The lattice evolving model change block information by using a quotient lattice, but mutation model change block information by using the probability, which we called mutation rate μ (this concept and the word highly relies on Eigen's model [90]). The mutation rate μ means the probability of copying error. All block information maintain if the mutation rate is zero. However, if the mutation rate becomes larger, unchanging positions tend to change changing position. Therefore, fitness of species becomes low and bit flip rate becomes high when the mutation rate is high. The type of bottom up model (such as mutation, extinction and collective phenomena etc.) uses the parameters which can control each behavior. Tuning these

parameters would lead the model to emerge some corrective properties. We construct the mutation model as one of typical example for the bottom up model.

Figure 3.5A and 3.5B shows the behavior of the mutation model when the mutation rate is controlled. Figure 3.5A is the relation between the mutation rate and the averaged distance to the target bit strings. It can be observed the proportional relation between them. Averaged distance is low (or fitness is high) if the mutation rate is low. We can observe the standard deviation of averaged distance also becomes larger in high mutation rate. This is because of high bit flip rate. In fact, Figure 3.5B shows the proportional relation between the mutation rate and bit flip rate. The high bit flip rate brings on the fluctuation around the mean averaged distance.

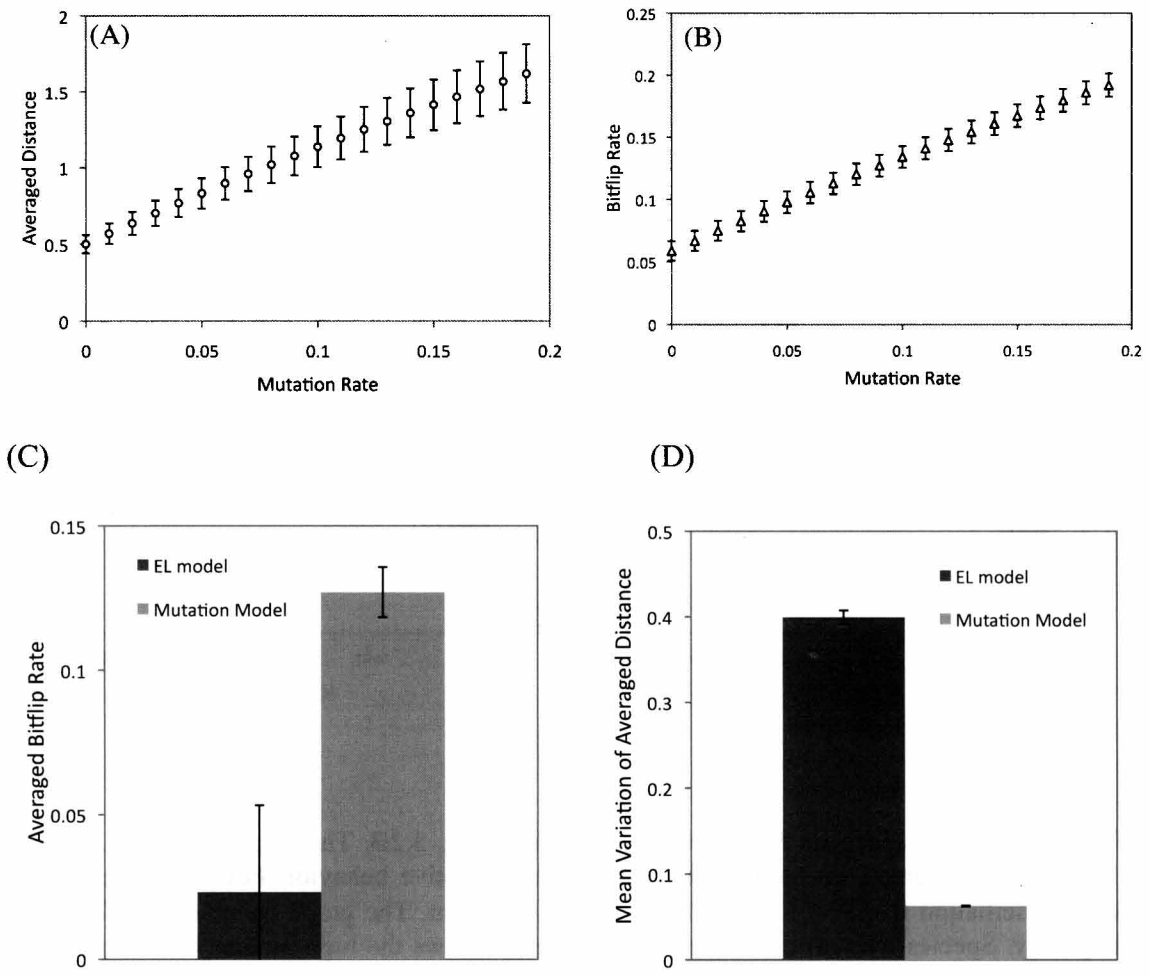

Figure 3.5 Figure 3.5A and 3.5B are the graph of the mutation model. The detail of algorithm is listed on Appendix B. (A) The graph of the relation between mutation rate and averaged distance to the target. Error bars are standard deviations. Averaged distance from the target becomes larger when the mutation rate μ rises. (B) The graph of the relation between mutation rate and bit flip rate. Error bars are standard deviation. The bit flip rate becomes larger when the mutation rate μ rises. Nonzero value of bit flip rate at μ =0 causes the concealed position of the target bit string.

Next two graphs show the comparison with the evolving lattice model and mutation model. The parameter μ in the mutation is fixed at 0.09. The number of species unifies at 2^8=256. (C) Both bars show averaged bit flip rate for the evolving lattice (colored black) model and the mutation model (colored gray). Error bars are standard deviations. The value of averaged bit flip rate of evolving lattice model is six times smaller than one of mutation model. (D) Both bars show mean variation from averaged distance for the evolving lattice (colored black) model and the mutation model (colored gray). Error bars are standard deviations. The value of the evolving lattice model is eight times larger than one of mutation model.

The mean averaged distance of the lattice evolving model is around d=1.1. This value corresponds to μ =0.09 for the mutation model. We fixed, thus, at μ =0.09 to compare with the lattice evolving model. We run the simulation for 8bit strings. First, we compare averaged bit flip rate for both models. Figure 3.5C shows this result. The black bar corresponds to the evolving lattice model and the gray bar corresponds to the mutation model. The graph shows averaged bit flip rate of the mutation model is six times larger than the evolving lattice model. In other words, the averaged bit flip rate of our model is very small (this value is smaller than μ = 0). We point out that bit flip rate of the mutation model hardly becomes zero like the evolving lattice model in Figure 3.2C because the error of the block information is determined stochastically. If the population becomes larger, it becomes impossible to occur no bit flip for every species. By contrast with the mutation model, the bit flip rate of the evolving lattice model never only depends on the probability, but also regulates a lattice structure (see Figure 3.2D). Therefore, bit flip event in the evolving lattice model never occurs as the same intensity.
Figure 3.5D also provides us interesting information. We examined the mean variation (standard deviation) around averaged distance between the target and species. The corresponding colors of Figure 3.5D are the same as the Figure 3.5C. Figure 3.5D shows opposite to the result of Figure 3.5C. The mean variation of averaged distance of the mutation model is eight times smaller than one of the evolving lattice model. This means that the distance to the target hardly moves around the mean averaged distance. High bit flip does not lead the mutation model to high fitness, but stays on low fitness. On the other hand, the evolving lattice model moves for a wide range around mean averaged distance despite low bit flip rate. This fact suggests that the evolving lattice model efficiently uses its bit flips to approach the target bit string. This efficient using bit flip never observed for the probabilistic mutation model because the mutation rate is uniformly distributed to each bit string.

3.5. Discussion

In this study, we start from the concept of incomplete information. Each species decides what are necessary traits by using his information, respectively. Although each species cannot obtain partial information from an environment, how does species can adapt an environment? To overcome this problem, we insisted that it is very important to consider the ceaseless negotiation between local incomplete information and dynamical global information.

We constructed the model with attention to these points. The lattice theory was employed to satisfy the interaction between global and local information. Elements (bit strings) in a set, which we called block information, are merely independent incomplete information per se. To construct the relation between elements, we used the topped intersection structure. By using the topped intersection structure, we can make a lattice from independent elements. Each element has some relation with other elements in a constructed lattice. There is no isolated element in a lattice. We considered that this lattice represents global information among species. This constructed lattice is not static, but dynamic for the time steps.

We observed that our evolving lattice model shows various properties such as power laws for the lifetime distribution and $1/f$ fluctuation for the adapting process. It should be noted that our model never needs bit flip events externally, but makes bit flip events inherently by negotiating between local and global information. The word of inherent here means that the rate of bit flips is never controlled by external parameters. Flipping rate of each bit string is determined by a structure of a lattice at time t. The importance of inherent bit flips rate becomes clear by comparing with the mutation model. The mutation model can control bit flip rate by the parameter μ. In other words, the bit flip events in each bit strings are determined stochastically. We observed that this stochastic event never showed variability of adapting to the target. We also observed that bit flip rate of the evolving lattice model was much smaller than one of the mutation model although our model showed high variability. This suggests that inherent bit flip events are used efficiently to approach the target bit string. Species of the evolving lattice model maneuvers less noise-like event to adapt the environment (the target bit string).

Next we consider the role of the reference point in our model. We suggested importance of the reference point in the lattice structure in adapting process. A reference point would become

the criteria when we make an ideal. This ideal induced a quotient lattice. By using a quotient lattice, all block information change its element to the upper limit in the congruence. Therefore, lower order elements are substituted by upper elements in a lattice. We have observed that this strong identification through a quotient lattice is important role for the population dynamics in species. However, we also observed that it was insufficient for the emergence of $1/f$ fluctuation if there is no reference point. There was a lack for the intensity in short time scale. The reference point in the evolving lattice played a role of adjusting high frequency. Recall the reference point was selected from a set $\overline{B}$. This selection suggests that a selected reference point has a property of an element as local information (one of the block information) and a set as global information (making ideal). In other words, the double meaning of reference point in a lattice activates more dynamical negotiation between global and local information for adaptive process.

One may wonder how is the relation between our model and self-organized criticality (SOC) because our model shows the power law and $1/f$ fluctuation which are often observed in SOC [38, 108, 109]. The concept of SOC is that nature evolves toward the critical state without any fine-tuning. Each species in the critical state connects each other for various time and special scales. The power law and $1/f$ fluctuation suggests self-similar structure for biological events. Bak et al. suggests that each species construct one organization when systems are on the critical state [83, 84]. Recently, it found that flock could move as one corrective because the collection of birds is on the critical state [110]. Many researchers often discussed the relation between SOC and these emergent behaviors as organism. In fact, there are many studies to insist on the biological events (fossil record, corrective behavior and ecology [105, 106, 107, 110]) can be explained by SOC. However, it is still controversial issue for the emergence of SOC.

The most general explanation of the emergence SOC is the balance between two factors, such as the balance between order and disorder or balance between birth and death etc. The simplest example is the random walk model which is discussed by Yang [110]. He considered the moving particle on the one-dimensional line. This particle can move right or left stochastically. In this model, the lifetime is, for instance, the returning time to the first position. Then power law of the lifetime distribution emerges when the probability of moving direction equals 1/2. The particle behaves the critical state when we gives equal probability. Here we must pay attention to the globality invades into this interpretation. Considering the balance between two powers is possible only when the state of two extremes is static. There is no room to consider the negotiation between local and global information once we consider the balance between two extremes. This static view, for example, emerges as the threshold, least fit species and equal probability for moving direction [83, 84, 105, 106, 107, 110]. Then the next question emerges the origin of the balance between two factors.

To consider the negotiation between globality and locality, we must avoid the static assumption between two factors. It would be difficult to explain the origin of the criticality if we assume these static perspectives. Our evolving lattice model proposes a different perspective. In fact, both of global and local information of our model change dynamically. The dynamical local information emerges as incomplete information for an environment. The dynamical global information also emerges as global information constructed from incomplete local information for every step. The incomplete information never works negatively here, but drives the active negotiation between globality and locality. There is no perspective to find the balance between them in our model. Our method would become important when we grasp the emergent property of biological phenomena.

4. Conclusion

Understanding a living system is a very important problem. Autopoiesis and self-organized criticality (SOC) provide some answers to these questions. Both approaches suggest that interfaces between parts and whole are needed to construct models. Autopoiesis intends to overcome this problem by constructing a one-to-one correspondence between parts and whole [7]. SOC intends to overcome this problem by using criticality [111]. In this paper, we insisted that understanding collective behavior helps to answer this question because individuals behave as one collective without any central control [28, 30, 31]. Collective behavior emerges only through local interactions. In fact, in order to explain flocking phenomena, the field naturalist Edmund Selous concluded that somehow, a connectivity of individual minds and transference of thoughts must underlie such behavior [28]. We could sometimes admit this kind of mind for a set of individuals. Therefore, the question of "what is a life?" lies closer to the question of "what is a collective behavior?" than we expected.

In this study, we discussed the collective behavior which is observed in a flocking and an evolutional system. Each individual tries to adjust type- and token- cognition. We have considered a type cognition as the class cognition in Chapter 2 and the global lattice structure in Chapter 3. By contrast, we have corresponded a token cognition to a collection cognition in Chapter 2 and a block information of partial ordered set in Chapter 3. Each individual becomes differentiate the type and the token cognition in its own experience.

We insisted in this study that the phenomenon of scale-free correlation might be a bridge between parts and whole in Chapter 2. Flocks always contain scale-independent correlated subparts that are represented by fluctuation vectors. Each correlated sub-domain provides an effective perception for each individual that belongs to the sub domain [34]. This means that a perception of one individual corresponds to the group perception. Cavagna and others, in fact, implied that scale-free correlation (or a criticality of flock) might contribute to the fascinating "collective mind" metaphor at a more quantity level. We observed that the MTI model satisfied various critical properties such as self-similar structure and $1/f$ fluctuation of the oscillation strength of fluctuations. For both cases, flocks in the MTI mode have a certain type of criticality for both extremes, such as spatial and temporal aspects. MTI flocks spontaneously direct and keep their fluctuations on the critical state for spatial and temporal aspects. These results are very consistent with SOC properties [36, 37, 111] and support Cavagna's presumption that flocks are on critical states, for various aspects. Furthermore, we have discussed an evolutionary system also has SOC properties such as -2 power low and $1/f$ fluctuation in adapting process in Chapter 3. These facts suggest that each species behaves as one collective like flocking phenomena when they adapt to an uncertain environment. In the evolving lattice model, the reference point has an important role for the $1/f$ fluctuation in a short time range. To achieve collectivity, it would need the connecting elements between the global and local information. This discussion also applies to the MTI model. The individual of the MTI model evaluated through observing concrete information of its neighbors by checking the difference between them when it uses the metric (type) interaction.

Is fulfilling these critical properties sufficient to understand a life or a mind? Critical properties are indeed very important for flocks to react more sensibly to external perturbations. Flocking behavior may be on the border between order and disorder. This interpretation resembles the idea of the edge of chaos as the metaphor for life [19, 20]. However, we consider that scale-free correlation in real flocks has a more suggestive aspect than the critical state. We recall that correlated domains not only have a role in effective perception that is suggested by Cavagna and others, but also are subparts that have the possibility to behave as an independent flock. This possibility was discussed in the section about splitting flocks. Extending an individual's perception range increases his ability to respond to external perturbation such as a predator at tack. There is no benefit for survival, however, if flocks promptly change their directions to another side. In a similar way, there is a difference between "a system" and "making a system".

This is a shortcoming of SOC because most SOC models focus on the problem of "keeping its critical state" [112, 113]. In fact, some SOC models are associated with a lack of efficiency of learning, despite showing versatility [36, 37, 112, 113]. In other words, critical fluctuations

never assist with efficient learning, although it shows criticality. If we want to discuss a living system, we must consider both sides, which are "system" and "making a system". "Making a system", in this case, corresponds to "using its critical state" to drive its own system. For example, MTI flocks rapidly change direction without any external noise. Noise is inherent. Each internal but scale-invariant fluctuation enables the flock to change direction abruptly. This fact suggests that criticality in MTI flocks never sacrifices their mobility as flocks. Thus, the MTI model holds both conditions, "system" and "making a system". In Chapter 3, we also observed that inherent noise is (bit flip rate) efficiently used in the adapting process, compared with the mutation model.

The general concept of "life on the critical state" is broadly embraced by several researchers [19, 20, 37, 112, 113, 114]. It is important in flocking cases that the critical state provides high sensibility to external perturbations to extend individuals' effective perception range. The critical state is also observed in MTI flocks for spatial and temporal cases. However, we observed that this critical state, which is a correlated sub-domain in this case, also has the potential to split the flock's body. Additionally, these correlated subparts behave as individual flocks after they split. Furthermore, MTI flocks can change their direction abruptly by using internal fluctuations. These facts suggest that internal fluctuations, which are on the critical state, contribute to dynamical flocking motion in reducing the risk of collapse. A system that utilizes critical fluctuations positively has to be distinguished from a system that passively receives critical fluctuations. Flocks maneuver internal fluctuations when they act. Evolving lattice model in ecology, in Chapter 3, suggests the same fact. Whole species could use the fluctuation, which seems random, efficiently as one system. It is suggested that critical phenomena play an essential role in driving a living system. This calls attention to another aspect, which is "how to use criticality for a living system". By using type and token perspective brought us new perspective of system theory.

Appendix A

The outline of the MTI model algorithm is as follows. All symbols that are used for equations from (1) to (8) is given an explanation as follows.

t : the time step
$i, k, s, \ldots$: the index of the individual
N: a set of individuals
n: the number of elements of set N
th: a threshold parameter
R^1_{min}: a minimum length of repulsion zone
R^2_{min}: a minimum length of alignment zone
V_0: the standard speed
V_+: the variation of speed

The symbol that is listed below is different for each time (indexed t) and each individual (indexed k). We added to all symbols as $(\text{-})_k^t$. This symbol means that the quantity of – for the individual k at time t.

$\mathbf{x}$: a position vector of each individual
$\mathbf{v}$: a velocity vector of each individual
v: a velocity (or norm of the velocity vector $\mathbf{v}$) of each individual
N-TOP : a set of the topological neighbors
n_T: the number of elements of the set *N-TOP*
R_1: a length of the repulsion zone
R_2: a length of the alignment zone
R_3: a length of the attraction zone
$N\text{-}MET_{Repulsion}$: a set of individuals on the repulsion zone
$N\text{-}MET_{alignment}$: a set of individuals on the alignment zone
$N\text{-}MET_{Attraction}$: a set of individuals on the attraction zone
n_{Rep}: the number of element of the set $N\text{-}MET_{Repulsion}$
n_{Align}: the number of element of the set $N\text{-}MET_{Alignment}$
n_{Attra}: the number of element of the set $N\text{-}MET_{Attraction}$

Each velocity vector can be also represented in the polar coordinate (v_k^t, θ_k^t) in two-dimension.

x-coordinate: $(\mathbf{v}_k^t)_x = v_k^t \cos(\theta_k^t)$
y-coordinate: $(\mathbf{v}_k^t)_y = v_k^t \sin(\theta_k^t)$

Each velocity vector can be also represented in the polar coordinate $(v_k^t, \varphi_k^t, \theta_k^t)$ in three-dimension.

x-coordinate: $(\mathbf{v}_k^t)_x = v_k^t \cos(\varphi_k^t)\sin(\theta_k^t)$
y-coordinate: $(\mathbf{v}_k^t)_y = v_k^t \sin(\varphi_k^t)\sin(\theta_k^t)$
z-coordinate: $(\mathbf{v}_k^t)_z = v_k^t \cos(\theta_k^t)$

Start the Algorithm
First, Each individual is allocated space and given a direction at random.

The algorithm at time t.
for(from k=1 to k= n){

if(individual k uses the topological interaction){

$$\hat{\mathbf{v}}_k^{t+1} = \hat{\mathbf{v}}_k^t + \frac{1}{(n_T)_k^t} \sum_{l \in N\text{-}TOP_k^t} \hat{\mathbf{v}}_l^t$$

$\cdot N\text{-}TOP_k^t \equiv \{l \in N \mid \text{rank}(l) \le n_t\}$
$\cdot (n_T)_k^t = \text{Num}(N\text{-}TOP_k^t)$

·rank(l): the order of the distance between $\mathbf{x}_k^t$ and $\mathbf{x}_l^t$.

$$v_i^{t+1} = V_0 - V_+ \cos(\theta)$$
$$\mathbf{v}_k^{t+1} = v_k^{t+1}\hat{\mathbf{v}}_k^{t+1}$$

if($\forall i \in N\text{-}TOP_k^t$, $\cos^{-1}\left\langle \hat{\mathbf{v}}_i^t, \langle \hat{\mathbf{v}}_l^t \rangle_{l \in N-TOP_k^t} \right\rangle < th$){

$$\#_k^t = \begin{cases} [(\|\mathbf{x}_k^t - \mathbf{x}_s^t\| - R_{\min}^2)/5] & \text{when } \|\mathbf{x}_k^t - \mathbf{x}_s^t\| - R_{\min}^2 > 0 \\ 0 & \text{otherwise} \end{cases}$$
$$(R_1)_k^t = R^1{}_{\min} + r \times \#_k^t$$
$$(R_2)_k^t = R^2{}_{\min} + al \times \#_k^t$$
$$(R_3)_k^t = (R_2)_k^t + at \times \#_k^t$$

· [] is a floor function.
· < , > is an inner product.
· $< >_S$ is an average of the individuals' direction on a set S.
· the individual indexed s is 6th neighbor from the individual indexed k.
The individual k uses the metric interaction for the next step.

}
else{
The individual k uses the topological interaction for the next step.
}
} **End topological interaction for an individual *k***

if(individual k uses the metric interaction){

<for repulsion zone>

$$(\hat{\mathbf{v}}^{Repulsion})_k^t = -\frac{1}{(n_{Rep})_k^t} \sum_{l \in (N-MET_{Repulsion})_k^t} \frac{\mathbf{x}_l^t - \mathbf{x}_k^t}{\|\mathbf{x}_l^t - \mathbf{x}_k^t\|}$$
· $(N\text{-}MET_{Repulsion})_k^t \equiv \{l \in N \mid 0 < \| \mathbf{x}'_k - \mathbf{x}'_l \| < (R_1)_k^t\}$
· $(n_{Rep})_k^t = \text{Num}((N\text{-}MET_{Repulsion})_k^t)$

<for alignment zone>

$$(\hat{\mathbf{v}}^{Alignment})_k^t = \frac{1}{(n_{Align})_k^t} \sum_{l \in (N-MET_{Alignment})_k^t} \frac{\mathbf{v}_l^t}{|\mathbf{v}_l^t|}$$
· $(N\text{-}MET_{Alignment})_k^t \equiv \{l \in N \mid (R_1)_k^t < \| \mathbf{x}'_k - \mathbf{x}'_l \| < (R_2)_k^t\}$
· $(n_{Align})_k^t = \text{Num}((N\text{-}MET_{Alignment})_k^t)$

<for attractive zone>

$$(\hat{\mathbf{v}}^{Attraction})_k^t = \frac{1}{(n_{Attra})_k^t} \sum_{l \in (N-MET_{Attraction})_k^t} \frac{\mathbf{x}_l^t - \mathbf{x}_k^t}{\|\mathbf{x}_l^t - \mathbf{x}_k^t\|}$$
·$(N\text{-}MET_{Attraction})_k^t \equiv \{l \in N \mid (R_2)_k^t < \| \mathbf{x}'_k - \mathbf{x}'_l \| < (R_3)_k^t\}$
· $(n_{Attra})_k^t = \text{Num}((N\text{-}MET_{Atrraction})_k^t)$

Then;
$$\hat{\mathbf{v}}_k^{t+1} = \hat{\mathbf{v}}_k^t + (\hat{\mathbf{v}}^{Repulsion})_k^t + (\hat{\mathbf{v}}^{Alignment})_k^t + (\hat{\mathbf{v}}^{Attraction})_k^t$$
$$v_i^{t+1} = V_0 - V_+ \cos(\theta)$$
$$\mathbf{v}_k^{t+1} = v_k \cdot \hat{\mathbf{v}}_k^{t+1}$$

if $(\forall i, j \in (N\text{-}MET_{Repulsion})_k^t \cup (N\text{-}MET_{Alignment})_k^t,\ \cos^{-1}(\langle \hat{\mathbf{v}}_i^t, \hat{\mathbf{v}}_j^t \rangle) > 2 * th$){
· i and j are randomly selected from the set $(N\text{-}MET_{Repulsion})_k^t$ or $(N\text{-}MET_{Alignment})_k^t$.
The individual k uses the topological interaction for the next step.
}
else{

The individual k uses the metric interaction for the next step.
The interaction domains, which are $(R_1)_k^t$, $(R_2)_k^t$ and $(R_3)_k^t$,
are preserved for next step.

}

} **End metric interaction for a individual *k***

} **End update all individuals**

Then back to the algorithm, which is **for**(from k=1 to k=n){–}, and repeat the same process to all individuals.

End all algorithm.

Here we set the parameter of MTI model. The threshold parameter *th* is fixed at 0.05 radians unless otherwise noted. This parameter determines the switching property of each individual. If *th* sets a small value, the individual tends to use the topological interaction. Or if *th* sets a large value, the individual tends to use the metric interaction. The number of individuals for the topological interaction is fixed at six through this study. V_0=3.0 and V_+ = 2.0. Thus the minimum speed is 1.0 and the max speed is 5.0. R_{min}^1=80 and R_{min}^2=100. The proportional constants are r=3.0, al=5.0, at= 2.5. These values selected to match with experimental data. If these value change, the slope of Figure. 2.22C and 2.22D will change or correlated relations would disappear. The space is set as $width^3$. The size of the space is fixed at $width$ = 2,000.

Appendix B

We give an explanation for a comparing model. The concept of the model comes from ideal copies and error. Each species tries to adapt its environment, which is represented by the target bit string. The target also has a randomly determined concealed position for every step. Then algorithm is as follows.

(1) Generating m n-bit strings $[s^1]_n^0$, $[s^2]_n^0$, ..., $[s^m]_n^0$ and a target $[t]_n$ string randomly.

(2) Determining a concealed position of the target is randomly selected from $\{1, 2, \ldots, n\}$. Making block information from a set of n-bit strings $M^t = \{[s^1]_n^t, [s^2]_n^t, \ldots, [s^m]_n^t\}$ by using Definition 3.2. A set of block information is denoted $B^t = \{[b^1]_n^t, [b^2]_n^t, \ldots, [b^{lt}]_n^t\}$.

(3) Changing each n-bit string by using block information. For $1 \le j \le n$ and $1 \le i \le m$,

$$s_j^{i,t+1} = \begin{cases} s_j^{i,t} & \text{if } (b_j^{i,t} = 1 \text{ and probability } (1-\mu)) \\ 0 \text{ or } 1 & \text{if } (b_j^{i,t} = 1 \text{ and probability } \mu) \\ 0 \text{ or } 1 & \text{(otherwise)} \end{cases}$$

And constructing new set of species $M^{t+1} = \{[s^1]_n^{t+1}, [s^2]_n^{t+1}, \ldots, [s^m]_n^{t+1}\}$.

Repeat the process (2) – (3). μ means a mutation rate for each bit in a string. Each species can copy completely without the concealed position when μ equals zero.

Bibliography

(1) von Bertalanffy, L., General System Theory: Foundations, Development and Applications, Penguin, 1973

(2) Letelier, J.C., Marin, G., & Mpodozis, J., 2003. Autopoietic and (M, R) systems. *J. Theor. Biol.* 222, 261-272.

(3) Letelier, J.C., Soto-Andrade, J., Abaruzia, F.G., Bowden, A.C., and Cardenas, M.L., 2006, Organizational invariance and metabolic closure: analysis in terms of (M, R) systems. *J. Theor. Biol.* 238, 949-961

(4) Maturana, H. and Varela, F. (1972). *Autopoeisis and Cognition*. Dordrecht: Reidel.

(5) Maturana, H. and Varela, F. (1980). *Autopoeisis and Cognition*. Dordrecht: Reidel.

(6) Maturana, H. and Varela, F. (1992). *The Tree of Knowledge: The Biological Roots of Human Understanding*. Boston: Shambhala.

(7) Varela, F. (1979). *The Principles of Biological Autonomy*. New York: North Holland.

(8) Rashevsky, N., 1954, Topology and life: in search of general mathematical principles in biology and sociology. *Bull. Math. Biophys.* 16, pp. 317–348.

(9) Rosen, R., 1958, A relational theory of biological systems. *Bull. Math. Biophys.* 20, pp. 245–341.

(10) Rosen, R., 1985, *Anticipatory Systems*, Pergamon, Oxford.

(11) Rosen, R., 1991, *Life Itself*, Columbia University Press, New York

(12) Bushev, M., 1994, *Synergetics: Chaos, Order, Self-Organization*. World Scientific Publishing CO. Pte. Ltd.

(13) Haken, H., 1978, *Synergetics – An Introduction*. Springer – Verlag.

(14) Haken, H., 1996, *Principles of Brain Functioning*. Springer – Verlag.

(15) Wolfram, S., 2002 *A New Kind of Science*, Wolfram Media, Inc., Cham- paign, Illinois.

(16) Cook, M., 2004, Universality in Elementary Cellular Automata, *Complex Systems* 15 (1) 1–40.

(17) Margolus, N., 1984, Physics-like models of computation, *Physica D.* 10: 81–95.

(18) Mitchell, M., 2011, *Complexity: A Guided Tour*. Oxford University Press.

(19) Kauffman, A., and Johnsen, S. 1991, Coevolution to the edge of chaos:coupled fitness landscapes, poised states, and coevolutionary avalanches. *J. Theor. Biol*, 149:467–505.

(20) Langton, C., 1990, Computation at the edge of chaos: Phase transitions and emergent computation. *Physica D*, 42:12–37

(21) Copelli, M., Roque, A. C., Oliveira, R. F. & Kinouchi, O., 2002, Physics of psychophysics: Stevens and Weber-Fechner laws are transfer functions of excitable media. *Phys. Rev. E* 65, 060901.

(22) Kinouchi, O and Copelli, M., 2006, Optimal dynamical range of excitable networks at criticality. *Nature*. 348-352.

(23) Stevens, S. S. 1975, *Psychophysics: Introduction to its Perceptual, Neural and Social Prospects*, Wiley, New York.

(24) N. Bertschinger and T. Natschläger. 2004, Real-time computation at the edge of chaos in recurrent neural networks. *Neural Computation*, 16(7): 1413-1436.

(25) Vicsek, T. 2001, *Fluctuations and Scaling in Biology*. Oxford University Press.

(26) Vicsek, T., Czir`ok, A., Ben-Jacob, E., Cohen, I., and Shochet, O. 1995, Novel type of phase transition in a system of selfdriven particles. *Phys. Rev. Lett.*, 75:1226.

(27) Couzin, I. 2008, Collective mind. *Nature*, 715.

(28) Couzin, I., Krause, J., James, R., Ruxtion, G., and Franks, N. 2002, Collective memory and spatial sorting in animal groups. *Journal of Theoretical Biology*, 218:1–11.

(29) Grégoire, G., Chaté, H., and Tu, Y. 2003, Moving and staying together without a leader. *Physica D*, 181:151–170.

(30) Sumpter, D. 2006. The principles of collective animal behavior. *Phil. Trans. Soc. B.*, 361:5–22.

(31) Sumpter, D. 2010, *Collective Animal Behavior*. Princeton University Press.

(32) Ballerini, M., Cabibbo, V., Candelier, R., Cisbani, E., Giardina, I.,Lecomte, V., Orlamdi, A., Parisi, G., Procaccini, A., Viale, M., and Zdravkovic, V. 2008, Iempirical investigation of starling flocks: A benchmark study in collective animal behavior. *Animal Behavior*, 76:201–215.

(33) Ballerini, M., Cabibbo, V., Candelier, R., Cisbani, E., Giardina, I., Lecomte, V., Orlamdi, A., Parisi, G., Procaccini, A., Viale, M., and Zdravkovic, V. 2008, Interaction ruling animal collective behavior depends on topological rather than metric distance: Evidence from a field study. *Proc. Natl. Acad. Sci. U.S.A.*, 105:1232–1237.

(34) Cavagna, A., Cimarelli, C., Giardina, I., Parisi, G., Santagati, R., S. F., and Viale, M. 2010, Scale-free correlation in the bird flocks. *Proc. Natl. Acad. Sci. U.S.A.*

(35) Mora, T. and Bialek, W. 2010, Are biological systems poised at criticality? arXiv.

(36) Bak, P. 1997, How Nature Works: The Science of Self-Organized Criticality. Oxford University Press.

(37) Bak, P. and Sneppen, K. 1993, Punctuated equilibrium and criticality in a simple model of evolution. Phys. Rev. Lett, 71:4083.

(38) Bak, P., Tang, C., and Wiesenfeld, K. 1987, Self organized criticality: An explanation of 1/f noise. Phys. Rev. Lett, 59(4):381–384.

(39) Penn, D.C., Holyoak, K.J. & Povinelli, D.J. 2008, Darwin's mistake: Explaining the discontinuity between human and nonhuman minds. Behavioral and Brain Sciences, 31: 109-178.

(40) Fodor, J.A., 1975, *The Language of Thought*. Crowell.

(41) Fodor, J.A., 1997, Connectionism and the problem of sytematicity (continued): Why Smolensky's solution still doesn't work. *Cognition* 62:109-119.

(42) Deneubourg, J.L. & Goss, S., 1989, Collective Patterns and Decision-Making. *Ethology Ecology & Evolution* 1: 295-311.

(43) Goldstone, R.L. & Gureckis, T.M., 2009, Collective Behavior. *Topics in Cognitive Science*, 412-438.

(44) Makris, N.C., Ratilal, P., Jagannathan, S., Gong, G., Andrew, M., Bertsatos, I., Godø, O.R., Nero, R.W. & Jech, M. 2009, Critical Population Density Triggers Rapid Formation of Vast Oceanic Fish Shoals. *Science*. 323: 1734-1737.

(45) Moussaid, M., Garnier, S., Theraulaz, G. & Helbing, D., 2009, Collective Information Processing and Pattern Formation in Swarms, Flocks, and Crowds. *Topics in Cognitive Science,* 469-497.

(46) Parrich, J.K., 1989, Layering with Depth in a Heterospecific Fish Aggregation. *Environmental Biology of Fishes*. 26: 79-85.

(47) Parrish, J.K. 1999, Complexity, Pattern, and Evolutionary Trade-Off in Animal Aggregation. *Science*; 284: 99-101.

(48) Parrish, J.K., Viscido, S.V. & Grunbaum, D., 2007, Self-Organized Fish Schools: An Examination of Emergent Properties. *Biol. Bull.*; 202: 296-305.

(49) Parrish, J.K. & Hammer, W.M., 2007, *Three Dimensional Animal Groups*. Cambridge University Press, Cambridge, England.

(50) Helbing, D., Keltsch, J. & Molnar, P., 1997, Modelling the evolution of human trail systems. *Nature*. 338: 47-50.

(51) Buhl, J., Sumpter, D.J.T., Couzin, I.D., Hale, J.J., Despland, E., Miller, E.R. & Simpson, S.J., 2006, From Disorder to Order in Marching Locusts. *Science*. 312: 1402-1406.

(52) Grégoire, G., Chaté, H. & Tu, Y., 2001, Commetnt on "Particle Diffusion in a Quasi-Two Dimensional Bacterial Bath". *Physical Review Letters*. 86(3): 556.

(53) Grégoire, G., Chaté, H. & Tu, Y., 2001, Active and Passive Particles: Modeling Bead in a Bacterial Bath. *Physical Review E*. 64: 011902-1.

(54) Giardina, I., 2008, Collective Behavior in Animal Groups: Theoretical Model and Empirical Studies. *HFSP Journal*. 2(4): 205-219

(55) Reynolds, C.W., 1987, Flocks, Herds, and Schools: A Distributed Behavioral Model. *Computer Graphics*. 21(4): 25-34.

(56) Szabó, P., Nagy, M. & Vicsek, T., 2009, Transition in a Self –Propelled-Particles model with Coupling of Accelerations. *Physical Review E*. 79: 021908-1.

(57) Czirok, A. & Vicsek, T., 2006, Collective Behavior of Interacting Self-Propelled Particles. *arXiv*.

(58) Grégoire, G. & Chaté, H., 2004, Onset of Collective and Cohesive Motion. *Physical Review Letters*. 92(2). 025702-4.

(59) Huth, A. & Wissel, C., 1992, The Simulation of the Movement of Fish School. *J. theor. Biol.* 156: 365-385.

(60) Aoki, I., 1982, A Simulation Study on the Schooling Mechanism in Fish. *Bulletin of the Japanese Society of Scientific Fisheries.* 40: 1081-1088.

(61) Bajec, I.L., Zimic, N. & Mraz, M., 2005, Simulating flocks on the wing: the fuzzy approach. *J. theor. Biol.* 233(2): 199-220.

(62) Bode, W. F., Franks, D.W. and Wood, A. J., 2010, Making Noise: Emergent Stochasticity in Collective Motion. *J. theor. Biol.* 267: 292-299.

(63) Bode, W. F., Franks, D.W. and Wood, A. J., 2010, Limited Interactions in Flocks: Relating Model Simulation to Empirical Data. *J. R. Soc. Interface.* Published Online.

(64) Ginelli, F. and Chaté, H., 2010, Relevance of Metric-Free Interaction in Flocking Phenomena. *Physical Review Letters.* 105: 168103-1 – 168103-4.

(65) Buscarino, A., Fortuna, L., Frasca, M. & Rizzo, A., 2009, Synchronization in Networks of Mobile Agents. in *Estimation and Control Networked Complex Systems.*

(66) Hildenbrandt, H., C. Carere, and C.K. Hemelrijk, 2010, Self-organized aerial displays of thousands of starlings: a model. *Behavioral Ecology*, 21(6): p. 1349-1359.

(67) Jadbadaie, A., Lin, J. & Morse, 2003, M. Coordination of Groups of Mobile Autonomous Agents Using Nearest Neighbor Rules. *IEEE Trans Auto Control.* 48: 988-1001.

(68) Hemelrijk, C.K. and H. Kunz., 2005, Density distribution and size sorting in fish schools: an individual-based model. *Behavioral Ecology.* 16(1): p. 178-187.

(69) Hemelrijk, C.K. and H. Hildenbrandt, 2008, Self-organized shape and frontal density of fish schools. *Ethology*, 114: p. 245-254.

(70) Reuter, H. and B., 1994, Breckling, 1984, Self organization of Fish Schools - an Object-Oriented Model. *Ecological Modelling.* 75: p. 147-159.

(71) Miller, G.A. 1953, The magical Number Seven, Plus or Minus Two: Some Limits on our Capacity for Processing Information. *Psychological Review.* 63: 81-97.

(72) Agrillo, C., Dadda, G., Serena, G. and Bisazza, A., 2008, Do fish count? Spontaneous Discrimination of Quantity in Female Mosquitofish. *Anim. Cogn.* 11: 495-503.

(73) Agrillo, C., Dadda, G., Serena, G. and Bisazza, A., 2009, Use of Number by Fish. *PLoS One.* 4(3): e4786.

(74) Feigenson, L., Dehaene, S. and Spelke, E., 2004, Core Systems of Number. *Trends in Cognitive Science.* 8(7): 307-314.

(75) Vos, P. G., Van Offelen, M. P, Tibosch, H.J. and Allik, J., 1988, Interaction between area and numerosity. *Phychol Res.* 50: 148-154.

(76) Huepe, C. & Aldana, M., 2004, Intermittency and Clustering in a System of Self-Driven Particle. *Phys. Lev. Lett.* 92(16) 168701-1-4.

(77) Dossetti, V., Sevilla, F.J. & Kenkre, V.M., 2009, Phase Transition Induced by Complex Nonlinear Noise in a System of Self-Propelled Agents. *Physical Review E.* 79: 051115-1.

(78) Strefler J, Erdmann U & Schimansky-Geier L., 2008, Swarming in three dimensions. *Physical Review E.* 78, 031927, 1- 8.

(79) Hemelrijk, C.K. and H. Hildenbrandt, 2011, Some cases of Variable Shape of Flock of Birds, *PLoS one.* 6(8): e22479.

(80) Yates CA, Erban R, Escudero C, Cousin I, Maini PK & Sumpter DJT, 2009, Inherent Noise Can Facilitate Coherence in Collective Swarm Motion. *PNaS.* 106. 14: 5464-5469.

(81) MacColl, A. D. C., 2011, The Ecological Causes of Evolution. Trends in Ecology and *Evolution.* 26 pp. 514-522.

(82) Darwin, C. *The Origin of Species by Means of Natural Selection* (1859)

(83) Sneppen, K., Bak, P, Flyvbjerg, H. and Jensen, M. H., 1995, Evolution as a Self-Organized Critical Phenomenon. *Proc. Natl. Acad. Sci. USA.* 92 pp. 5209- 5213.

(84) Mustonen, V. and Lässig, M., 2010, Fitness flux and Ubiquity of Adaptive Evolution. *Proc. Natl. Acad. Sci. USA.* 107 pp. 4248- 4253.

(85) Solè, R. V. and Manrubia, S. C., 1996, Extinction and Self-Organized Criticality in a Model of Large-Scale Evolution. *Phys. Rev. E.* 54.

(86) Nunes, L. A. and Meyer, M., 1999, Environmental changes, Coextinction, and Patterns in Fossil Record. *Phys. Rev. Lett.* 18. pp. 652-655.

(87) Sato, M. and Waxman, 2008, D. Adaptation to Slow Environmental change, with Apparent Anticipation of Selection. *J. Theor. Biol.* 252 pp. 166-172.

(88) Droz, M and Pękalski, A. Dynamics of Populations in a Changing Environment. *Phys. Rev. E.* 65. pp. 051911-1 - 051911-6.

(89) Wilke, C. O., 2005, Quasispecies Theory in the Context of Population Genetics. *BMC Evolutional Biology.* 5.

(90) Eigen M, McCaskill J, Schuster P, 1989, The Molecular Quasi-Species. *Adv Chem Phys* 75 pp.149-263.

(91) Clune, J., Misevic, D., Ofria, C., Lenski, R. E., Elena, S. F. and Sanjuán, R., 2008, Natural Selection Fails to Optimize Mutation Rate for Long-Term Adaptation on Rugged Fitness Landscapes. *PloS Computational Biology.* 4 e1000187.

(92) Hermisson, J., Redner, O., Wagner, H And Baake, E., 2002, Mutation–Selection Balance: Ancestry, Load, and Maximum Principle. *Theoretical Population Biology.* 62. pp. 9-46.

(93) Sasaki, A. and Nowak. M. A., 2003, Mutation Landscape. *J. Theor. Biol.* 181. 224 pp. 241-247.

(94) Lachmann, M. and Jablonka, E., 1991, The Inheritance of Phenotypes: an Adaptation to Fluctuating Environments. *J. Theor. Biol.* 181. pp. 1-9.

(95) Jansen, V. A. A. and Stumpf. M. P. H., 2005, Making Sense of Evolution in an Uncertain World. *Science.* 309 pp. 2005-2007.

(96) Lande. R. and Shannon. S., 1996, The role of Genetic Variation in Adaptation and Population Persistence in a Changing Environment. *Evolution.* 50. pp. 434-437.

(97) Carja, O. and Feldman. M. W., 2011, An Equilibrium for Phenotypic Variance in Fluctuating Environments Owing to Epigenetics. *J. R. Soc. Interface*. 17.

(98) Martins, J. S. S., Stauffer, D., De Oliveira, P. M. C. and De. Oliveira. S. M. Simulated Self-Organization of Death by Inherited Mutations. Annals of the Brazilian Academy of Science. 81. (2009) pp. 707- 714.

(99) Gunji, Y-P., Haruna, T. and Sawa, K., 2006, Principles of Biological Organization: Local-Global Negotiation Based on "Material Cause". *Physica D*. 219 pp. 152-167.

(100) Niizato, T. and Gunji, Y-P., 2010, Imperfect Identity of Autonomous Living Systems. *Biosystems*. 100 pp. 159-165.

(101) Niizato, T. and Gunji, Y-P., 2010, Applying Weak Equivalence of Categories Between Partial Map and Pointed Set Against Changing the Condition of 2-Arms Bandit Problem. *Complexity*. 16 pp. 10-21.

(102) Davey, B. A. and Priestelely, H. A., 2005, *Introduction to Lattices and Oder*. Cambridge. Cambridge University Press.

(103) Vecchio, D. D., Murray, R. M. and Klavins, E., 2006, Descrete State Estimators for Systems on a Lattice. *Automatica*. 42. 271-285.

(104) Pigolotti, S. Flammini, A. Marsili, M. and Maritan, A., 2005, Species Lifetime Distribution for Simple Models of Ecologies. *Proc. Natl. Acad. Sci. USA*. 102. pp. 15747-15751.

(105) Newman, M. E. J. and Eble, G. J., 1999, Power Spectra of Extinction in the Fossil Record. *Proc. R. Soc. Lond. B*. 266. pp. 1267-1270.

(106) Newman, M. E. J. and Eble, G. J., 1999, Decline in Extinction Rates and Scale Invariance in the Fossil Record. *Paleobiology* 2. pp. 434-439.

(107) West, G. B. and Brown, J. H., 2004, Life's Universal Scaling Laws. *Physics Today*. pp. 36- 42.

(108) Jensen, H. J., 1998, *Self-Organized Criticality: Emergent Complex Behavior in Physical and Biological Systems*. Cambridge. Cambridge University Press.

(109) Adami. C., 1995, Self-Organized Criticality in Living Systems. *Phys. Lett. A*. 203 29-32.

(110) Yang. C. B., 2004, The origin of Power-law Distribution in Self-Organized Criticality. J. Phys. A: *Math. Gen*. 37. L523-L529.

(111) Stassinopoulos, D. and Bak, P. 1995, Democratic reinforcement: A principle for brain function. *Phys. Rev. E*, 51:5033.

(112) Alstrøm, P. and Stassinopoulos, D. 1995, Versatility and adaptive performance. *Phys. Rev. E*, 51:5027–5032.

(113) Arcangelis, D., Capano, C. P., and Herrmann, H. 2006, Selforganized criticality model for brain plasticity. *Phys. Rev. Lett*, 96:0281071–4.

(114) Tagliazucchi, E. and Chialvo, D. R. 2011, The collective brain is critical. *arXiv*.